Characterization of the Warburg Effect and Crabtree Effect in Barrett's Esophagus Cell Lines and Development of a Chip-Based Single-Cell Respirometry System

Martin Thomas Suchorolski

A dissertation

submitted in partial fulfillment of the

requirements for the degree of

Doctor of Philosophy

University of Washington

2011

Nina Salama, Chair

Brian Reid

Peter Nelson

Program Authorized to Offer Degree:

Molecular and Cellular Biology

DEDICATION

In memory to Pavel, Antoni, Stefa and Zenia;

To my family Janusz, Wiera, Mike, Roxana, and Nicholas, for their love;

To Joan Henjum and Chris Marsh, for their daily fellowship and wisdom.

ACKNOWLEDGEMENTS

I would like to acknowledge all of the members of the Reid lab, specifically Thomas Paulson, PhD, Carissa Sanchez, and my advisor Brian Reid, MD PhD, for their rigorous coaching, attention to detail in reviewing this dissertation and support on a daily basis as I navigated skills that were sometimes very foreign to me or in very rough shape at commencement. At times it was a struggle and at others a real joy, but from experience I can say now that I had chosen the best lab in which to grow as a scientist and a human being. Other members that directly contributed to this work include Xiaohong Li, PhD, with guidance in statistical analysis, and Amber Karnofski for helping me coordinate meetings with Brian's busy schedule. I will always look back with admiration at the cohesiveness displayed by every single member of the Reid lab and the dependability they showed in any request made of them; other current and past members I had the pleasure of working alongside and would like to thank for their encouragement and camaraderie include Jessica Arnaudo, Valerie Cerera, Dennis Chao, PhD, David Cowan, Pui-Yee Fong, Patty Galipeau, Heather Kissel, Carlo Maley, PhD, Jesse Salk, PhD, and Lianjun Xu, MD. I would also like to thank Rachelle Kosoff and Lauren Merlo, PhD, from the Maley lab for critical discussion regarding tissue culture, and Corinna Palanca-Wessels, MD PhD, for initially establishing the Barrett's esophagus cell lines.

I would like to acknowledge David Hockenbery, MD PhD, for sharing in advisor duties, training me in the details of cellular metabolism and significant contributions to the experimental design and review of experiments in Chapter One, Daciana Margineantu, MD PhD, for input during experimental design, analysis and critical review of Chapter One, and John Fry for technical training with the Seahorse XF24 analyzer.

I would also like to thank Julio Vasquez and Dave McDonald in Scientific Imaging, Andrew Berger and other staff in Flow Cytometry Shared Resources at the FHCRC, and Peter Rabinovitch, MD PhD, at UW Pathology for training, technical advice and experience.

As part of the mentorship I received from Dr. Brian Reid, I was given the opportunity to collaborate with the bioengineers at the University of Washington Microscale Life Science Center, who contributed to the technology development project that is presented in Chapter Two: Engineering Lead Lloyd Burgess, PhD, Michael Konopka, PhD, Tim Strovas, PhD, Tim Molter, PhD, Sarah McQuaide, MS, Noel Fitzgerald, James Etzkorn, and Judy Anderson. I also appreciated all of the support given by Dr. Mary Lidstrom and Lidstrom lab members, in which the single-cell technology experiments were performed. I would also like to acknowledge all of the lab members that contributed from Dr. Alex Jen's lab (UW), Dr. Babak Parviz's lab (UW), Dr. Brad Cookson's lab (UW), Dr. Norm Dovichi's lab (UW), Dr. Larry Wangh's lab (Brandeis University), and Dr. Deidre Meldrum's lab (Arizona State University).

Early in my work at the Reid lab, I also had the pleasure to collaborate with Georg Luebeck, PhD, Jihyoun Jeon, PhD and Larry Jean, PhD at the FHCRC to write a mathematical modeling paper, which was not included in this dissertation.

I would like to thank all of the scientists, friends and acquaintances at the FHCRC for creating a vibrant and collaborative community for making an impact in diseases that claim so many lives. Great thanks for Michelle Karantsavelos, who supports every single FHCRC graduate student to get the best experience possible. I would also like to acknowledge the organizers, staff and

fellow graduate students with the Molecular and Cellular Biology department at the University of Washington, for creating a vision of an interdisciplinary training program that provided an unprecedented opportunity for growth.

I would like to acknowledge my thesis committee members, Dr. Nina Salama (chair), Dr. Pete Nelson, Dr. Joshua Akey, and Dr. Paul Lampe (graduate student representative), for their ideas, advice, and critical review of my work.

Finally, I would like to thank the Microscale Life Sciences Center and the National Institutes of Health funding agency (Grant CEGSTECHP5002360) for funding this work and other past and currently existing projects in the Reid lab.

TABLE OF CONTENTS

ABSTRACT

This thesis consisted of two distinct parts: In the first part, Warburg and Crabtree effects on energy metabolism were characterized in cell lines derived from premalignant Barrett's esophagus patients; in the second part, I participated in developing a microscopy-based single-cell oxygen consumption rate measurement device for determining metabolic diversity in cell populations.

Increased glycolysis is a hallmark of cancer metabolism, yet relatively little is known about this phenotype at premalignant stages of progression. Periodic ischemia occurs in premalignant Barrett's esophagus (BE) due to tissue damage from chronic acid-bile reflux and may select for early adaptations to hypoxia, including upregulation of glycolysis.

We compared metabolic rates of glycolysis and oxidative phosphorylation in four cell lines derived from patients with the premalignant condition Barrett's esophagus (CP-A, CP-B, CP-C and CP-D) in response to metabolic inhibitors and changes in glucose concentration. We report that cell lines derived from the dysplastic Barrett's esophagus have up to two-fold higher glycolysis compared to a cell line derived from non-dysplastic tissue; however, the dysplastic lines preserve active mitochondria. In response to the glycolytic inhibitor 2-deoxyglucose, the most glycolytic cell lines (CP-C and CP-D) had the greatest suppression of extra-cellular acidification, but were able to compensate with upregulation of oxidative phosphorylation. In addition, these cell lines showed the lowest compensatory increases in glycolysis in response to mitochondrial uncoupling by 2,4-dinitrophenol. Finally, these cell lines also upregulated their oxidative phosphorylation in response to glucose, demonstrating an elevated Crabtree effect.

Our findings suggest that cells from premalignant Barrett's esophagus tissue may adapt to an ever-changing selective microenvironment by increasing energy metabolic pathways typically associated with cancer cells.

In the second part of my thesis, I assisted in the development and testing of a system to measure single-cell oxygen consumption rates (OCR). Compared to systems that perform similar measurements, our instrument was able to perform single-cell OCR measurements in gas-impermeable chambers on a population of CP-A with minimal toxicity. I also established methods for serially measuring cell cycle and OCR on single-cells cells in this system.

INTRODUCTION

THE WARBURG EFFECT, CRABTREE EFFECT AND RECENT FOCUS OF RESEARCH ON CANCER METABOLISM

The interaction between the two major energy metabolism pathways in cells, glycolysis and oxidative phosphorylation, was initially studied by Louis Pasteur in 1857. Pasteur observed that when oxygen was provided to cells growing anaerobically, oxygen consumption rates increased while glucose consumption and lactate production rates decreased, a phenomenon named the Pasteur effect. Contrary to the Pasteur effect which occurs in normal cells, in 1927 Otto Heinrich Warburg first reported that cancer cells instead have increased lactate production even under aerobic oxygen conditions, a phenomenon that he named the Warburg effect (Warburg, Wind et al. 1927). The Warburg effect was discovered in mouse ascites tumors compared to normal liver and kidney cells of adult animals and confirmed in Earle's cancer cells, where more malignant cells of the same genetic background had elevated glycolysis (Warburg 1956). Since tumors failed to increase oxidative phosphorylation with addition of oxygen via the Pasteur effect, Warburg hypothesized that mitochondria were impaired. At that point, studies by Goldblatt and Cameron had shown that intermittent oxygen disturbances could produce cancer and Warburg speculated that the Warburg effect arose due to an irreversible "damage to respiration", which led to a rise in glycolysis to compensate for the loss of mitochondrial energy production (Goldblatt and Cameron 1953). Although Warburg remarked that the rise in glycolysis occurred progressively and with many cell divisions during growth in tumors, the origins of the Warburg effect have not been investigated in pre-malignant tissue.

Several groups have reported the Warburg effect in a variety of tumors; however Warburg's generalization that all cancer cells are glycolytic was challenged by Sidney Weinhouse, who insisted that glycolytic upregulation is not unique to cancers, since normal tissues such as brain, retina, kidney medulla and intestinal mucosa are also glycolytic (Weinhouse 1956). Weinhouse later showed that Warburg's observations applied to subsets of tumors since in slow growing rat hepatomas, developed by H. P. Morris, the metabolism was more reliant on oxidative phosphorylation than faster growing, more glycolytic hepatomas (Weinhouse 1967). Warburg's hypothesis that tumor mitochondria are damaged was also refuted since many tumors actively respire to produce ATP (Weinhouse 1976). With the exception of brain cancers, which are unable to obtain non-glycolytic substrates due to the blood/brain barrier, it has been discovered that many cancers use mitochondria to produce energy via non-glycolytic substrates including glutamine and lipids (Souba 1993; Przybytkowski, Joly et al. 2007). Finally, it was realized that even in cancers where the glycolysis is upregulated, the energy production was still largely dependent on mitochondrial function (Zu and Guppy 2004), suggesting other roles for glycolysis.

In addition to upregulated glycolysis due to the Warburg effect, a less studied metabolic phenomenon in cancer cells is their ability to decrease oxygen consumption in response to increasing glucose concentrations: the Crabtree effect (Crabtree 1929). The Crabtree effect has also been observed in other continuously replicating cells, such as thymocytes and intestinal mucosa, as well as in yeast and bacterial cells (Mustea and Muresian 1967; Leese and Bronk 1975; Postma, Verduyn et al. 1989; Guppy, Greiner et al. 1993). The molecular mechanism for the Crabtree effect is not clearly defined but is thought to be mediated through hexokinase

binding to mitochondria, downregulating complex I of the electron transport chain, and through sensitization of cells to [ATP]/[ADP][Pi] (Sussman, Erecinska et al. 1980; Golshani-Hebroni and Bessman 1997). The interactions between the Warburg and Crabtree effect remains uninvestigated, despite knowledge that ischemia occuring in tumors affects oxygen and glucose concentrations and is known to influence the rate of glucose consumption (Lopaschuk and Stanley 1997). Similar to the Warburg effect, the Crabtree effect is thought to provide cancer cells with an adaptive advantage to fluctuations in available substrate. It is currently unknown whether the Crabtree effect arises during the progression of neoplastic tissue to cancer.

With the advent of gene-centric cancer research in the 1980s and 1990s, cancer metabolism research declined and the Warburg and Crabtree effects wereeffectively ignored in several later oncology and mitochondrial reviews (Hanahan and Weinberg 2000; Scheffler 2001). A re-examination of the Warburg effect was necessitated by the discovery of hypoxia-inducible factor-1 (HIF-1) by Greg Semenza's group (Zhong, De Marzo et al. 1999). Upon reviewing prior studies, several groups remarked that the importance of glycolysis on energy production in cancer was indeed over-emphasized (Zu and Guppy 2004; Moreno-Sanchez, Rodriguez-Enriquez et al. 2007; Dang 2010). A meta-analysis of studies with different tissue types demonstrated that several tissues maintain functional mitochondria as they progress to cancer (Moreno-Sanchez, Rodriguez-Enriquez et al. 2007). Warburg's damaged mitochondria hypothesis was further refuted with the discoveries that active mitochondria play novel roles in some cancers, including allowing the cells to switch to alternate oxidative substrates and to metastasize (Souba 1993; Berridge, Herst et al. 2010).

Despite the initial overgeneralization of Warburg's findings, the discovery that most cancers increase their glycolysis relative to normal tissue suggested a number of practical applications that have enhanced medical care and treatment of many cancers. The discovery that most tumors require higher glucose flux to maintain increased levels of glycolysis was applied successfully in positron emission tomography (PET), an imaging technique which can detect greater than 90% of human primary and metastatic tumors by monitoring increased concentrations of labeled glucose analogues (Czernin and Phelps 2002). Also as a result of Warburg's findings, glycolysis has been targeted for therapy, and a number of drugs have been identified to disrupt the glycolytic pathway (Chen, Lu et al. 2007).

Although early detection and treatment of cancer has been proposed as a viable and potentially effective strategy, the Warburg and Crabtree effects have not been investigated in early neoplastic lesions. Cancers develop genetic heterogeneity in advanced stages, so early detection and therapy, coupled with a specific assay for progression may provide much more effective treatment results. Given that most tumors display high glycolysis, surprisingly little is known of the evolutionary origins of the Warburg and Crabtree effects.

SELECTIVE PRESSURES AND MECHANISMS OF WARBURG EFFECT IN CANCER

The Warburg and Crabtree effect are thought to be protective against substrate fluctuation in the presence of ischemia, which arises in tumors due to chronic wounding, inflammation or uncontrolled growth. Ischemia can lead to hypoxic (low oxygen), anoxic (no oxygen) and hypoglycemic (low glucose) conditions that are toxic to cells. In this section I describe how these environments arise in tumors, the mechanisms that provide protection under these

conditions and theories for how increased glycolysis and/or decreased mitochondrial function would benefit cancer cells.

Cells progressing to cancer undergo clonal selection as a function of selective pressures caused by their neighboring cells and extracellular environment, with surviving populations passing on genetic and epigenetic changes to future generations (Nowell 1976). To survive periodic near-anoxic events, cells upregulate survival mechanisms for hypoxia which are conserved in eukaryotes and play critical roles during development, differentiation and survival in response to injury.

Hypoxic conditions arise when cells grow beyond 100-150 microns from nearby vasculature: the Thomlinson-Gray limit (Thomlinson and Gray 1955). Beyond this limit, oxygen is at too low concentrations for cells to produce adequate energy via oxidative phosphorylation; however glycolysis is still possible in this environment (Casciari, Sotirchos et al. 1988). Hypoxic and anoxic environments are known to arise in intermediate stages of solid tumor growth, prior to vascularization and at later stages due to poorly designed and leaky vascularization that is present in tumors. Hypoxia can also occur in wounding, especially in chronic wounds such as ulceration, burns or scarring. Fluctuations to near-anoxia and reoxygenation generate reactive oxygen species (ROS), due to inefficient electron transport chain function in mitochondria, and are toxic to cells. ROS can also be produced by chronic inflammation, which is associated with numerous premalignant conditions that increase risk of progression to cancer, including ulcerative colitis, gastric ulcers and Barrett's esophagus. It is unknown whether adaptation to hypoxia occurs at earlier premalignant stages in most cancers.

Several genes are involved in hypoxic protection and their alteration results in constitutive upregulation of glycolysis, thought to be protective from periodic fluctuations to anoxia. The major conserved hypoxia-mediating factors in eukaryotes are the hypoxia-inducible transcription factors, HIF-1α and HIF-2α. These genes become stabilized under hypoxic conditions, form heterodimeric transcription complexes with HIF-1β, and activate over 100 downstream genes important in hypoxic survival. Their targets include glycolytic enzymes (hexokinase, aldolase), glucose transporters (GLUT-family transporters), angiogenic factors (VEGF), haematopoetic factors (erythropoietin) and anti-apoptotic factors (Bcl-2, IAP-2) (Semenza 2001). HIF-1α expression is regulated transcriptionally by several factors, notably COX-2, ERBB2, PI3K and h-RAS (Semenza 2002). In the presence of oxygen, HIF-1α activity is also negatively regulated post-translationally by a family of oxygen-dependent prolyl and asparagine hydroxylases, which begin the enzymatic sequence that leads to ubiquitination and proteolytic degradation (Epstein et al, 2001 Cell 107; Ivan et al, 2001 Science 292; Jaakkola 2001 Science 292)(Hewitson, McNeill et al. 2002). Von Hippel Lindau protein is also critical for HIF-1α ubiquitination and degradation, such that patients that inherit two mutant copies develop constitutively increased glycolysis and early onset renal carcinoma (Latif, Tory et al. 1993). p53 and p14/ARF, two critical tumor suppressors, have been reported to regulate HIF-1α post-translationally: p53 reduces levels of HIF-1α by targeting it for proteolytic degradation (Blagosklonny, An et al. 1998), while p14 sequesters HIF-1α to the nucleolus, preventing transcription under hypoxic conditions (Fatyol and Szalay 2001). Although p53 mutations can be selected for in hypoxic tumors (Graeber, Osmanian et al. 1996), selection may also be due to suppression of hypoxia-induced apoptosis. Since several genes are commonly mutated in cancer have a role in HIF regulation, constitutively upregulated glycolysis may result from cumulative loss of regulation. Increased glycolysis was initially believed to be an evolutionary

adaptation by tumors to overcome hypoxic conditions (Gatenby and Gillies 2004); however upregulated glycolysis is also found in several cancers, such as leukemia or lung tumors (Nolop, Rhodes et al. 1987; Elstrom, Bauer et al. 2004), prior to onset of hypoxic conditions which suggests that a different role for glycolysis in these cells.

New findings have discovered alternate methods for regulating the Warburg effect and novel roles for increased glycolysis. Myc and p53, two genes important in growth factor signaling and cell cycle control in cancer progression, were found to play roles in regulating both glycolysis and mitochondrial function (Bensaad, Tsuruta et al. 2006; Matoba, Kang et al. 2006; Diaz-Ruiz, Rigoulet et al. 2011). p53 loss results in the Warburg effect by upregulating glycolysis and the pentose phosphate pathway, suggesting that the primary function of glycolytic upregulation in cancers is to generate substrates for nucleotides, non-essential amino acids, and NADPH+, a critical co-factor in recharging glutathione, to mediate ROS from mitochondrial, inflammatory or extracellular sources (Bensaad, Tsuruta et al. 2006). P53 loss *in vitro* and *in vivo* also decreased oxidative phosphorylation through a decrease in transcription of SCO2 (synthesis of cytochrome c oxidase), a critical factor for cytochrome III assembly (Blagosklonny, An et al. 1998; Matoba, Kang et al. 2006). Recently the pyruvate kinase isoform M2 was found to be upregulated in cancer cells, causing a bypass of substrate-level phosphorylation of ADP, resulting in non-energetic glycolytic metabolism (Vander Heiden, Locasale et al. 2010). Since mitochondria appear to be active in many cancers, it is reasonable for glycolysis to no longer be thought of as mainly an energy-producing pathway, but to benefit proliferation in these cells instead.

An effect of increased glycolysis in tumors is the transport of lactate into extracellular spaces, acidifying surrounding tissue to toxic levels for normal cells (Schornack and Gillies 2003), breaking down extra-cellular matrix and promoting invasion and metastasis of healthy tissue (Gatenby and Gillies 2008). Since adjacent healthy tissue is not able to survive the lower pH conditions, this acidification has been suggested as a form of intercellular competion. To overcome the toxic effects of decreased intracellular pH, several carbonic anhydrase and other acid-transporters are upregulated in cancers (Cardone, Casavola et al. 2005; Chiche, Ilc et al. 2009). Simulation models by Gatenby and Smallbone predict a step-wise progression of cells which become glycolytic, followed by acid-tolerance and invasion by mutant cells into normal epithelium (Smallbone, Gatenby et al. 2007); although glycolysis is often associated with more invasive phenotypes, these models of progression have not been explicitly validated *in vivo*.

Despite the recent increase in knowledge about the mechanisms controlling the Warburg effect, there is a lack of studies which investigate when it originates during cancer progression. At least two studies have examined how Warburg effect can be induced experimentally in cell lines that simulate progressive transformation through step-wise gene transfection (Ramanathan, Wang et al. 2005; de Groof, te Lindert et al. 2009); however these are largely artificial systems which begin with previously transformed cells and ignore many of the selective pressures that affect *in vivo* evolution. Cell lines derived from different cancer types have heterogeneous levels of constitutive HIF-1α upregulation (Zhong, Mabjeesh et al. 2002), but the progression resulting in the tissue-specific differences at proteomic or metabolic levels is poorly understood. Studies of the evolution of glycolysis in tissue have historically been limited by the absence of a model in which periodic surveillance can occur, from premalignant tissue to cancer tissue. In this thesis we propose such a model in Barrett's esophagus.

BARRETT'S ESOPHAGUS MODEL OF CANCER EVOLUTION

It is impossible to follow most premalignant conditions in the human body because they are either removed upon detection (eg. polyps in the colon) or clinical complications preclude systematic sampling (eg. pancreatic cancer). In contrast, the pre-malignant condition Barrett's esophagus (BE) provides an opportunity to study neoplastic progression longitudinally because periodic endoscopic biopsy surveillance is recommended for early detection of cancer (Sampliner 2002). In this section, I present our knowledge of BE, known biomarkers of progression and cell lines that allow for monitoring metabolic changes *ex vivo* in the experiments performed in this thesis.

Barrett's esophagus is a columnar epithelium that replaces normal esophageal squamous epithelium, secretes mucin and bicarbonate, and is thought to be protective against chronic acid-bile refluxate, typically occuring in patients with gastroesophageal reflux disease (GERD) which commonly precedes BE (Orlando 2006). Although BE is believed to be protective, patients are at risk of progressing to esophageal adenocarcinoma at a rate of 0.5% per year (Thomas, Abrams et al. 2007; Yousef, Cardwell et al. 2008). Esophageal adenocarcinoma has increased >600% in incidence in the past three decades in the United States (Pohl and Welch 2005) and results in survival of less than one year in most patients (Polednak 2003). In the United States, incidence of BE is highest in Caucasian men, in whom it is eight times higher than in Caucasian women and five times higher than in African-American men (Holmes and Vaughan 2007). Several risk factors are associated with progression to EA including symptomatic GERD, obesity (especially waist-to-hip ratio), cigarette smoking and a diet low in fruits and vegetables (reviewed in (Reid, Li et al. 2010)). Use of non-steroidal anti-inflammatory drugs have been associated with a reduction in risk (Vaughan, Dong et al. 2005; Abnet, Freedman et al. 2009). COX2, a gene that encodes a cyclooxygenase that is targeted by NSAIDs has also been expressed at higher levels in BE and OE (Moons, Kuipers et al. 2007; Ferguson, Wild et al. 2008). Although COX2 is primarily thought to regulate inflammation, it also interacts with HIF-1α and may be protective in an ulcerative environment (Greenhough, Smartt et al. 2009). Several markers of hypoxia, including HIF-2α and VEGF, have been reported previously in advanced BE (Lord, Park et al. 2003; Griffiths, Pritchard et al. 2007), however levels of glycolysis and oxidative phosphorylation metabolism have never been directly characterized.

The current standard of care for BE patients is detection and classification of changes in epithelial structure by pathological examination for the early development of EA. In BE, the assessment of dysplasia is subject to substantial observer variation between pathologists and has been limited at discriminating premalignant lesions which are at risk of progressing (Reid, Haggitt et al. 1988; Montgomery, Bronner et al. 2001). Several studies have identified genetic lesions such as 9pLOH (p16 locus), 17pLOH (p53 locus), as well as DNA content abnormalities, tetraploidy, and aneuploidy, which provide an accurate method for predicting BE patient progression to cancer (Li, Galipeau et al. 2008). In a novel method for measuring progression, Maley et al demonstrated that increased clonal diversity, as measured by Shannon Index and pairwise divergence of genetic content by flow cytometry, and genetic alteration can result in increased risk for EA (Maley, Galipeau et al. 2006). Diversity between crypts or single cells has not been thoroughly investigated yet, however new methods of microdisection and assay technologies at a single-cell level are now bringing this into the realm of possibility.

Even with surveillance, most cases of EA present with no prior diagnosis of BE (Bytzer, Christensen et al. 1999; Corley, Levin et al. 2002), presenting an opportunity for novel biomarkers and/or surveillance strategies to improve detection and prevention of this disease. Several imaging methods have previously detected signs of upregulated glycolysis and altered redox in BE and EA. Like many other advanced solid tumors, EA displays high glycolytic flux by positron emission tomography (PET), indicating increased levels of glycolysis (Taylor, Smith et al. 2009). It is unknown if this glycolysis occurs in premalignant lesions; however fluorescent tissue imaging of NADH/ NADPH levels in BE by resemble hypoxic tissue and can discriminate BE from surrounding normal tissue(Georgakoudi, Jacobson et al. 2002). The technology to discriminate localized regions of glycolysis *in vivo* is still under development, thus for this thesis *ex vivo* models were chosen to characterize levels of glycolysis and oxidative phosphorylation.

Both animal and cell line models exist for studying BE progression to adenocarcinoma. Although rat models of BE exist, these have particular difficulties associated with them. The first model, which requires surgical alteration to create chronic acid conditions which allows BE to arise, is technically difficult to construct and is unable to replicate BE to EA progression faithfully, resulting in a mix of squamous carcinoma and adenocarcinoma (Bonde, Gao et al. 2007). In a more recent genetic model, rats with intestinal transcription factor Cdx2 ectopically expressed in the esophagus replaced normal squamous epithelium with an epithelium that shared characteristics intermediate with BE and keratinocytes (Kong, Crissey et al. 2011). Finally, Frank McKeon's group has recently discovered that p63 null mice which have acid-damaged esophagi re-epithelialize their tissue with residual embryonic-like cells which appear to authentically reproduce BE (Wang, Ouyang et al. 2011). Cell lines, derived from patients with premalignant BE and immortalized with hTERT, provide a reusable model for studying BE *ex vivo.* These cells display similar genetic and epigenetic alterations to source tissue including alterations and methylation in p16, alterations in p53, deletions at fragile sites and genetic instability resulting in aneuploidy and tetraploidy (Palanca-Wessels, Barrett et al. 1998; Palanca-Wessels, Klingelhutz et al. 2003; Lai, Kostadinov et al. 2010). While acid-bile mixtures are known to result in increased apoptosis (Dvorak, Payne et al. 2007) they also result in a variety of responses in the cell lines. Studies with BE cell lines have shown that bile acid receptors are upregulated (De Gottardi, Dumonceau et al. 2006) and acid-bile reflux is able to activate the COX-2 pathway (Song, Guha et al. 2007), the mTOR metabolic pathway (Yen, Izzo et al. 2008) and is able to stimulate cell differentiation and tissue remodeling (Chang, Lao-Sirieix et al. 2007). COX-2 has been previously mentioned as a transcriptional co-activator with HIF-1α and upregulating mTOR increases glycolysis in pancreatic, prostate and hepatic cancer cell lines (Greenhough, Smartt et al. 2009; Sun, Chen et al. 2011). Several EA cell lines also exist, however BIC-1, SEG-1 and TE-7 were recently found to be contaminated and/or mis-identified (Boonstra, van Marion et al. 2010). Other EA cell lines are either of non-BE origin (OE-19) or are only privately available (OE-24, BE-3, SK-4), which dramatically limits the number of available EA lines. Recently, organotypic culture with BE cell lines on collagen substrate has been developed to recreate a more representative *in vivo* tissue structure (Kosoff, Gardiner et al. 2011). In this study, I used cell lines that were representative of early (CP-A) and late (CP-B, C, and D) stages in neoplastic progression in order to characterize evolutionary changes to energy metabolism that have persisted in culture.

OUTLINE OF THESIS

This thesis investigates two energy metabolism alterations occurring in cancer, the Warburg and Crabtree effects, in cell lines derived from patients with premalignant Barrett's esophagus. BE is an excellent model system for studying cellular changes that predict progression, since candidate biomarkers can be validated in longitudinal studies incorporating periodic surveillance in patients. BE is one of the few neoplasias for which a panel of hTERT-immortalized cell lines exist which allow for rapid characterization of glycolysis and oxidative phosphorylation *in vitro*.

In the first chapter of my thesis, I tested the hypothesis that BE cell lines that are more advanced in genetic instability display higher levels of glycolysis. I also tested that more glycolytic cell lines display higher Crabtree effect. In this chapter I took advantage of recent technology advances in measuring metabolic flux, the Seahorse XF24 analyzer, which enabled rapid characterization of glycolysis and oxidative phosphorylation in BE cell lines. I present my characterization of the levels of glycolysis and oxidative phosphorylation in existing BE cell lines and their changes in response to glycolytic and mitochondrial inhibitors and conditions that would stimulate the Crabtree effect. I also examined nuclear and mitochondrial genome changes, which are remarkably similar to changes observed in patients from which the cell lines were derived.

Since diversity measures are predictive for BE progression to EA, as part of this thesis I also had the opportunity to participate in the development of a microscopy system for measuring single-cell oxygen consumption rates in order to measure heterogeneity of energy metabolism at single-cell levels. This part of the thesis was done with the help of bioengineers in Mary Lidstrom's group and chemists in Lloyd Burgess' group at the University of Washington, as part of a Centers for Excellence in Genome Sciences (CEGS) multi-center interdisciplinary grant. In the second chapter of the thesis, I present the development of the microscopy system for measuring single-cell oxygen consumption rates (OCR) and methods for serially measuring cellular parameters such as cell cycle, mitochondrial mass and apoptosis. This system enables measurements of OCR heterogeneity and related cellular parameters critical to cellular life and death decisions.

In the third chapter, I propose novel directions for future research given the findings with our cell lines and how these findings may apply to diagnostic and therapeutic applications. In this chapter, I also suggest potential applications for the prototype single-cell oxygen consumption system we developed and tested.

REFERENCES

Abnet, C. C., N. D. Freedman, et al. (2009). "Non-steroidal anti-inflammatory drugs and risk of gastric and oesophageal adenocarcinomas: results from a cohort study and a meta-analysis." Br J Cancer **100**(3): 551-557.

Bensaad, K., A. Tsuruta, et al. (2006). "TIGAR, a p53-inducible regulator of glycolysis and apoptosis." Cell **126**(1): 107-120.

Berridge, M. V., P. M. Herst, et al. (2010). "Metabolic flexibility and cell hierarchy in metastatic cancer." Mitochondrion **10**(6): 584-588.

Blagosklonny, M. V., W. G. An, et al. (1998). "p53 inhibits hypoxia-inducible factor-stimulated transcription." Journal of Biological Chemistry **273**(20): 11995-11998.

Bonde, P., D. Gao, et al. (2007). "Duodenal reflux leads to down regulation of DNA mismatch repair pathway in an animal model of esophageal cancer." The Annals of thoracic surgery **83**(2): 433-440; discussion 440.

Boonstra, J. J., R. van Marion, et al. (2010). "Verification and unmasking of widely used human esophageal adenocarcinoma cell lines." Journal of the National Cancer Institute **102**(4): 271-274.

Bytzer, P., P. B. Christensen, et al. (1999). "Adenocarcinoma of the esophagus and Barrett's esophagus: a population- based study." Am J Gastroenterol **94**(1): 86-91.

Cardone, R. A., V. Casavola, et al. (2005). "The role of disturbed pH dynamics and the Na+/H+ exchanger in metastasis." Nature reviews. Cancer **5**(10): 786-795.

Casciari, J. J., S. V. Sotirchos, et al. (1988). "Glucose diffusivity in multicellular tumor spheroids." Cancer Res **48**(14): 3905-3909.

Chang, C. L., P. Lao-Sirieix, et al. (2007). "Retinoic acid-induced glandular differentiation of the oesophagus." Gut **56**(7): 906-917.

Chen, Z., W. Lu, et al. (2007). "The Warburg effect and its cancer therapeutic implications." Journal of bioenergetics and biomembranes **39**(3): 267-274.

Chiche, J., K. Ilc, et al. (2009). "Hypoxia-inducible carbonic anhydrase IX and XII promote tumor cell growth by counteracting acidosis through the regulation of the intracellular pH." Cancer research **69**(1): 358-368.

Corley, D. A., T. R. Levin, et al. (2002). "Surveillance and Survival in Barrett's Adenocarcinomas: A Population- Based Study." Gastroenterology **122**(3): 633-640.

Crabtree, H. G. (1929). "Observations on the carbohydrate metabolism of tumours." The Biochemical journal **23**(3): 536-545.

Czernin, J. and M. E. Phelps (2002). "Positron emission tomography scanning: current and future applications." Annual review of medicine **53**: 89-112.

Dang, C. V. (2010). "p32 (C1QBP) and cancer cell metabolism: is the Warburg effect a lot of hot air?" Molecular and cellular biology **30**(6): 1300-1302.

De Gottardi, A., J. M. Dumonceau, et al. (2006). "Expression of the bile acid receptor FXR in Barrett's esophagus and enhancement of apoptosis by guggulsterone in vitro." Mol Cancer **5**: 48.

de Groof, A. J., M. M. te Lindert, et al. (2009). "Increased OXPHOS activity precedes rise in glycolytic rate in H-RasV12/E1A transformed fibroblasts that develop a Warburg phenotype." Molecular cancer **8**: 54.

Diaz-Ruiz, R., M. Rigoulet, et al. (2011). "The Warburg and Crabtree effects: On the origin of cancer cell energy metabolism and of yeast glucose repression." Biochimica et biophysica acta **1807**(6): 568-576.

Dvorak, K., C. M. Payne, et al. (2007). "Bile acids in combination with low pH induce oxidative stress and oxidative DNA damage: relevance to the pathogenesis of Barrett's oesophagus." Gut **56**(6): 763-771.

Elstrom, R. L., D. E. Bauer, et al. (2004). "Akt stimulates aerobic glycolysis in cancer cells." Cancer research **64**(11): 3892-3899.
Fatyol, K. and A. A. Szalay (2001). "The p14(ARF) tumor suppressor protein facilitates nucleolar sequestration of hypoxia-inducible factor-1 alpha (HIF-1 alpha) and inhibits HIF-1-mediated transcription." Journal of Biological Chemistry **276**(30): 28421-28429.
Ferguson, H. R., C. P. Wild, et al. (2008). "Cyclooxygenase-2 and inducible nitric oxide synthase gene polymorphisms and risk of reflux esophagitis, Barrett's esophagus, and esophageal adenocarcinoma." Cancer epidemiology, biomarkers & prevention : a publication of the American Association for Cancer Research, cosponsored by the American Society of Preventive Oncology **17**(3): 727-731.
Gatenby, R. A. and R. J. Gillies (2004). "Why do cancers have high aerobic glycolysis?" Nature Reviews Cancer **4**(11): 891-899.
Gatenby, R. A. and R. J. Gillies (2008). "A microenvironmental model of carcinogenesis." Nat Rev Cancer **8**(1): 56-61.
Georgakoudi, I., B. C. Jacobson, et al. (2002). "NAD(P)H and collagen as in vivo quantitative fluorescent biomarkers of epithelial precancerous changes." Cancer research **62**(3): 682-687.
Goldblatt, H. and G. Cameron (1953). "Induced malignancy in cells from rat myocardium subjected to intermittent anaerobiosis during long propagation in vitro." The Journal of experimental medicine **97**(4): 525-552.
Golshani-Hebroni, S. G. and S. P. Bessman (1997). "Hexokinase binding to mitochondria: a basis for proliferative energy metabolism." Journal of bioenergetics and biomembranes **29**(4): 331-338.
Graeber, T. G., C. Osmanian, et al. (1996). "Hypoxia-mediated selection of cells with diminished apoptotic potential in solid tumours." Nature **379**(6560): 88-91.
Greenhough, A., H. J. Smartt, et al. (2009). "The COX-2/PGE2 pathway: key roles in the hallmarks of cancer and adaptation to the tumour microenvironment." Carcinogenesis **30**(3): 377-386.
Griffiths, E. A., S. A. Pritchard, et al. (2007). "Increasing expression of hypoxia-inducible proteins in the Barrett's metaplasia-dysplasia-adenocarcinoma sequence." Br J Cancer **96**(9): 1377-1383.
Guppy, M., E. Greiner, et al. (1993). "The role of the Crabtree effect and an endogenous fuel in the energy metabolism of resting and proliferating thymocytes." European journal of biochemistry / FEBS **212**(1): 95-99.
Hanahan, D. and R. A. Weinberg (2000). "The hallmarks of cancer." Cell **100**(1): 57-70.
Hewitson, K. S., L. A. McNeill, et al. (2002). "Hypoxia-inducible factor (HIF) asparagine hydroxylase is identical to factor inhibiting HIF (FIH) and is related to the cupin structural family." The Journal of biological chemistry **277**(29): 26351-26355.
Holmes, R. S. and T. L. Vaughan (2007). "Epidemiology and pathogenesis of esophageal cancer." Semin Radiat Oncol **17**(1): 2-9.
Kong, J., M. A. Crissey, et al. (2011). "Ectopic Cdx2 expression in murine esophagus models an intermediate stage in the emergence of Barrett's esophagus." PloS one **6**(4): e18280.
Kosoff, R. E., K. L. Gardiner, et al. (2011). "Development and characterization of an organotypic model of Barrett's esophagus." Journal of cellular physiology.
Lai, L. A., R. Kostadinov, et al. (2010). "Deletion at fragile sites is a common and early event in Barrett's esophagus." Mol Cancer Res **8**(8): 1084-1094.
Latif, F., K. Tory, et al. (1993). "Identification of the Vonhippel-Lindau Disease Tumor-Suppressor Gene." Science **260**(5112): 1317-1320.
Leese, H. J. and J. R. Bronk (1975). "Lactate formation by rat small intestine in vitro." Biochimica et biophysica acta **404**(1): 40-48.

Li, X., P. C. Galipeau, et al. (2008). "Single nucleotide polymorphism-based genome-wide chromosome copy change, loss of heterozygosity, and aneuploidy in Barrett's esophagus neoplastic progression." Cancer Prev Res (Phila Pa) **1**(6): 413-423.
Lopaschuk, G. D. and W. C. Stanley (1997). "Glucose metabolism in the ischemic heart." Circulation **95**(2): 313-315.
Lord, R. V., J. M. Park, et al. (2003). "Vascular endothelial growth factor and basic fibroblast growth factor expression in esophageal adenocarcinoma and Barrett esophagus." The Journal of thoracic and cardiovascular surgery **125**(2): 246-253.
Maley, C. C., P. C. Galipeau, et al. (2006). "Genetic clonal diversity predicts progression to esophageal adenocarcinoma." Nat Genet **38**(4): 468-473.
Matoba, S., J. G. Kang, et al. (2006). "p53 regulates mitochondrial respiration." Science **312**(5780): 1650-1653.
Montgomery, E., M. P. Bronner, et al. (2001). "Reproducibility of the diagnosis of dysplasia in Barrett esophagus: a reaffirmation." Hum Pathol **32**(4): 368-378.
Moons, L. M., E. J. Kuipers, et al. (2007). "COX-2 CA-haplotype is a risk factor for the development of esophageal adenocarcinoma." The American journal of gastroenterology **102**(11): 2373-2379.
Moreno-Sanchez, R., S. Rodriguez-Enriquez, et al. (2007). "Energy metabolism in tumor cells." The FEBS journal **274**(6): 1393-1418.
Mustea, I. and T. Muresian (1967). "Crabtree effect in some bacterial cultures." Cancer **20**(9): 1499-1501.
Nolop, K. B., C. G. Rhodes, et al. (1987). "Glucose utilization in vivo by human pulmonary neoplasms." Cancer **60**(11): 2682-2689.
Nowell, P. C. (1976). "The clonal evolution of tumor cell populations." Science **194**(4260): 23-28.
Orlando, R. C. (2006). Mucosal Defense in Barrett's Esophagus. Barrett's Esophagus and Esophageal Adenocarcinoma. S. R. ed. Sharma P. Oxford, UK, Blackwell Publishing, Ltd**:** pp. 60-72.
Palanca-Wessels, M. C., M. T. Barrett, et al. (1998). "Genetic analysis of long-term Barrett's esophagus epithelial cultures exhibiting cytogenetic and ploidy abnormalities." Gastroenterology **114**(2): 295-304.
Palanca-Wessels, M. C., A. Klingelhutz, et al. (2003). "Extended lifespan of Barrett's esophagus epithelium transduced with the human telomerase catalytic subunit: a useful in vitro model." Carcinogenesis **24**(7): 1183-1190.
Pohl, H. and H. G. Welch (2005). "The role of overdiagnosis and reclassification in the marked increase of esophageal adenocarcinoma incidence." J Natl Cancer Inst **97**(2): 142-146.
Polednak, A. P. (2003). "Trends in survival for both histologic types of esophageal cancer in US surveillance, epidemiology and end results areas." Int J Cancer **105**(1): 98-100.
Postma, E., C. Verduyn, et al. (1989). "Enzymic analysis of the crabtree effect in glucose-limited chemostat cultures of Saccharomyces cerevisiae." Applied and environmental microbiology **55**(2): 468-477.
Przybytkowski, E., E. Joly, et al. (2007). "Upregulation of cellular triacylglycerol - free fatty acid cycling by oleate is associated with long-term serum-free survival of human breast cancer cells." Biochemistry and cell biology = Biochimie et biologie cellulaire **85**(3): 301-310.
Ramanathan, A., C. Wang, et al. (2005). "Perturbational profiling of a cell-line model of tumorigenesis by using metabolic measurements." Proc Natl Acad Sci U S A **102**(17): 5992-5997.
Reid, B. J., R. C. Haggitt, et al. (1988). "Observer variation in the diagnosis of dysplasia in Barrett's esophagus." Human Pathology **19**(2): 166-178.

Reid, B. J., X. Li, et al. (2010). "Barrett's oesophagus and oesophageal adenocarcinoma: time for a new synthesis." Nat Rev Cancer **10**(2): 87-101.
Sampliner, R. E. (2002). "Updated guidelines for the diagnosis, surveillance, and therapy of Barrett's esophagus." Am J Gastroenterol **97**(8): 1888-1895.
Scheffler, I. E. (2001). "A century of mitochondrial research: achievements and perspectives." Mitochondrion **1**(1): 3-31.
Schornack, P. A. and R. J. Gillies (2003). "Contributions of cell metabolism and H+ diffusion to the acidic pH of tumors." Neoplasia **5**(2): 135-145.
Semenza, G. L. (2001). "Hypoxia-inducible factor 1: control of oxygen homeostasis in health and disease." Pediatric research **49**(5): 614-617.
Semenza, G. L. (2002). "HIF-1 and tumor progression: pathophysiology and therapeutics." Trends in Molecular Medicine **8**(4): S62-S67.
Smallbone, K., R. A. Gatenby, et al. (2007). "Metabolic changes during carcinogenesis: potential impact on invasiveness." Journal of theoretical biology **244**(4): 703-713.
Song, S., S. Guha, et al. (2007). "COX-2 induction by unconjugated bile acids involves reactive oxygen species-mediated signalling pathways in Barrett's oesophagus and oesophageal adenocarcinoma." Gut **56**(11): 1512-1521.
Souba, W. W. (1993). "Glutamine and cancer." Annals of surgery **218**(6): 715-728.
Sun, Q., X. Chen, et al. (2011). "Mammalian target of rapamycin up-regulation of pyruvate kinase isoenzyme type M2 is critical for aerobic glycolysis and tumor growth." Proceedings of the National Academy of Sciences of the United States of America **108**(10): 4129-4134.
Sussman, I., M. Erecinska, et al. (1980). "Regulation of cellular energy metabolism: the Crabtree effect." Biochimica et biophysica acta **591**(2): 209-223.
Taylor, M. D., P. W. Smith, et al. (2009). "Correlations between selected tumor markers and fluorodeoxyglucose maximal standardized uptake values in esophageal cancer." European journal of cardio-thoracic surgery : official journal of the European Association for Cardio-thoracic Surgery **35**(4): 699-705.
Thomas, T., K. R. Abrams, et al. (2007). "Meta analysis: Cancer risk in Barrett's oesophagus." Aliment Pharmacol Ther **26**(11-12): 1465-1477.
Thomlinson, R. H. and L. H. Gray (1955). "The histological structure of some human lung cancers and the possible implications for radiotherapy." British Journal of Cancer **9**: 539-549.
Vander Heiden, M. G., J. W. Locasale, et al. (2010). "Evidence for an alternative glycolytic pathway in rapidly proliferating cells." Science **329**(5998): 1492-1499.
Vaughan, T. L., L. M. Dong, et al. (2005). "Non-steroidal anti-inflammatory drugs and risk of neoplastic progression in Barrett's oesophagus: a prospective study." Lancet Oncol **6**(12): 945-952.
Wang, X., H. Ouyang, et al. (2011). "Residual embryonic cells as precursors of a Barrett's-like metaplasia." Cell **145**(7): 1023-1035.
Warburg, O. (1956). "On the origin of cancer cells." Science **123**(3191): 309-314.
Warburg, O., F. Wind, et al. (1927). "The Metabolism of Tumors in the Body." The Journal of general physiology **8**(6): 519-530.
Weinhouse, S. (1956). "On respiratory impairment in cancer cells." Science **124**(3215): 267-269.
Weinhouse, S. (1967). "Glycolysis, respiration, and enzyme alterations in rat liver neoplasia." Science **158**(3800): 537.
Weinhouse, S. (1976). "The Warburg hypothesis fifty years later." Zeitschrift fur Krebsforschung und klinische Onkologie. Cancer research and clinical oncology **87**(2): 115-126.

Yen, C. J., J. G. Izzo, et al. (2008). "Bile acid exposure up-regulates tuberous sclerosis complex 1/mammalian target of rapamycin pathway in Barrett's-associated esophageal adenocarcinoma." Cancer research **68**(8): 2632-2640.
Yousef, F., C. Cardwell, et al. (2008). "The incidence of esophageal cancer and high-grade dysplasia in Barrett's esophagus: a systematic review and meta-analysis." Am J Epidemiol **168**(3): 237-249.
Zhong, H., A. M. De Marzo, et al. (1999). "Overexpression of hypoxia-inducible factor 1alpha in common human cancers and their metastases." Cancer research **59**(22): 5830-5835.
Zhong, H., N. Mabjeesh, et al. (2002). "Nuclear expression of hypoxia-inducible factor 1alpha protein is heterogeneous in human malignant cells under normoxic conditions." Cancer letters **181**(2): 233-238.
Zu, X. L. and M. Guppy (2004). "Cancer metabolism: facts, fantasy, and fiction." Biochemical and biophysical research communications **313**(3): 459-465.

CHAPTER 1

BARRETT'S ESOPHAGUS CELL LINES DISPLAY THE WARBURG EFFECT WITH ACTIVE MITOCHONDRIA AND THE CRABTREE EFFECT

Suchorolski, MT, Paulson TG, Sanchez CA, Hockenbery D, Reid BJ

ABSTRACT:

Background:

Increased glycolysis is a hallmark of cancer metabolism, yet relatively little is known about this phenotype at premalignant stages of progression. Periodic ischemia occurs in premalignant Barrett's esophagus (BE) due to tissue damage from chronic acid-bile reflux and may select for early adaptations to hypoxia, including upregulation of glycolysis.

Methodology/Principal Findings:

We compared metabolic rates of glycolysis and oxidative phosphorylation in four cell lines derived from patients with the premalignant condition Barrett's esophagus (CP-A, CP-B, CP-C and CP-D) in response to metabolic inhibitors and changes in glucose concentration. We report that cell lines derived from the dysplastic Barrett's esophagus have up to two-fold higher glycolysis compared to a cell line derived from non-dysplastic tissue; however, the dysplastic lines preserve active mitochondria. In response to the glycolytic inhibitor 2-deoxyglucose, the most glycolytic cell lines (CP-C and CP-D) had the greatest suppression of extra-cellular acidification, but were able to compensate with upregulation of oxidative phosphorylation. In addition, these cell lines showed the lowest compensatory increases in glycolysis in response to mitochondrial uncoupling by 2,4-dinitrophenol. Finally, these cell lines also upregulated their oxidative phosphorylation in response to glucose, demonstrating an elevated Crabtree effect.

Conclusions/Significance:

Our findings suggest that cells from premalignant Barrett's esophagus tissue may adapt to an ever-changing selective microenvironment by increasing energy metabolic pathways typically associated with cancer cells.

BACKGROUND:

Two well-known differences in energy metabolism have been shown to exist between normal and cancer cells: the Warburg and Crabtree effects. In 1927, Otto Warburg discovered that cancer cells produce twice as much ATP as normal cells through glycolysis, even in oxygenated tissue (Warburg, Wind et al. 1927). Warburg also measured reduced oxygen consumption in several cancers and postulated that mitochondria were damaged (Warburg 1956). This hypothesis was later contested, as non-glycolytic cancers were also discovered (Weinhouse 1956) and it was found that even in primarily glycolytic tumors mitochondria were essential for

proliferation and metastasis (Zu and Guppy 2004; Berridge, Herst et al. 2010). Although mitochondria have been traditionally studied as sources of cellular energy, these organelles also provide vital biosynthetic, anabolic and apoptotic functions, some of which are altered in cancer cells (Frezza and Gottlieb 2009). Cancer cells have been shown to be different from normal cells by reversibly down-regulating their oxygen consumption in response to increases in glucose: the Crabtree effect (Crabtree 1929). Both of these metabolic effects are thought to be protective and contribute to cancer cell survival in a dynamic environment periodically experiencing hypoxia (Diaz-Ruiz, Rigoulet et al. 2011). Given that hypoxia and glycolytic adaptation is common in a large variety of cancers, these metabolic adaptations in cancer have been targeted for therapy; however clones refractory to treatment may evolve from the clonal heterogeneity in cancers. (Chen, Lu et al. 2007). Although the Warburg and Crabtree effects have been well characterized in cancer cells for nearly a century, their role in premalignant conditions, which are less likely to develop resistance, have not been closely investigated.

Barrett's esophagus (BE) is a premalignant condition in which intestinal metaplasia replaces normal esophageal squamous epithelium and is associated with an increased risk of esophageal adenocarcinoma (EA) (Cook, Wild et al. 2007). BE is a unique model for investigating neoplastic progression *in vivo* because periodic endoscopic surveillance is recommended in BE patients for early detection of cancer, allowing intermediate stages of intestinal metaplasia to be characterized and monitored at regular intervals (Levine and Reid 1992; Wang and Sampliner 2008). While a panel of biomarkers, including 9pLOH, 17pLOH, tetraploidy, and aneuploidy provide a method for predicting BE patient progression to cancer (RR = 38.7; 95% CI 10.8-138.5, $p < 0.001$)(Galipeau, Li et al. 2007), little is known about the state of energy metabolism in BE. hTert immortalized BE cell lines containing similar genomic alterations to primary biopsies *in vivo* have been derived from primary premalignant tissue at different stages of progression and provide an opportunity to study cellular metabolism of premalignant lesions *in vitro* (Palanca-Wessels, Barrett et al. 1998).

BE develops as an adaptation to the erosive environment of acid-reflux with periodic hypoxic events due to ulceration and ischemia(Baatar, Jones et al. 2002). Given that esophageal adenocarcinoma (EA) has been shown to display the Warburg effect (Taylor, Smith et al. 2009). premalignant BE cells may be subject to selective pressure to adapt to variable oxygen and glucose concentrations before progression to EA. Although BE rarely displays levels of glucose flux that can be detected by positron emission tomography (PET) (Neto, Zhuang et al. 2001), Georgakoudi et al have successfully discriminated localized regions of BE from normal tissue by fluorescent tissue imaging of regions with elevated NADH/NADPH levels, characteristic of hypoxic tissue (Georgakoudi, Jacobson et al. 2002). Several markers of hypoxia, including HIF-2α and VEGF, have been reported previously in advanced BE (Lord, Park et al. 2003; Griffiths, Pritchard et al. 2007), however levels of glycolysis and oxidative phosphorylation metabolism have never been directly characterized.

Since metaplastic esophageal mucosa from individuals with BE have phenotypes suggesting selective adaptation to hypoxia we hypothesized that BE cell lines display increased glycolysis and decreased oxidative phosphorylation, and that glycolytic BE cell lines display the Crabtree effect. To test our hypotheses, we compared metabolic rates of glycolysis and oxidative phosphorylation in four cell lines derived from individuals with BE and measured changes in response to metabolic inhibitors and glucose concentrations. If BE cell lines representing different stages of progression to cancer have characteristic metabolic features, then it may be

possible to develop novel metabolic biomarkers for EA risk or therapeutic targets for pre-malignant stages.

MATERIALS AND METHODS:

Tissue Culture. Barrett's esophageal cell lines CP-A, CP-B, CP-C and CP-D derived from premalignant Barrett's esophagus tissue (Palanca-Wessels, Barrett et al. 1998) and adapted for serum-free growth by the Carlo Maley lab (University of California San Francisco) were cultured in keratinocyte serum-free media (KSFM) with 5ug/L human epithelial growth factor and 50mg/L bovine pituitary extract (media and supplements from Invitrogen). All cell lines except CP-A were derived from patients with metaplastic Barrett's esophagus containing high levels of genetic alterations and cell lines alterations were verified to be similar to those found in patient biopsies (Tables S1 and S2). The patient from which CP-B was derived was also diagnosed with EA. Research participants from whom the biopsies for cell lines were derived were followed in a separate longitudinal study that evaluated changes in genetic biomarkers and progression to cancer and were further characterized for nuclear and mitochondrial alterations as part of this study (Figures S1 and S2, and Table S2).

Since Barrett's epithelium is a metaplasia which is of different origin than normal esophageal squamous epithelium, there is no "normal" tissue control; therefore CRL-4001/BJ-5ta (Geron Corporation, ATCC), a genetically stable immortalized foreskin fibroblast cell line, was cultured as a control cell line in four parts of DMEM Dulbecco's Modified Eagle's Medium (Invitrogen), containing 4 mM L-glutamine and 4.5 g/L glucose, to one part of Medium 199, supplemented with 0.01 mg/ml hygromycin B (all supplements from Sigma) and 10% fetal bovine serum (Gemini Bioproducts #100-106). OE-33, an esophageal adenocarcinoma line (Health Protection Agency, UK) (Rockett, Larkin et al. 1997), was cultured as a control cancer cell line in RPMI 1640 (Invitrogen), supplemented with 2mM Glutamine (Invitrogen) and 10% fetal bovine serum (Gemini Bioproducts). Since OE-33 adhered poorly to Seahorse assay plates, assays with this cell line could not be normalized, however results of estimated assay values for this cell line were still reported (Text S1). We also investigated two cell lines derived from esophageal squamous epithelium as potential controls, but the EPC-2 cell line (from the Carlo Maley lab, UCSF) was aneuploid (data not shown) and HET-1A cell-line was transformed by SV40 T-antigen, making them unsuitable as 'normal' esophageal squamous controls (Text S1).

All cell lines were grown in a humidified 37°C incubator with 5% CO_2, and passaged upon reaching 50-80% confluency, once to twice weekly. To minimize over-trypsinization, passaging was performed using 0.05% Trypsin-EDTA (Invitrogen).

Several esophageal adenocarcinoma cell lines in existing cell banks have been reported to be contaminated and/or mis-identified (Boonstra, van Marion et al. 2010). We therefore confirmed that the cell line DNA matched the normal DNA from each of the individuals from whom the BE cell lines were originally derived using the AmpFlSTR Identifiler kit (Applied Biosystems). In addition, we evaluated the cell lines by DNA content flow cytometry. Cell cultures were confirmed to be free of mycoplasma by MycoSensor PCR kit (Stratagene). Cell lines were refreshed from stock after 20 passages, or upon detection of changes in DNA content.

Seahorse XF24 metabolic measurements. The Seahorse XF24 flux analyzer (Seahorse Bioscience Inc, North Billerica, MA, USA) is capable of simultaneously measuring changes in pH and oxygen levels from cells seeded on 24-well plates. Extracellular acidification rates (ECAR), representative of glycolysis, and oxygen consumption rates (OCR), representative of oxidative phosphorylation, were measured on the Seahorse XF24. Since carbon dioxide produced by cells also acidifies the culture medium, glycolysis accounts for approximately 80% of the ECAR, and has been shown to be consistent with the amount of lactate measured in cells (Wu, Neilson et al. 2007; Xie, Valera et al. 2009).

Two days prior to seeding Seahorse plates, cell lines were passaged and seeded at cell densities that produce 50-70% confluency and consistent rates of proliferation. Prior to harvesting and re-seeding, the cell confluency was visually inspected.

Since ECAR and OCR measurements with the Seahorse instrument are confined to the media beneath the fluorescent sensors, localized differences in cell density contribute to noise in the Seahorse assay. Thus, consistent cell seeding is critical to minimize measurement noise. Optimal cell densities were established for Seahorse plates by plating two seeding densities for each cell line and determining well-to-well variability in ECAR and OCR. Since ECAR and OCR were highly reproducible for each seeding density, to avoid the potential for over-growth, the lower of the two seeding densities was determined to be optimal. To plate cells for Seahorse measurement, cells were concentrated in 100µl medium specific to the cell line (described in Tissue Culture methods) and gently seeded with a pipette tip positioned at a 45-degree angle into 24-well Seahorse culture plates (Seahorse Bioscience Inc, part #100777-004). Three hours later, cells had adhered to the wells and 150µl of medium was added. After overnight growth, medium was replaced with buffer-free Seahorse assay medium: Dulbecco's Modified Eagle's Medium (Sigma Product #D5030) supplemented with 5mM glucose, 2mM glutamine, 10mg/L phenol red and 1.85g/L NaCl. The plates were equilibrated for one hour in a 37°C room-air incubator and sensors calibrated in calibration solution (Seahorse Bioscience Inc, part #100840-000). The plates were then evaluated on the Seahorse XF24. Five consecutive measurements were obtained on each well, however since the initial measurement was consistently greater than two standard deviations different in OCR from the subsequent measurements, it was discarded. Outlier data from wells that produced two-fold or greater increases in ECAR or OCR standard deviation when pooled were excluded from the analysis, since noisy sensors or poor signal from uneven seeding were suspected. Data from three to four wells per experiment were combined across at least six experiments for each cell line.

Preliminary analysis was performed using the Seahorse XF24 software (Version 1.7.0.74). Statistical analyses of differences in ECAR and OCR between cell lines were performed using ANOVA and Tukey-Kramer test on STATA software (Version 11.1, http://www.stata.com).

Response to metabolic inhibitors measurements. Glycolytic inhibition was tested with 2-deoxyglucose (2-DG), a glucose analogue that inhibits hexokinase activity in the first enzymatic step of glycolysis (Kern and Norton 1987; Dwarkanath, Zolzer et al. 2001). Changes in ECAR and OCR were measured on the Seahorse XF24 in response to addition of 2-DG in consecutive injections that produced final concentrations of 1, 10, 25 and 50mM. Five consecutive measurements were performed per well prior to and after each addition. Differences between cell line changes in ECAR and OCR at 50mM 2-DG were analyzed with ANOVA and Tukey-Kramer tests using STATA software.

2,4-dinitrophenol (2,4-DNP), a well-established protonophore and mitochondrial uncoupling agent, causes depolarization of the inner mitochondrial membrane, resulting in a dramatic arrest of ATP generation. Cell line changes in ECAR and OCR were measured on the Seahorse XF24, in response to addition of 2,4-DNP in consecutive injections that produced final concentrations 2, 20, 50 and 200μM. Five consecutive measurements were performed per well, prior to and after each addition. In most cell lines, 200μM 2,4-DNP produced a sudden collapse of OCR below baseline levels, indicating toxicity, thus only data from 2 to 50 μM were used for further analysis. Differences between cell line changes in ECAR and OCR at 50 μM 2,4-DNP were analyzed with ANOVA and Tukey-Kramer tests using STATA software.

Crabtree effect measurements. Cell lines were cultured in Seahorse plates as described above, except glucose-free buffer-free assay medium was substituted for the standard Seahorse assay medium. Following room air and buffer-free media equilibration and sensor calibration, the plates were run on the Seahorse XF24 instrument. Cell line changes in ECAR and OCR were measured in response to addition of glucose in consecutive injections that produced final concentrations of 0.25, 0.5 and 5mM. Five consecutive measurements were obtained prior to and following each addition. Data were evaluated for inter-replicate variability as above and pooled from four experiments. Differences between cell line changes in ECAR and OCR at 5 mM glucose were analyzed with ANOVA and Tukey-Kramer tests using STATA software.

Seahorse data normalization per cell by image cytometric cell counting. Following each experiment, Seahorse assay media was replaced with 50μl freezing media (Minimal Essential Media (Gibco) with 10% DMSO (Sigma), 5% heat deactivated fetal calf serum, 5mM Hepes Buffer) and stored at -25°C. On the week of cell counting, plates were thawed, washed with PBS at room temperature, fixed with 70% ethanol for 10 minutes at 4°C, washed again with PBS and stained with 5 μg/ml DAPI. The plates were stored at 4°C in the dark until data collection. Image data were acquired using a Nikon-Ti microscopy platform equipped with a Sutter Instruments Lambda LS 300W xenon arc lamp, 360/BP40 excitation and 460/BP50 emission filters, and automated stage. Image cytometry analysis was performed using ImageJ (Version 1.45i, http://rsbweb.nih.gov/ij/index.html) with a software macro that identified and counted nuclei. In each well, cells were imaged in four separate fields of view, each located in a distinct quadrant and visually verified to contain no staining artifacts. The mean from the four fields was extrapolated to the area of the well to estimate total number of cells. ECAR and OCR values were normalized using these cell counts within the Seahorse XF24 software (Version 1.7.0.74).

BARRETT'S ESOPHAGUS CELL LINES DISPLAY HETEROGENEITY IN GLYCOLYSIS AND OXIDATIVE PHOSPHORYLATION

To determine if BE cell lines demonstrate increased glycolysis and/or decreased oxidative phosphorylation, extracellular acidification rates (ECAR) and oxygen consumption rates (OCR) were measured using the Seahorse XF24 analyzer in four BE cell lines, and a fibroblast control cell line.

ECAR in CP-D was two-fold higher than in CP-A ($p<10^{-7}$; Figure 1a and Table S6). ECAR in CP-B and CP-C were also higher than in CP-A, but only reached significance in CP-C ($p<0.001$). OCR was higher in CP-B and CP-C than in CP-A ($p<10^{-7}$ and $p<0.001$ respectively; Figure 1b and Table S6). OCR in CP-D was not found to be statistically different than in CP-A. There was no correlation found between levels of ECAR and OCR for the cell lines (R=0.288).

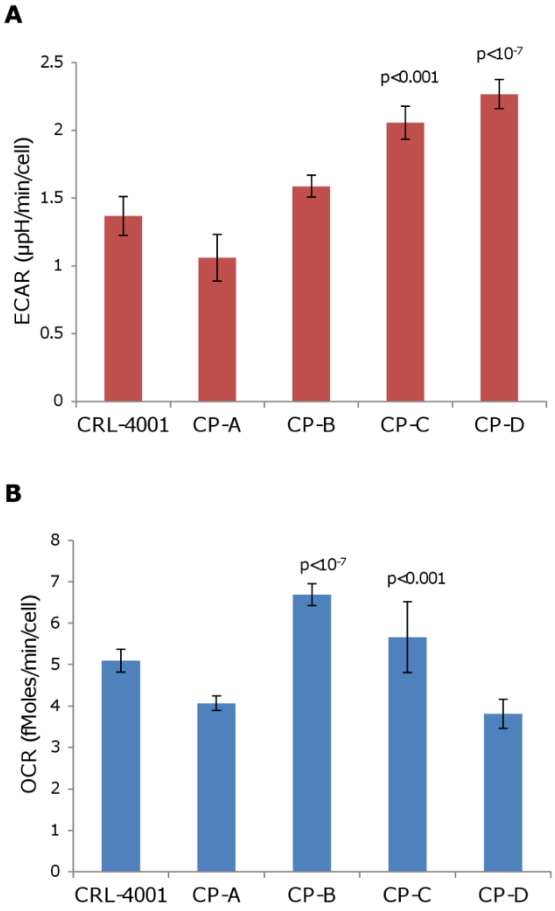

Figure 1. CP-D demonstrates a significantly elevated glycolysis than other BE cell lines. Shown above are mean measures of total (a) ECAR/cell and (b) OCR/cell. Error bars represent standard-deviation of mean between experiments (N=6-11). Each experiment consisted of 3 to 4 replicate wells per cell line with four serial measures performed on each well. p-values (Tukey-Kramer test) of statistically significant differences from CP-A are shown.

CP-D IS THE MOST SENSITIVE CELL LINE TO GLYCOLYTIC INHIBITION BY 2-DEOXYGLUCOSE, BUT COMPENSATES WITH MITOCHONDRIAL ACTIVITY

To test the effects of glycolytic inhibition on the BE cell lines, ECAR and OCR changes were measured in response to 2-deoxyglucose (2-DG), a competitive inhibitor of the glycolytic pathway. If a cell line has elevated glycolysis (such as CP-C and CP-D), a greater decrease in ECAR would be expected in response to 2-DG compared to cells that are less glycolytic. In cell lines that have functional mitochondria, OCR would also increase to compensate for the decrease in glycolytic ATP production. If OCR does not increase in response to glycolytic inhibition, then the cells would have adequate ATP production by oxidative phosphorylation alone, have dysfunctional mitochondria or are unable to oxidize alternative substrates (eg. glutamine or fatty acids). If OCR instead decreases in response to glycolytic inhibition, then the rate of oxidative phosphorylation in that cell line would likely be limited by the rate of synthesis of pyruvate or other mitochondrial substrates.

In response to 2-DG, ECAR decreased more in CP-C and CP-D than in CP-A ($p<10^{-4}$ and $p<10^{-7}$ respectively; Figure 2a,c and Table S7). In response to 2-DG, OCR increased more in CP-D compared to other BE cell lines ($p<0.01$; Figure 2b,d and Table S7).

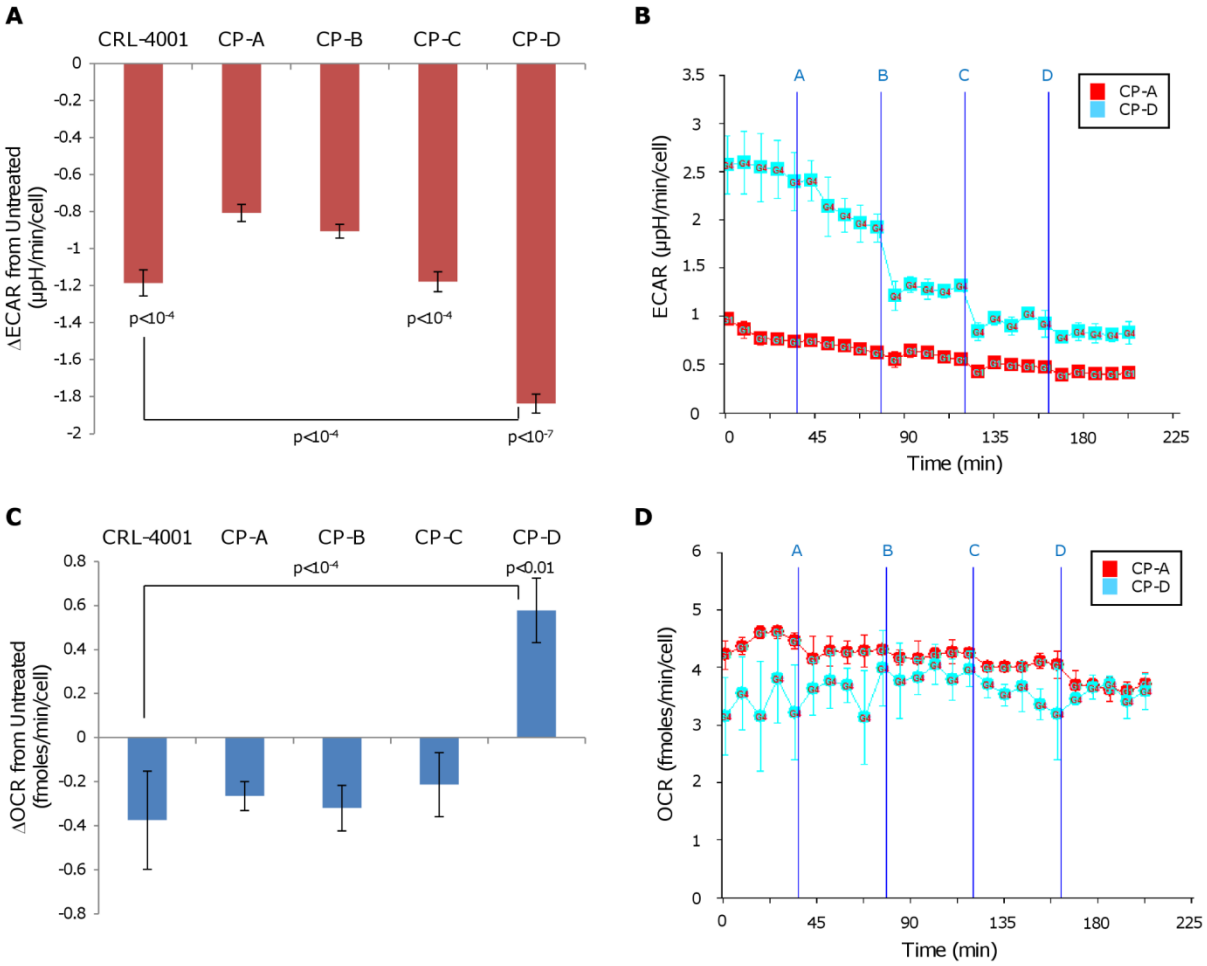

Figure 2. CP-D displays a greater OCR and ECAR response to glycolytic inhibition than other cell lines. Following addition of 50mM 2-DG, total (a) ECAR and (c) OCR were measured on the Seahorse XF24 analyzer for each cell line and changes versus untreated baseline are plotted. Error bars represent standard-deviation of means between experiments (N=2-4). Each experiment consisted of 3-4 replicate wells per cell line with four serial measures performed on each well. p-values (Tukey-Kramer test) of statistically significant differences from CP-A are shown, or between cell lines indicated by bars. Representative measurements of (b) ECAR and (d) OCR are shown in response to consecutive addition of 2-DG resulting in final concentrations of 1, 10, 25 and 50mM, indicated at A, B, C and D respectively. Error bars represent standard deviation of 3-4 replicate wells.

CP-C AND CP-D ARE THE LEAST SENSITIVE BE CELL LINES TO MITOCHONDRIAL UNCOUPLING BY 2,4-DINITROPHENOL

CP-C and CP-D are the least sensitive BE cell lines to mitochondrial uncoupling by 2,4-dinitrophenol.

Uncoupling agents such as 2,4-dinitrophenol (2,4-DNP) dissipate mitochondrial potential that would results in an immediate arrest in ATP generation. In an attempt to restore potential, mitochondrial ATPases would consume ATP to pump protons in reverse across the inner mitochondrial membrane. As a result of these two events, uncoupled cells would rapidly deplete their ATP levels and upregulate glycolysis to compensate. Since glycolytic cell lines are known to have greater resistance to uncoupling agents and mitochondrial poisons (Harper, Antoniou et al. 2002; Suganuma, Miwa et al. 2010), we tested cell line ECAR and OCR responses to 2,4-DNP. If the cells are more glycolytic, a lower increase in ECAR would result in response to uncoupling, due to 1) lower disturbance in ATP/ADP levels since the cells are less reliant on oxidative phosphorylation and/or 2) an inability to further increase glycolysis beyond its already elevated levels. In cells having uncoupled mitochondria or a lower ADP/ATP ratio, a lower OCR increase would result upon 2,4-DNP addition, since the mitochondria are already functioning near maximum respiratory capacity.

In response to 2,4-DNP, CP-C and CP-D had a lower increase in ECAR than CP-A ($p<0.001$ and $p<10^{-7}$ respectively; Figure 3a,c and Table S8). In response to 2,4-DNP, CP-B and CP-D had a higher increase in OCR than CP-A ($p<10^{-7}$ and $p<0.05$ respectively; Figure 4b,d and Table S8).

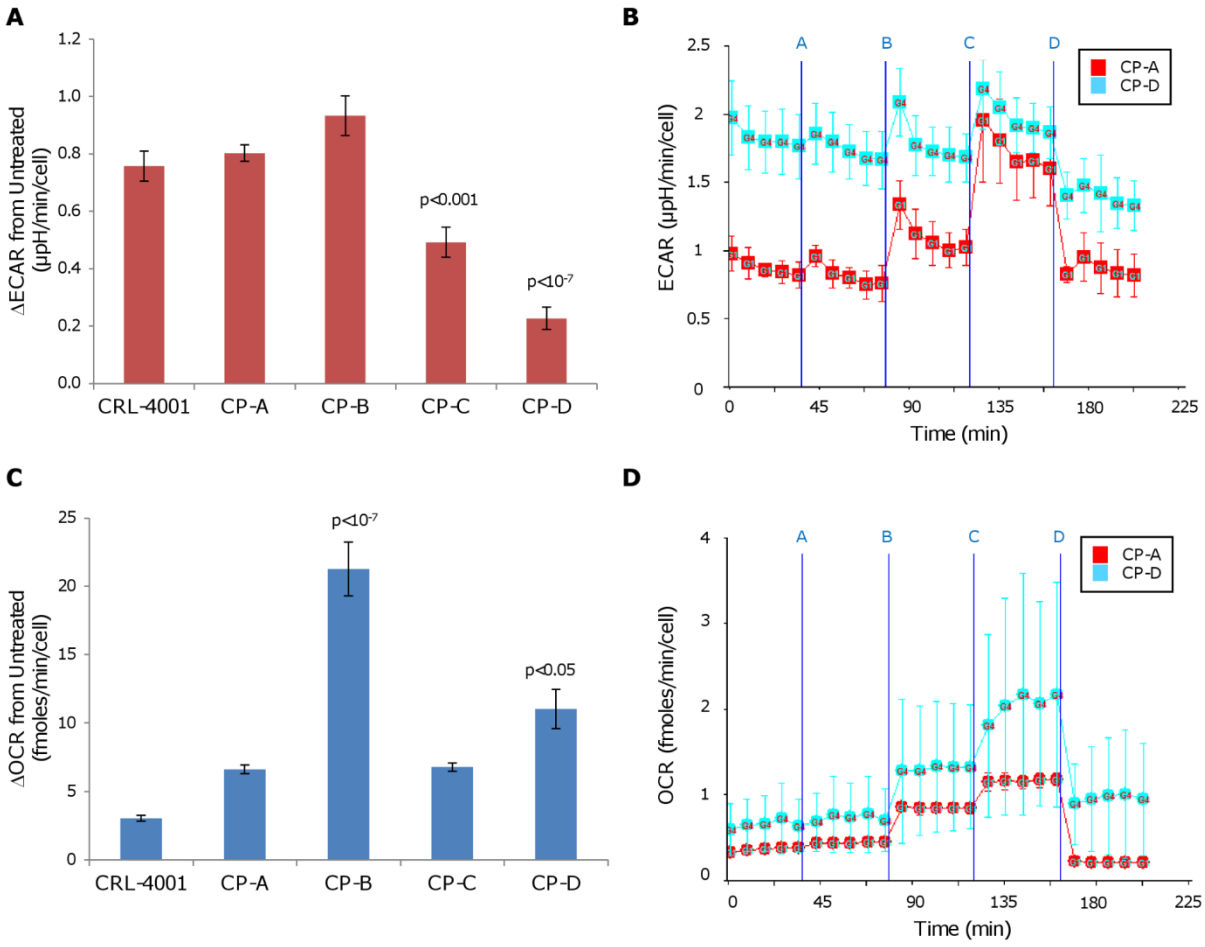

Figure 3. CP-C and CP-D display a lower ECAR increase after mitochondrial uncoupling than other cell lines. Following addition of 50μM 2,4-DNP, total (a) ECAR and (c) OCR were measured on the Seahorse XF24 analyzer for each cell line and changes versus untreated baseline are plotted. Error bars represent standard-deviation of means between experiments (N=2-4). Each experiment consisted of 3-4 replicate wells per cell line with four serial measures performed on each well. p-values (Tukey-Kramer test) of statistically significant differences from CP-A are shown. Representative measurements of (b) ECAR and (d) OCR are shown in response to consecutive addition of 2,4-DNP resulting in final concentrations of 2, 20, and 50μM, indicated at A, B, C and D respectively. Error bars represent standard deviation of 3-4 replicate wells.

CP-C AND CP-D CELL LINES HAVE A GREATER MODULATION OF OCR VIA THE CRABTREE EFFECT

The Crabtree effect decreases oxidative phosphorylation in response to increasing glucose concentration and allows cancer and proliferating cells to adjust their energy metabolism depending on substrate availability. Since some BE cell lines displayed upregulated glycolysis while maintaining the ability to upregulate oxidative phosphorylation, we tested whether glycolytic cells displayed the Crabtree effect, another phenotype associated with progression to cancer.

In response to increased glucose concentrations from 0mM to 5mM, OCR decreased more in CP-C and CP-D than in CP-A ($p<10^{-7}$ and $p<10^{-6}$, respectively; Figure 4b,d). With the same treatment, ECAR increased more in CP-C than in CP-A ($p<10^{-7}$; Figure 4a,c and Table S9). ECAR in CP-D also increased more than in CP-A, but was not statistically significant ($p<0.12$).

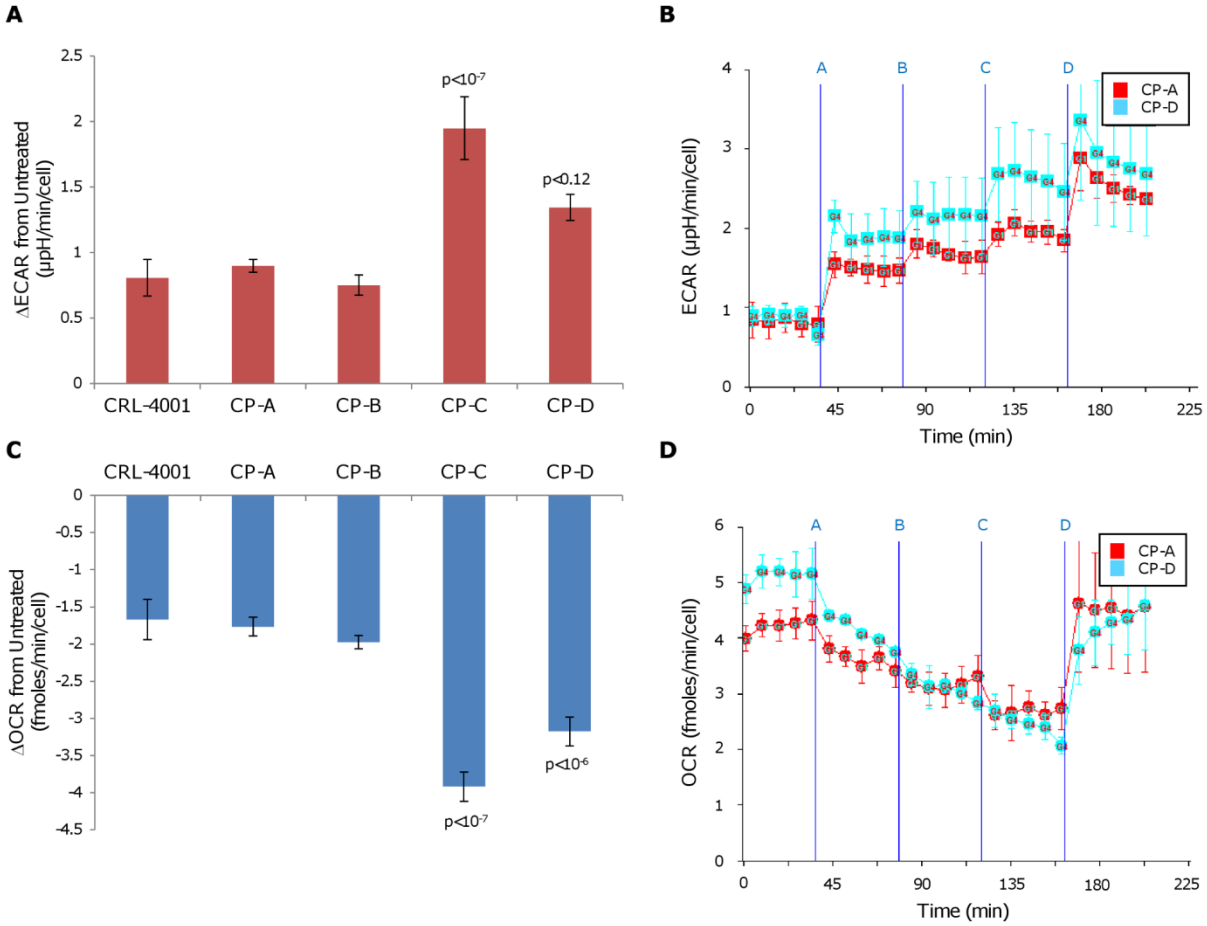

Figure 4. CP-C and CP-D demonstrate a stronger Crabtree effect response than other cell lines. Following the increase of glucose concentration in media from 0mM to 5mM, total (a) ECAR and (c) OCR were measured on the Seahorse XF24 analyzer for each cell line and changes versus untreated baseline are plotted. Error bars represent standard-deviation of means between experiments (N=2-4). Each experiment consisted of 3-4 replicate wells per cell line with four serial measures performed on each well. p-values (Tukey-Kramer test) indicating significant differences from CP-A are shown. Representative measurements of (b) ECAR and (d) OCR are shown in response to consecutive addition of glucose resulting in final concentrations of 0.25, 0.5 and 5mM, indicated at A, B, and C. CCCP (an uncoupling agent similar to 2,4-DNP) was added at D to verify that mitochondria remained functional despite a drop in OCR following glucose addition.

DISCUSSION:

This study provides the first evidence that cell lines derived from the premalignant dysplastic Barrett's esophagus have increased glycolysis while preserving mitochondrial function. Furthermore, we found these cell lines modulate their oxidative phosphorylation with an elevated Crabtree effect. Both of these phenotypic alterations are hallmarks of cancer metabolism and suggest that BE cell lines likewise are able to rapidly adapt their energy metabolism in response to variable nutrient levels.

We found that ECAR was highest in the three BE cell lines derived from patients with the highest genomic instability (CP-B, CP-C and CP-D) and lowest in the cell line derived from a patient with relatively more stable genome (CP-A), suggesting that a glycolytic phenotype is selected during the process of neoplastic progression. In addition, CP-D is more glycolytic than the other BE cell lines, confirmed by its greatest ECAR decrease following 2-DG addition and lowest ECAR increase following 2,4-DNP addition. However, mitochondrial function is conserved during CP-D's "glycolytic switch" since it is able to compensate for glycolytic inhibition by upregulating oxidative phosphorylation. Although CP-B and CP-C are more glycolytic than CP-A, they also display a high level of oxidative phosphorylation and are therefore more resistant to glycolytic inhibition than CP-D. However, ECAR in CP-C (but not in CP-B) is also more resistant to uncoupling by 2,4-DNP than CP-A due to increased glycolysis in CP-C.

OCR in the BE cell lines does not correlate with ECAR, resulting in heterogeneous responses to metabolic inhibitors. The lack of OCR increase in CP-A, CP-B and CP-C cell lines in response to glycolytic inhibition suggests that ATP/ADP levels do not fall below a threshold that would stimulate mitochondrial activity, since oxidative phosphorylation supplies the majority of energy in these cell lines. Likewise, in response to 2,4-DNP, OCR increases were not significantly different in CP-A and CP-C, and marginally higher in CP-D, suggesting that their mitochondria maintain a similar level of mitochondrial coupling. This was also confirmed in an independent experiment in which oligomycin-treated BE cells had similar percentage OCR decreases (Supplemental Materials Table S6). CP-B, the BE cell line displaying the highest OCR, also displayed the highest OCR increase in response to 2,4-DNP, indicating that this cell line has the highest level of mitochondrial coupling or utilizes different mitochondrial substrates. Despite evidence that suggest mitochondrial differences between the BE cell lines, mitochondrial mass and potential assessed by flow cytometric assays were not found to be different (Supplemental Materials Figures S2 and S3).

Finally, CP-C and CP-D cell lines demonstrate a greater change in OCR via Crabtree effect than the less glycolytic CP-A and CP-B cell lines, further suggesting adaptation towards a more cancer-like phenotype. Increased Crabtree effect predicts a greater survival advantage to BE cells by allowing them to adapt to conditions where glucose fluctuates, such as during periodic ulceration or ischemia.

Difficulties associated with OE-33 cell adhesion prevented normalization of data collected for this EA cell line for direct comparison to the BE cell lines. However, based on normalization estimated from a limited set of wells, OE-33 had the highest levels of ECAR out of the cell lines tested and had percent ECAR that decreased as much as CP-D following 2-DG addition, indicating that it is a significantly glycolytic cell line (Supplemental Materials Section S3). OE-33 also had the highest levels of OCR and was sensitive to oligomycin, indicating a glycolytic cell

line with functionalmitochondria. Finally, OE-33 had OCR upregulated less than CP-A following 2,4-DNP addition and a lower mitochondrial potential (Supplemental Materials Figure S3) than any of the BE cell lines, suggesting partially uncoupled mitochondria. Altogether, OE-33 appears to be a cancer cell line with increased glycolysis and oxidative phosphorylation, but with some mitochondrial inefficiency.

Given our findings, we propose a model in which BE begins with a metabolism which is largely dependent on oxidative phosphorylation, as seen in CP-A, but then progresses through a metabolic phenotype which is intermediate between normal and cancer (Figure 6). This intermediate stage consists of increases in glycolysis while mitochondria remain functional. As the cells progress, later stages of BE display a Crabtree effect which is more responsive to substrate, which enables mitochondrial downregulation while increasing glycolysis. Mitochondrial activity and uncoupling subsequently increase as the tissue progresses to EA.

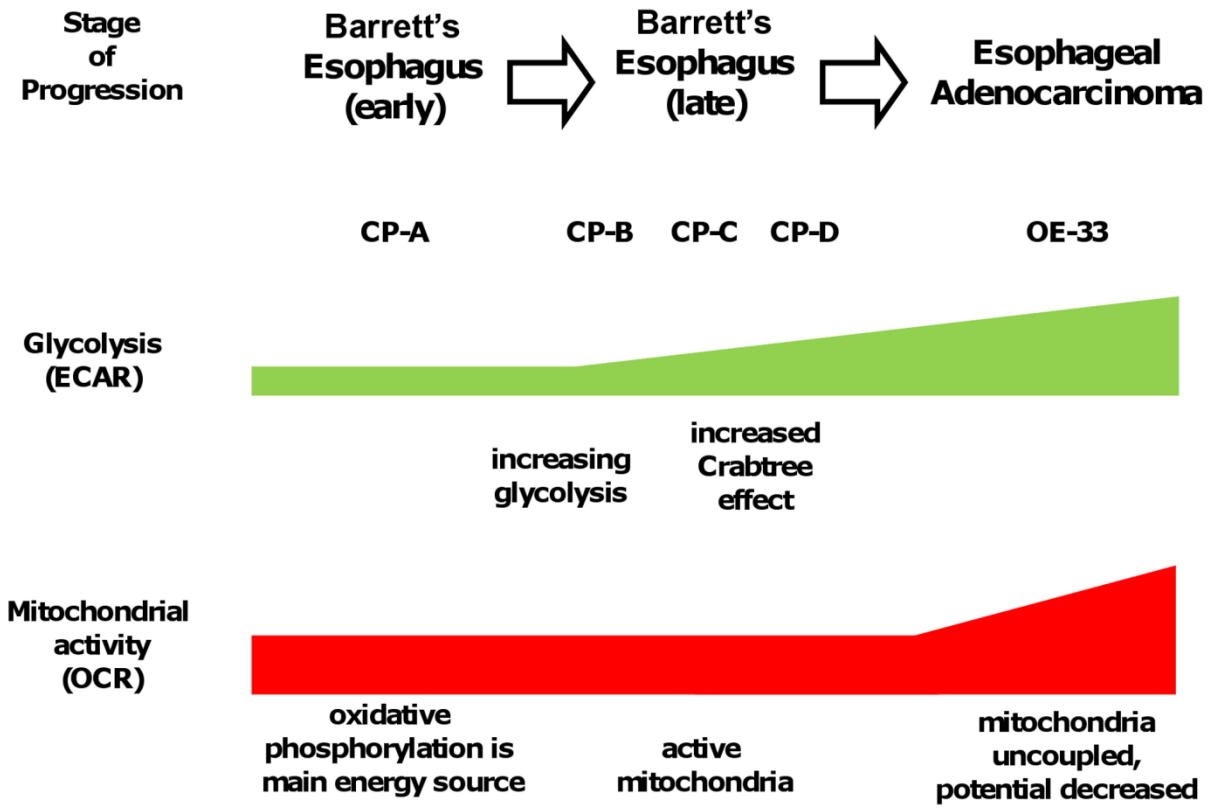

Figure 5. Barrett's esophagus progression involves an intermediate metabolic stage with increased glycolysis and functional mitochondria. Early BE cells (e.g. CP-A), rely mainly on mitochondrial oxidative phosphorylation for energy needs prior to the glycolytic increase which occurs in late BE cells (CP-B, CP-C and CP-D), which demonstrate elevated ECAR (all) and the Crabtree effect (CP-C and CP-D). Finally in adenocarcinoma (OE-33) mitochondrial uncoupling occurs with increased OCR and glycolysis.

Several mechanisms are likely to contribute to the metabolic changes in the BE cell lines. p53 has both copies mutated and/or altered in CP-B, CP-C and CP-D (Supplemental Materials Table S2) and has been reported to upregulate glycolysis and downregulate mitochondrial activity to produce the Warburg effect in several cell lines (Bensaad, Tsuruta et al. 2006; Matoba, Kang et

al. 2006). Notably the p53-wild type BE cell line, CP-A, which is more representative of the genotype of BE patients that do not progress to cancer, demonstrated lower levels of glycolysis. A number of hypoxia-response genes have also been reported in BE tissue: glucose transporter Glut-1 (Younes, Ertan et al. 1997), known to be associated with elevated glycolysis, vascular endothelial growth factor (VEGF), and erythropoietin (Griffiths, Pritchard et al. 2007), which are upregulated by hypoxia-induced transcription factors HIF-1α and HIF-2α respectively. The genomic analysis performed in our study revealed that CP-D has a single copy of HIF-1α, however, the condition of the remaining allele is unknown (Supplemental Materials Table S3). CP-D was also found to contain an amplified PHDGH gene (Human Cancer Genome Atlas), which is related to serine biogenesis and suggests an alternate use of the upregulated glycolytic pathway in this cell line (Possemato, Marks et al. 2011). The identification of a glycolytic phenotype in BE should bring to attention the increased importance of glycolytic and hypoxia-resistance genes, which are routinely investigated in cancers but may also become altered earlier in progression.

Since endogenous reactive oxygen species (ROS) are produced by mitochondria, the mitochondrial genome is particularly susceptible to ROS-mediated damage. Although CP-A has the fewest nuclear genome alterations, it displays the most mitochondrial genome mutations of all the cell lines (Supplemental Materials Figure S1 and Table S4). Most of the CP-A mutations are heteroplasmic which suggests a higher number of different clones present. However, this diversity may also indicate that the predominantly oxidative phosphorylation metabolism in this cell line generates higher ROS levels, consistent with findings by Chen et al (Chen, Izzo et al. 2009). Remarkably, we found that the cell line displaying the most nuclear genomic alterations, CP-D, had the fewest number of mitochondrial genome mutations (Supplemental Materials Table S4), suggesting that it is effective at suppressing ROS in the mitochondria and/or has undergone a mitochondrial genetic sweep event.

Although the Warburg and Crabtree effects have been commonly associated with cancer progression, higher glycolysis and Crabtree effect have also been observed in actively replicating non-cancerous cells, such as stem cells and lymphocytes (Crabtree 1929; Vander Heiden, Cantley et al. 2009). Since BE is a tissue responsible for repeatedly healing damaged epithelium, higher rates of growth in this tissue could be promoted by elevated glycolysis providing higher levels of anabolic substrates and NADPH, an important cofactor responsible for glutathione regeneration which suppresses ROS. Chen et al reported that CP-C had lower toxicity than CP-A to exogenous ROS species, although glutathione levels were not different (Chen, Izzo et al. 2009) and toxicity may be due to CP-A's more sensitive wild type p53, which has intact apoptotic signaling. Although we did not study ROS levels in the BE cell lines, altering metabolism may be a mechanism for preventing higher levels of mutation during BE progression. Interestingly of the patients that produced biopsies that produced cell lines, the patient from whom the most mitochondrially active BE cell line (CP-B) was derived was the only patient in which EA was detected.

Given the preliminary nature of our findings, it is important to determine if the metabolic changes found in BE cell lines are also found in patient lesions. Although tissue culture is clearly an artificial model system, all of the metabolic measurements of ECAR and OCR were done at confluency, similar to the structure of cells in tissue. Also, the BE cell lines in this study are immortalized using hTERT, avoiding potential metabolic effects of other immortalization methods that affect p53 or Myc activity such as SV40 large T antigen. However, since the BE

and EA cell lines used in this study are derived from different patients, further analysis of longitudinally collected samples within the same patient would more directly address these questions. The most promising support for our findings *in vivo* are from BE tissue quantitative fluorescent imaging which displays elevated NAD(P)H levels representative of glycolytic tissue (Georgakoudi, Jacobson et al. 2002), suggesting that our observation in BE cell lines may translate to BE segments in patients.

SUPPLEMENTAL MATERIALS:

Text S1: BE and control cell line background and characterization.

BE cell lines. The BE cell lines were previously shown to contain the same genetic lesions as BE segments of patients from whom the lines were derived (Palanca-Wessels, Barrett et al. 1998). CP-A is the only cell line derived from an individual without dysplasia and contains a wild-type p16 and p53 (Supplemental Materials Table S1). CP-B, CP-C and CP-D cell lines were derived from patients with high grade dysplasia; all contain bi-allelic p16 or p53 alterations and have greater genomic aberrations, with CP-D displaying the most genetic instability and multiple aneuploid sub-populations. Cell lines were started at low passage numbers indicated in Table S1 to avoid development of extra aneuploid sub-populations, and were refreshed from stock after 20 passages, or upon detection of changes in DNA content.

The research participant from whom the CP-A cell line was developed never developed high-grade dysplasia or esophageal adenocarcinoma and has been active in the Seattle Barrett's Esophagus study for 21 years. The research participant from whom the CP-B cell line was developed had esophageal adenocarcinoma detected during the same endoscopy and 1cm below the level of the biopsy that produced the cell line. The research participant from whom the CP-C cell line was developed was followed with high-grade dysplasia for 6.3 years and opted for an esophagectomy for high-grade dysplasia and died of mesothelioma 11.9 years later. The research participant from whom the CP-D cell line was developed was followed with high-grade dysplasia for 8.3 years and died of natural causes (pneumonia) 9.6 years later.

Genetically stable control cell line. As potential esophageal squamous control cell lines, we considered cell lines EPC-2 and HET-1A. EPC-2, an esophageal squamous cell line was initially proposed as a normal cell line control since it was reported to have wild-type p16 and p53 loci (Harada, Nakagawa et al. 2003). However, the cell line that was provided from the Carlo Maley lab (UCSF) was abandoned after it was found to be aneuploid by flow cytometric DNA content quantitation (data not shown). HET-1A was not used since it was transformed with simian virus 40 large T-antigen, which inhibits Rb and p53 activity, a modulator of glycolytic and oxidative phosphorylation in cells (Matoba, Kang et al. 2006). Recently, HET-1A has also been reported to form irregular dysplastic epithelial organotypic culture by Underwood et al (Underwood et al, 2010), further indicating that this cell line is not suitable as a normal esophageal control.

Since an esophageal squamous control cell line was not available, in this study we decided to use CRL-4001/BJ-5ta, a genetically stable hTERT-immortalized foreskin fibroblast cell line, which is guaranteed by ATCC to display genetic stability for up to ten passages (Geron Corporation, ATCC). Although it has been shown that fibroblasts and keratinocytes typically display different energy metabolism characteristics (Hornig-Do, von Kleist-Retzow et al. 2007), this cell line was used as an inter-experimental control due to its genetic stability, and it remained phenotypically consistent across our experiments.

Adenocarcinoma cell line. OE-33 was established from a Barrett's associated adenocarcinoma of the distal esophagus and was chosen as an adenocarcinoma cell line control in this study (Nishihira, Hashimoto et al. 1993). OE-33 is a hyperploid p53-inactive cell line with high mitotic index and was recently authenticated by Boonstra et al (Boonstra, van Marion et al. 2010; Fichter, Herz et al. 2011).

Difficulties associated with cell adhesion prevented normalization of the EA cell line OE-33 and direct comparison to the BE cell lines. However based on cell counts obtained from a limited set of wells, we estimate that OE-33 was the most glycolytic out of the cell lines tested with ECAR up to four-fold higher compared to the other cell lines (4.1 μpH/min/cell). It also had the highest levels of oxidative phosphorylation with OCR five-fold higher compared to the other cell lines (27.6 fmol/min/cell). This higher OCR suggests a glycolytic cell line with 1) increased oxidative phosphorylation and/or 2) mitochondrial uncoupling. OCR in OE-33 was also highly decreased following treatment with ATPase inhibitor oligomycin, suggesting that mitochondrial are involved in ATP synthesis in this cell line.

In response to 2-DG, percent ECAR decreased in OE-33 to levels similar to CP-D, however contrary to other cell lines, OCR in OE-33 decreased suggesting that the rate of pyruvate production from glycolysis is the rate limiting step for oxidative phosphorylation in this cell line (data not shown). In response to 2,4-DNP uncoupling, OE-33's smaller increase in percent OCR than in the other BE cell lines suggests that mitochondria are already partially uncoupled (data not shown). Lower levels of mitochondrial potential in OE-33, assessed by flow cytometry, provide further evidence for uncoupling (Supplemental Materials Figure S3). Altogether, OE-33 displays characteristics of a glycolytic cancer cell line with active but partially uncoupled mitochondria. Thus, consistent with numerous other groups' findings that mitochondria maintain their function in several cancers (Vander Heiden, Cantley et al. 2009),(Dang 2010),(Berridge, Herst et al. 2010), in the EA cell line that we examined, mitochondria remained functional while glycolysis was upregulated. In response to elevated glucose, OE-33 did not have percent ECAR and percent OCR increases that were significantly different compared to CRL-4001, CP-A, or CP-B, however absolute changes in OCR were estimated to be significantly higher than in other cell lines.

Cell line	Patient Diagnosis	Genetics Summary	DNA Content	Starting Passage Number
CP-A	Negative for dysplasia	p16del/del, p53WT	2.7	33
CP-B	High-grade Dysplasia*	p16-/del, p53-/del	2.6, 4.5	26
CP-C	High-grade dysplasia	p16+/del, p53-/del	2.2, 4.4	24
CP-D	High-grade dysplasia	p16del/del, p53-/del	2.4, 3.6, 4.2	21

Table S1: Genetic characteristics of Barrett's esophagus cell lines. DNA content was characterized using flow-cytometry with DAPI staining versus chick-red blood cell internal controls. Patient diagnosis is the maximum abnormality in the Barrett's segment at the endoscopy from which the cultures were derived. Genetics summary describes alterations in the p16 and p53 loci. DNA content is compared to normal (2N) cells and in CP-D multiple hyperploid populations are indicated. Mutations in p16 and p53 were determined by Palanca-Wessels et al (Palanca-Wessels, Barrett et al. 1998). * The patient from whom CP-B was derived also had EA detected in the same endoscopy.

Text S2: Nuclear genome characterization. BE cell lines were analyzed for somatic genetic alterations (copy number alterations or copy-neutral LOH) using Illumina Omni-quad 1M SNP arrays. DNA was isolated from an early passage of each cell line as well as from constitutive normal tissue (blood or gastric tissue) from the individual from which each cell line originated. Samples were processed and hybridized according to manufacturer's protocol. Data were initially processed using Illumina Bead Studio, and regions of gain, loss and copy neutral LOH were determined using Partek Genomics Suite v6.5.

EPC-2, CRL-4001 or OE-33 were excluded from nuclear genome characterization since they did not have patient-matched normal controls.

All cell lines were previously characterized by cytogenetic analysis as having genetic instability prior to being adapted to serum-free media (Palanca-Wessels, Barrett et al. 1998). In this study, we confirmed that serum-adapted CP-B, CP-C and CP-D have the largest number of chromosomal aberrations (Fig S1).

Comparing the cell lines to patient-derived biopsies acquired at several time points, most of the alterations in genomic copy number were consistent between the cell lines and patient biopsies, with the exception of the several notable changes (Table S2). CP-B is clonally related to samples taken from the patient, similar to a clone with deleted 17p, but displays an additional loss of sequence in the 17q chromosomal region and other chromosomal alterations. Losses on chromosome 17 were not observed in most biopsies taken from this patient. Since this patient went on to cancer, this may represent inherent genetic instability in this line. CP-C is nearly identical genetically to biopsies from multiple time points in the patient, with the exception of chromosome 4 and 14. We also observed additional alterations in evolved clones *in vivo*. The differences in genetics observed between biopsies and cell lines may be due to clonal evolution and/or sampling error. Patient biopsies for CP-D were not available for comparison.

The nuclear genome loci of 30 genes of particular importance in regulating glycolysis, oxidative phosphorylation, acid transport and hypoxia resistance were investigated for copy number status (Table S3). CP-A had gain of copy number in three genes, CP-B had single copy deletions in three genes and CP-C had single copy deletions in 11 genes. Calls for CPD are difficult since by flow cytometry the cell line appears to be a mixture of a "tetraploid" population that also has some alterations with another aneuploid population that has a different subset of alterations. The tetraploid fraction is likely masking deletion events commonly seen in BE samples. In both CP-C and CP-D, hypoxia inducible factor 1-alpha (HIF-1α) has a single copy deletion. With a single HIF-1α copy remaining, the remaining allele may be subject to constitutive upregulation. HIF-1α is negatively regulated post-translationally by a family of oxygen-dependent prolyl and asparagine hydroxylases which modify residues 402, 564 and 803 for ubiquitination by Von-Hippel Lindau ubiquitin ligase which targets the protein for proteosomal degradation (Epstein, Gleadle et al. 2001; Ivan, Kondo et al. 2001; Jaakkola, Mole et al. 2001; Hewitson, McNeill et al. 2002). Modification of any of these residues would constitutively stabilize this transcription factor, causing an upregulation in target glycolysis and hypoxia-resistance genes.

Since the majority of the mitochondrial proteome is coded in the nuclear genome, we analyzed the 1023 nuclear-encoded genes in the four BE cell lines. CP-D had the most nuclear genome alterations which affect mitochondrial genes, however, since this cell line still retains mitochondrial activity these alterations do not appear to produce loss-of-function in the mitochondria (Supplemental Materials Table S4). Although there are many single-copy mutations in the nuclear-encoded mitochondrial genes, only a single double-deletion was reported: POLRMT, the DNA-directed mitochondrial RNA polymerase, in CP-B. This is the primase required for initiation of DNA synthesis from the light-strand origin of DNA replication. Since this polymerase function is vital to mitochondrial replication, another polymerase must be complementing its function by synthesizing the primer necessary for replication.

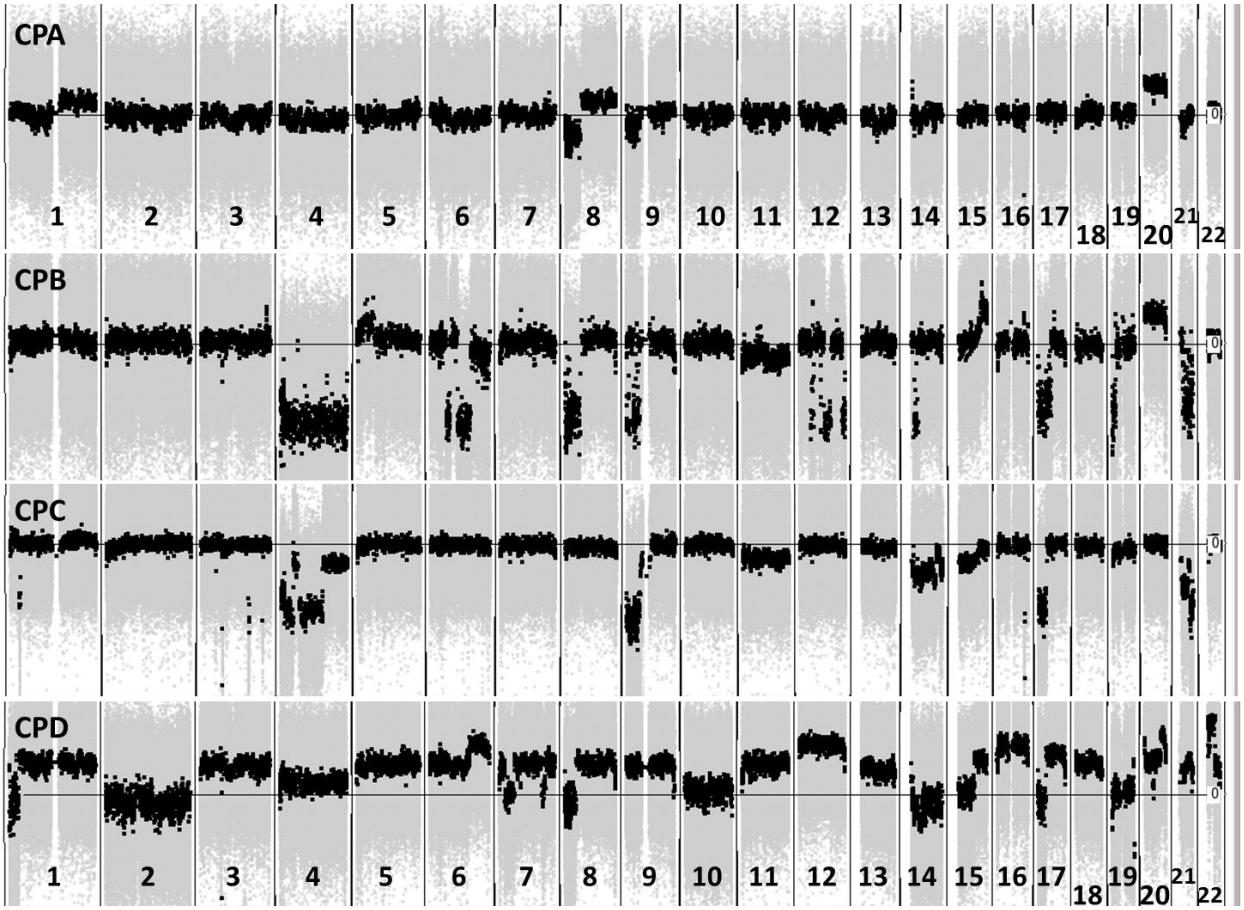

Figure S1. Barrett's esophagus cell lines CP-B, CP-C and CP-D display higher genome instability than CP-A. Genome copy number alterations, relative to normal patient-derived diploid matched control (horizontal line), were plotted for each of the cell lines. CP-B, CP-C and CP-D display a large number of chromosomal alterations, compared to CP-A. Black dots represent moving averages of copy number.

	Gene deletions				Somatic Genomic Alterations		
	p16	p53	FHIT	WWOX	CNLOH SGA (Mb)	SCNA SGA (Mb)	Combined SGA (Mb)
CPA	double deletion	Wt	double deletion	double deletion	126	229	355
CPB	single deletion	single deletion	double deletion	weak call increase in copy number	66	527	593
CPC	single deletion	single deletion	double deletion	double deletion	15	552	567
CPD	no deletion	no deletion	single deletion	single deletion	373	2067	2440

Table S2: BE cell lines display genomic alterations that confer risk of progression (p16, p53) or are genetically unstable (FHIT, WWOX). Number of somatic genome alterations (SGA) are shown categorized by type (CNLOH = copy number loss of heterozygosity, SCNA = somatic copy number alterations) and indicate the total amount of the genome affected by CNLOH or SCNA in each respective cell line.

		----------Cell line----------				
Gene function	Gene Symbol	CP-A	CP-B	CP-C	CP-D	Gene name
Glycolysis	HK1					hexokinase 1
	HK2					hexokinase 2
	LDHA			-	+	lactate dehydrogenase A
	LDHB	+			+	lactate dehydrogenase B
	LDHC			-	+	lactate dehydrogenase C
	LDHD				+	lactate dehydrogenase D
	PFKL			-	+	phosphofructokinase, liver
	PFKM				+	phosphofructokinase, muscle
	PFKP					phosphofructokinase, platelet
	PGK1				+	phosphoglycerate kinase 1
	PGK2	+	-		+	phosphoglycerate kinase 2
	PKM2				+	pyruvate kinase, muscle
	SLC2A1				+	solute carrier family 2 (facilitated glucose transporter), member 1
Regulation of	PDHA2		-	-		pyruvate dehydrogenase (lipoamide) alpha 2
Oxidative Phosphorylation	PDHB					pyruvate dehydrogenase (lipoamide) beta
	PDHX			-	+	pyruvate dehydrogenase complex, component X
	SCO2				p+	SCO cytochrome oxidase deficient homolog 2 (yeast)
Acid transporters	CA9			-	+	carbonic anhydrase IX
	CA12					carbonic anhydrase XII
	SLC9A1			p-		solute carrier family 9 (sodium/hydrogen exchanger), member 1
Hypoxia resistance	EPO				+	erythropoietin
	HIF1A			-	-	hypoxia inducible factor 1, alpha subunit
	HIF2A/EPAS1					endothelial PAS domain protein 1
	HIF3A					hypoxia inducible factor 3, alpha subunit
	P4HA1*					prolyl 4-hydroxylase, alpha polypeptide I
	P4HA2*	+			+	prolyl 4-hydroxylase, alpha polypeptide II
	P4HA3*			-	+	prolyl 4-hydroxylase, alpha polypeptide III
	VEGFA				+	vascular endothelial growth factor A
	VEGFB			-	+	vascular endothelial growth factor B
	VEGFC		-	-		vascular endothelial growth factor C
	VHL					von Hippel-Lindau tumor suppressor

Table S3: Analysis of copy number alterations of genes involved glycolysis, oxidative phosphorylation and hypoxia regulation in BE cell lines. Gene symbol is the human genome Gene Symbol for the gene. Copy number gains are marked as '+', single copy losses as '-', and gains or losses of a part of a gene locus are 'p+' or 'p-' respectively. *Note that prolyl 4-hydroxylases are inhibitors of HIF-1 mediated hypoxic resistance.

Cell line	Single-copy deletions	Double deletions	Gains	Copy-neutral loss of heterozygosity
CP-A	10	0	211	61
CP-B	174	1	33	47
CP-C	156	0	6	1
CP-D	11	0	667	113

Table S4: Summary of copy number alterations in nuclear-encoded mitochondrial genes. 1023 mitochondrial genes were characterized for deletions, gains of copy number, and copy neutral loss of heterozygosity (LOH).

Text S3: Mitochondrial genome characterization. Cell line mitochondrial genomes were assessed using MitoChip v2.0 oligonucleotide arrays from Affymetrix. Sequences were compared to matched constitutive normal samples to ensure the alterations detected were somatic changes. Since EPC-2, CRL-4001 or OE-33 did not have patient-matched normal controls, they were excluded from mitochondrial genome characterization. For cell lines, DNA was extracted by standard protocol on Qiagen columns (Germantown, MD, USA). For constitutive DNA, DNA was extracted from gastric biopsies using Qiagen columns or Gentra DNA isolation kit (Minneapolis, MN, USA). mtDNA was amplified using two sets of PCR primers and samples were quantitated, fragmented and labeled according to the MitoChip v2.0 protocol.

MitoChip data were then analyzed using Affymetrix GCOS v1.3d and GSEQ v4.1 software and the putative mutations were verified on both forward and reverse strands. Cell line alterations that were detected were compared with matched constitutive DNA. Further characterization of the location of mutations, affected mitochondrial genes, and mitochondrial haplogroup for each cell line were determined using the Mitomaster mtDNA sequence analysis program (Brandon, Ruiz-Pesini et al. 2009) (Supplemental Materials Table S5).

Multiple mtDNA mutations were detected in each of the cell lines, ranging from 2 in CP-D to 26 in CP-A (Supplemental Materials Table S5). The resequencing data from cell line CP-C indicate the presence of multiple sequences, suggesting the presence of multiple mitochondrial genomes in the cell line, representing either a mixed clonal population or mixed mitochondrial species in each cell (heteroplasmy). Having mixed clonal populations in CP-A and CP-C would explain the abundance of mutations found in these cell lines.

Cell line	Haplogroup	Mitochondrial Mutation (basepair)	Mitochondrial mutation	Gene affected
CP-A	H2	72*	(a > g)	D-Loop
		194	(t > c)	D-Loop
		1437*	(a > g)	12S ribosomal RNA
		2580	(a > g)	16S ribosomal RNA
		2705*	(a > g)	16S ribosomal RNA
		4644	(t > c)	NADH dehydrogenase subunit 0
		4767*	(a > g)	NADH dehydrogenase subunit 1
		4809	(a > g)	NADH dehydrogenase subunit 2
		5997	(t > c)	Cytochrome c oxidase subunit I
		6045	(a > g)	Cytochrome c oxidase subunit I
		6144	(a > g)	Cytochrome c oxidase subunit I
		6258	(g > a)	Cytochrome c oxidase subunit I
		7026	(c > t)	Cytochrome c oxidase subunit I
		9068	(t > g)	ATP synthase F0 subunit 6
		10596	(a > g)	NADH dehydrogenase subunit 4L
		10905	(t > c)	NADH dehydrogenase subunit 4
		11007	(t > c)	NADH dehydrogenase subunit 5
		11330	(c > t)	NADH dehydrogenase subunit 6
		11465	(a > g)	NADH dehydrogenase subunit 7
		11717*	(g > a)	NADH dehydrogenase subunit 8
		12306	(a > g)	tRNA leucine2
		12370	(g > a)	NADH dehydrogenase subunit 5
		14618	(c > t)	NADH dehydrogenase subunit 6
		14764*	(c > t)	Cytochrome b
		14864	(c > t)	Cytochrome b
		15691	(t > c)	Cytochrome b
CB-B	H1	151	(t > c)	D-Loop
		6717	(t > c)	Cytochrome c oxidase subunit I
		8243	(a > g)	Cytochrome c oxidase subunit II
		12616	(g > a)	NADH dehydrogenase subunit 6
CP-C	U	145	(t > c)	D-Loop
		152	(a > g)	D-Loop
		194	(t > c)	D-Loop
		1718	(g > a)	16S ribosomal RNA
		2180	(a > g)	16S ribosomal RNA
		3916	(g > a)	NADH Dehydrogenase subunit 1
		6219	(t > c)	Cytochrome c oxidase subunit I
		6369	(c > t)	Cytochrome c oxidase subunit I
		12649	(g > a)	NADH dehydrogenase subunit 7
		12703	(c > t)	NADH dehydrogenase subunit 8
		13964	(a > g)	NADH dehydrogenase subunit 9
		14468	(t > c)	NADH dehydrogenase subunit 5
		14770	(c > t)	Cytochrome b
		15312	(g > a)	Cytochrome b
		16221	(c > t)	D-Loop
		16253	(g > a)	D-Loop
		16276	(c > t)	D-Loop
		16292	(c > t)	D-Loop
CP-D	H1	256	(a > g)	D-Loop
		476	(t > c)	D-Loop

Table S5. Summary of mitochondrial mutations in BE derived cell lines. Nucleotides for mutation locations and Haplogroup designation based upon data from Mitomaster mitochondrial mutation database and analysis tool (Brandon, Ruiz-Pesini et al. 2009). * indicates mutations that share their location with a known human mitochondrial polymorphism.

Text S4: Mitochondrial mass measurements by flow cytometry. All cell lines were grown to 50-70% confluency and harvested with 0.05% trypsin. Cells were centrifuged at 100g for six minutes and resuspended in KSFM media (Invitrogen) to a concentration of 4 million cells/ml. Cells were then diluted 1:2 and stained for 30 minutes at 37°C in a staining solution containing final concentrations of 10nM mitotracker green, 10µM Hoechst 33342 and 5µM Sytox Orange (all dyes from Invitrogen). Samples were measured by flow cytometry on the Beckton-Dickinson LSR-2 instrument. Dead cells were gated out using Sytox Orange, and were less than 0.1% for each cell line. Analysis was performed using FlowJo software (Treestar, Ashland, OR) on whole-cell and G1-phase fractions that were gated using the Hoechst 33342 cell cycle profile.

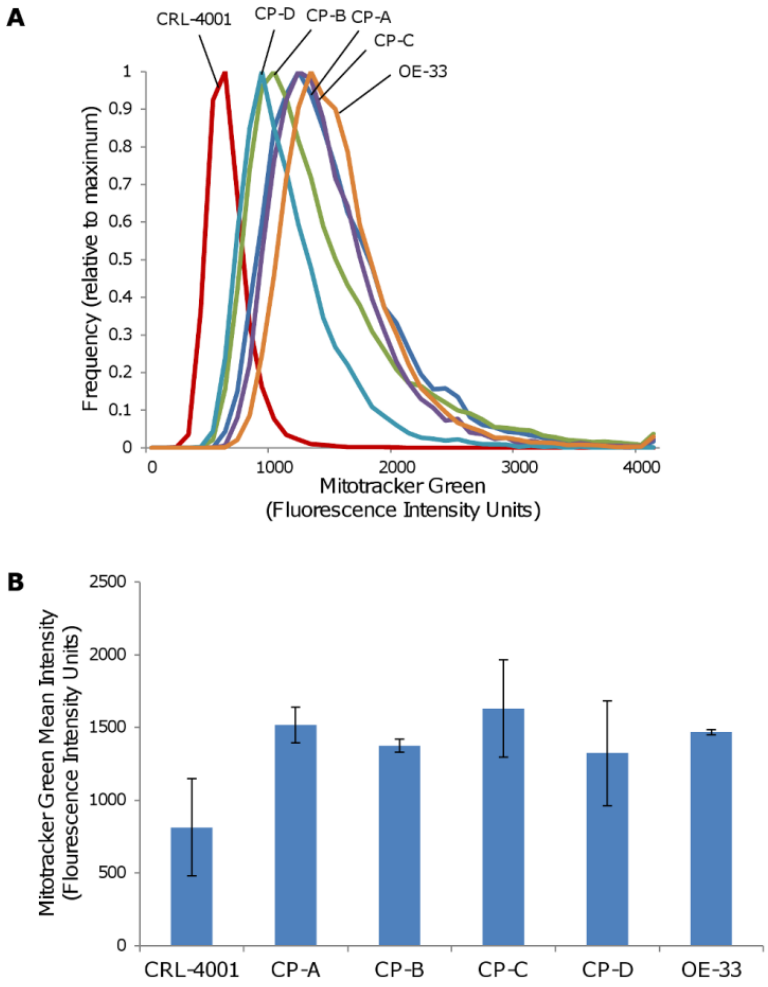

Figure S2. Barrett's esophagus cell lines are not significantly different in mitochondrial mass. Representative experiments are shown above with (a) profiles of relative mitotracker green intensity (linear scale) for each of the cell lines, gated on live fraction by Sytox Orange and G1-fraction by Hoechst 33342 staining; and (b) comparisons of mean mitotracker ratios from two repeat experiments. Error bars represent standard deviation between experiments (N=2). Comparable results are obtained when non-G1 fractions are included in the analysis.

Text S5: Mitochondrial potential measurements by flow cytometry. To assess mitochondrial potential, cells were passaged, harvested and concentrated as for mitochondrial mass measurements prior to staining with 10μM JC-1 and 10μM Hoechst 33342 for 45 minutes at 37°C (all dyes from Invitrogen). Samples were measured by flow cytometry on Beckton-Dickinson LSR-2 system, with the green JC-1 monomer excited with 488nm and emission detected with 530nm/30; the red JC-1 aggregate was excited with 532nm and emission was detected with 585nm/42. Analysis was performed using FlowJo software (Treestar, Ashland, OR). Debris was gated out by forward scatter and side-scatter. Whole-cell and G1-phase fractions were selected for analysis using the Hoechst 33342 cell cycle profile.

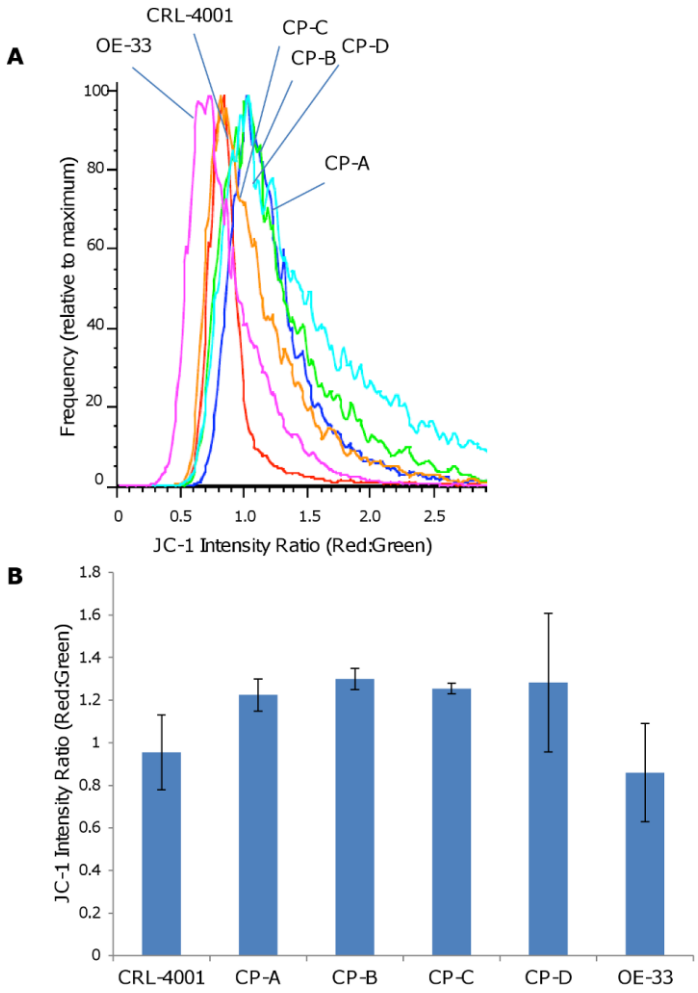

Figure S3. Barrett's esophagus cell lines are not significantly different in mitochondrial potential. Representative experiments are shown above with (a) profiles of JC-1 red:green intensity ratios from cells stained with JC-1 and gated on G1-fraction by Hoechst 33342 staining; and (b) comparisons of mean JC-1 red:green ratios from two repeat experiments. Error bars represent standard deviation between experiments (N=2). Comparable results are obtained when non-G1 fractions are included in the analysis.

Text S6: Tabulated Seahorse ECAR and OCR measures

Oligomycin treatment. To measure the amount of OCR which is dependent on ATP synthesis in each cell line, cells were treated with 3.2μM oligomycin, an ATP synthase inhibitor. By subtracting the residual OCR from the total OCR (OCR_{Total}), the OCR dependent on oxidative phosphorylation (OCR_{OxPhos}) was obtained. In response to oligomycin treatment, cell lines demonstrated a 60-70% decrease in OCR_{Total}, which corresponds to their OCR_{OxPhos} (Supplemental Materials Table S6).

	ECAR (μpH/min/cell)			OCR_{Total} (fmoles/min/cell)			OCR_{OxPhos} (fmoles/min/cell)		ΔOCR from untreated baseline following oligomycin addition (% change)
Cell line	mean	SD	p-value	mean	SD	p-value	mean	SD	
CRL-4001	1.4	0.2	n.s.	4.9	0.2	n.s.	3.6	0.2	-73
CP-A	1.1	0.1	-	4.1	0.3	-	2.7	0.3	-66
CP-B	1.6	0.1	n.s.	6.7	0.9	$<10^{-7}$	4.2	0.9	-63
CP-C	2.1	0.1	<0.001	5.7	0.3	<0.001	3.4	0.3	-60
CP-D	2.2	0.2	$<10^{-7}$	3.7	0.8	n.s.	2.1	0.8	-57

Table S6: BE cell lines have significant differences in ECAR and OCR. The mean of OCR and ECAR measurements by Seahorse XF24 is reported (N=6-11). Abbreviations: SD = standard-deviation of means; OCR_{OxPhos} = OCR resulting from oxidative phosphorylation; p-value (Tukey-Kramer test) of statistically significant differences from CP-A are shown.

	ΔECAR from untreated baseline (μpH/min/cell)			ΔECAR from untreated baseline (% change)	ΔOCR from untreated baseline (fMoles/min/cell)			ΔOCR from untreated baseline (% change)
Cell line	mean	SD	p-value		mean	SD	p-value	
CRL-4001	-1.19	0.07	$<10^{-4}$	-66	-0.37	0.22	n.s.	-7
CP-A	-0.81	0.05	-	-67	-0.26	0.07	-	-6
CP-B	-0.91	0.04	n.s.	-60	-0.32	0.10	n.s.	-6
CP-C	-1.18	0.05	$<10^{-4}$	-54	-0.21	0.15	n.s.	-4
CP-D	-1.84	0.05	$<10^{-7}$	-70	0.58	0.15	<0.01	+21

Table S7: Effects of 2-DG treatment on ECAR and OCR in cell lines. The mean changes in ECAR and OCR after addition of 50mM 2-DG compared to untreated baseline measured by Seahorse XF24 (N=2-4). Abbreviations: SD = standard-deviation of means; p-value (Tukey-Kramer test) of statistically significant differences from CP-A are shown.

	ΔECAR from untreated baseline (μpH/min/cell)			ΔECAR from untreated baseline (% change)	ΔOCR from untreated baseline (fMoles/min/cell)			ΔOCR from untreated baseline (% change)
Cell line	mean	SD	p-value		mean	SD	p-value	
CRL-4001	0.76	0.05	n.s.	+73	3.0	0.2	n.s.	+69
CP-A	0.80	0.03	-	+79	6.6	0.3	-	+156
CP-B	0.93	0.07	n.s.	+53	21.3	2.0	$<10^{-7}$	+271
CP-C	0.49	0.05	<0.001	+26	6.8	0.3	n.s.	+122
CP-D	0.23	0.04	$<10^{-7}$	+8	11.0	1.4	<0.05	+157

Table S8: Effects of 2,4-DNP treatment on ECAR and OCR in cell lines. The mean changes in ECAR and OCR after addition of 50μM 2,4-DNP compared to untreated baseline measured by Seahorse XF24 (N=2-4). Abbreviations: SD = standard-deviation of means; p-value (Tukey-Kramer test) of statistically significant differences from CP-A are shown.

	ΔECAR from baseline (μpH/min/cell)			ΔECAR from baseline (% change)	ΔOCR from baseline (fMoles/min/cell)			ΔOCR from baseline (% change)
Cell line	mean	SD	p-value		mean	SD	p-value	
CRL-4001	0.81	0.14	n.s.	104	-1.7	0.3	n.s.	-45
CP-A	0.90	0.05	-	130	-1.8	0.1	-	-34
CP-B	0.75	0.08	n.s.	67	-2.0	0.1	n.s.	-25
CP-C	1.95	0.24	$<10^{-7}$	196	-3.9	0.2	$<10^{-7}$	-60
CP-D	1.34	0.10	<0.12	132	-3.2	0.2	$<10^{-6}$	-53

Table S9: Effects of glucose on changes in ECAR and OCR in cell lines via the Crabtree effect. The mean changes in ECAR and OCR after addition of 5mM glucose compared to glucose-free baseline measured by Seahorse XF24 (N=2-4). Abbreviations: SD = standard-deviation of means; p-value (Tukey-Kramer test) of statistically significant differences from CP-A are shown.

REFERENCES

Baatar, D., M. K. Jones, et al. (2002). "Esophageal ulceration triggers expression of hypoxia-inducible factor-1 alpha and activates vascular endothelial growth factor gene - Implications for angiogenesis and ulcer healing." American Journal of Pathology **161**(4): 1449-1457.

Bensaad, K., A. Tsuruta, et al. (2006). "TIGAR, a p53-inducible regulator of glycolysis and apoptosis." Cell **126**(1): 107-120.

Berridge, M. V., P. M. Herst, et al. (2010). "Metabolic flexibility and cell hierarchy in metastatic cancer." Mitochondrion **10**(6): 584-588.

Boonstra, J. J., R. van Marion, et al. (2010). "Verification and unmasking of widely used human esophageal adenocarcinoma cell lines." Journal of the National Cancer Institute **102**(4): 271-274.

Brandon, M. C., E. Ruiz-Pesini, et al. (2009). "MITOMASTER: a bioinformatics tool for the analysis of mitochondrial DNA sequences." Hum Mutat **30**(1): 1-6.

Chen, G., J. Izzo, et al. (2009). "Different redox states in malignant and nonmalignant esophageal epithelial cells and differential cytotoxic responses to bile acid and honokiol." Antioxidants & redox signaling **11**(5): 1083-1095.

Chen, Z., W. Lu, et al. (2007). "The Warburg effect and its cancer therapeutic implications." Journal of bioenergetics and biomembranes **39**(3): 267-274.

Cook, M. B., C. P. Wild, et al. (2007). "Risk of mortality and cancer incidence in Barrett's esophagus." Cancer Epidemiol Biomarkers Prev **16**(10): 2090-2096.

Crabtree, H. G. (1929). "Observations on the carbohydrate metabolism of tumours." The Biochemical journal **23**(3): 536-545.

Dang, C. V. (2010). "p32 (C1QBP) and cancer cell metabolism: is the Warburg effect a lot of hot air?" Molecular and cellular biology **30**(6): 1300-1302.

Diaz-Ruiz, R., M. Rigoulet, et al. (2011). "The Warburg and Crabtree effects: On the origin of cancer cell energy metabolism and of yeast glucose repression." Biochimica et biophysica acta **1807**(6): 568-576.

Dwarkanath, B. S., F. Zolzer, et al. (2001). "Heterogeneity in 2-deoxy-D-glucose-induced modifications in energetics and radiation responses of human tumor cell lines." International journal of radiation oncology, biology, physics **50**(4): 1051-1061.

Fichter, C. D., C. Herz, et al. (2011). "Occurrence of multipolar mitoses and association with Aurora-A/-B kinases and p53 mutations in aneuploid esophageal carcinoma cells." BMC cell biology **12**: 13.

Frezza, C. and E. Gottlieb (2009). "Mitochondria in cancer: not just innocent bystanders." Seminars in cancer biology **19**(1): 4-11.

Galipeau, P. C., X. Li, et al. (2007). "NSAIDs modulate CDKN2A, TP53, and DNA content risk for future esophageal adenocarcinoma." PLoS Med **4**: e67.

Georgakoudi, I., B. C. Jacobson, et al. (2002). "NAD(P)H and collagen as in vivo quantitative fluorescent biomarkers of epithelial precancerous changes." Cancer research **62**(3): 682-687.

Griffiths, E. A., S. A. Pritchard, et al. (2007). "Increasing expression of hypoxia-inducible proteins in the Barrett's metaplasia-dysplasia-adenocarcinoma sequence." Br J Cancer **96**(9): 1377-1383.
Harada, H., H. Nakagawa, et al. (2003). "Telomerase induces immortalization of human esophageal keratinocytes without p16INK4a inactivation." Molecular cancer research : MCR **1**(10): 729-738.
Harper, M. E., A. Antoniou, et al. (2002). "Characterization of a novel metabolic strategy used by drug-resistant tumor cells." The FASEB journal : official publication of the Federation of American Societies for Experimental Biology **16**(12): 1550-1557.
Hewitson, K. S., L. A. McNeill, et al. (2002). "Hypoxia-inducible factor (HIF) asparagine hydroxylase is identical to factor inhibiting HIF (FIH) and is related to the cupin structural family." The Journal of biological chemistry **277**(29): 26351-26355.
Hornig-Do, H. T., J. C. von Kleist-Retzow, et al. (2007). "Human epidermal keratinocytes accumulate superoxide due to low activity of Mn-SOD, leading to mitochondrial functional impairment." The Journal of investigative dermatology **127**(5): 1084-1093.
Kern, K. A. and J. A. Norton (1987). "Inhibition of established rat fibrosarcoma growth by the glucose antagonist 2-deoxy-D-glucose." Surgery **102**(2): 380-385.
Levine, D. S. and B. J. Reid (1992). Endoscopic diagnosis of esophageal neoplasms. Gastrointestinal Endoscopy Clinics of North America. G. A. Boyce and H. W. J. Boyce. Philadelphia, W. B. Saunders Co.**:** 395-413.
Lord, R. V., J. M. Park, et al. (2003). "Vascular endothelial growth factor and basic fibroblast growth factor expression in esophageal adenocarcinoma and Barrett esophagus." The Journal of thoracic and cardiovascular surgery **125**(2): 246-253.
Matoba, S., J. G. Kang, et al. (2006). "p53 regulates mitochondrial respiration." Science **312**(5780): 1650-1653.
Neto, C. A., H. Zhuang, et al. (2001). "Detection of Barrett's esophagus superimposed by esophageal cancer by FDG positron emission tomography." Clinical nuclear medicine **26**(12): 1060.
Nishihira, T., Y. Hashimoto, et al. (1993). "Molecular and cellular features of esophageal cancer cells." Journal of cancer research and clinical oncology **119**(8): 441-449.
Palanca-Wessels, M. C., M. T. Barrett, et al. (1998). "Genetic analysis of long-term Barrett's esophagus epithelial cultures exhibiting cytogenetic and ploidy abnormalities." Gastroenterology **114**(2): 295-304.
Possemato, R., K. M. Marks, et al. (2011). "Functional genomics reveal that the serine synthesis pathway is essential in breast cancer." Nature.
Rockett, J. C., K. Larkin, et al. (1997). "Five newly established oesophageal carcinoma cell lines: phenotypic and immunological characterization." British journal of cancer **75**(2): 258-263.
Suganuma, K., H. Miwa, et al. (2010). "Energy metabolism of leukemia cells: glycolysis versus oxidative phosphorylation." Leukemia & lymphoma **51**(11): 2112-2119.
Taylor, M. D., P. W. Smith, et al. (2009). "Correlations between selected tumor markers and fluorodeoxyglucose maximal standardized uptake values in esophageal cancer." European journal of cardio-thoracic surgery : official journal of the European Association for Cardio-thoracic Surgery **35**(4): 699-705.
Vander Heiden, M. G., L. C. Cantley, et al. (2009). "Understanding the Warburg effect: the metabolic requirements of cell proliferation." Science **324**(5930): 1029-1033.
Wang, K. K. and R. E. Sampliner (2008). "Updated guidelines 2008 for the diagnosis, surveillance and therapy of Barrett's esophagus." Am J Gastroenterol **103**(3): 788-797.
Warburg, O. (1956). "On the origin of cancer cells." Science **123**(3191): 309-314.

Warburg, O., F. Wind, et al. (1927). "The Metabolism of Tumors in the Body." The Journal of general physiology **8**(6): 519-530.
Weinhouse, S. (1956). "On respiratory impairment in cancer cells." Science **124**(3215): 267-269.
Wu, M., A. Neilson, et al. (2007). "Multiparameter metabolic analysis reveals a close link between attenuated mitochondrial bioenergetic function and enhanced glycolysis dependency in human tumor cells." American journal of physiology. Cell physiology **292**(1): C125-136.
Xie, H., V. A. Valera, et al. (2009). "LDH-A inhibition, a therapeutic strategy for treatment of hereditary leiomyomatosis and renal cell cancer." Molecular cancer therapeutics **8**(3): 626-635.
Younes, M., A. Ertan, et al. (1997). "Human erythrocyte glucose transporter (Glut1) is immunohistochemically detected as a late event during malignant progression in Barrett's metaplasia." Cancer Epidemiology Biomarkers & Prevention **6**(5): 303-305.
Zu, X. L. and M. Guppy (2004). "Cancer metabolism: facts, fantasy, and fiction." Biochemical and biophysical research communications **313**(3): 459-465.

CHAPTER 2

DEVELOPMENT OF A PROTOTYPE MICROSCOPY SYSTEM FOR THE MEASUREMENT OF OXYGEN CONSUMPTION RATE HETEROGENEITY IN SINGLE CELLS

BACKGROUND

HETEROGENEITY IN LIFE AND DEATH EVENTS

Phenotypic heterogeneity is one of the fundamental principles of evolution (Lewontin 1970) and allows a population of cells to buffer the effects of extracellular and intracellular events which cause injury. To adapt to changes in their environment (e.g. a novel nutrient or toxin), it is critical for living systems to be able to sense and respond appropriately to maintain homeostasis. Within a population the ability of any individual cell to adapt to a particular change is limited by the state of that particular cell. Prior conditions, such as cell cycle, organelle content, transcript and protein content influence the ability of a cell to adapt to its environment. Novel protein-length transcripts are created in a matter of hours, translation of proteins take longer, and assembly of organelles substantially longer. Single-cell cell cycle studies have characterized heterogeneity that would go unnoticed when studied at a population level in cell metabolism, infectivity, and response to treatments (eg. radiation therapy) (Novak and Mitchison 1990; Cooke, Temple et al. 2011).

Cells in a tissue may also display heterogeneity due to mutation, which can affect transcriptional regulation, translation, protein stability and/or protein function. These changes in turn can affect responses at metabolic, signaling and structural levels of the cell. In extreme cases, mutations can also affect the synthesis of organelles and rewire metabolism (Harper, Antoniou et al. 2002; Wright, Maroulakou et al. 2008). Some of these changes affect how a cell interacts with its neighbours: at one extreme, if cell fitness is reduced below levels for successful survival in an organism then degenerative diseases due to cell death can result (eg. neural degeneration), while at the other extreme, an increase in cell fitness can allow cells to overcome restrictions imposed by the organism for cell growth, resulting in hyperproliferative disorders and cancer. In both cases, heterogeneity at a single-cell level has significant implications for the organism.

HETEROGENEITY AND ITS EFFECT IN CANCER

Cancer progression was described by Dr. Peter Nowell as an evolutionary disease in which heterogeneous populations of premalignant clones undergo selection (Nowell 1976). Clones having an increased fitness can come to predominate in a population, resulting in clonal expansion of cells with altered genomes and potentially cancer. This process is accelerated by mutations in DNA proof-reading, repair, and check-point control, which increase the rate of mutations and chromosomal aberrations, leading to increased heterogeneity of tumor cells

(Salk, Fox et al. 2010). Monitoring genetic instability and genetic heterogeneity in tumors has demonstrated that late stage tumors have a significant number of translocations, loss of heterozygosity events (LOH), amplifications and deletion events (Coons, Johnson et al. 1995; Gonzalez-Garcia, Sole et al. 2002). The development of assays that screen for premalignant lesions and tumors in the early stages of chromosomal instability and neoplastic progression may benefit prevention and early detection of cancer.

Heterogeneity at the single cell level impacts efforts to control cancer through early diagnosis and therapy. A common problem in cancer control is therapeutic resistance which arises as a result of treatment of late stages tumors when enough heterogeneity may be present within a population to produce surviving resistant clones. Measuring genetic and/or phenotypic heterogeneity in tumors may allow clinicians to determine a more effective therapeutic strategy to treat a particular cancer while minimizing resistance. Genetic heterogeneity has recently been used as a method to measure progression in Barrett's Esophagus, where clonal diversity (as measured by Shannon Index) and genetic divergence were observed to result in increased risk for EA (Maley, Galipeau et al. 2006). Technologies that function at a single-cell level may improve resolution of heterogeneity assays, require fewer or smaller biopsies to be collected and provide more information from regular-sized biopsies.

EXISTING AND NOVEL METHODS FOR MEASURING HETEROGENEITY

Biological research has traditionally used assays for measuring effects at the population-level but novel technology is now enabling measurements that are able to be done at a single-cell level and analyze variation within a population (Limke and Atchison 2009; Ryan, Ren et al. 2011). Multi-parameter staining and analysis by flow cytometry is routinely used to characterize sub-populations of cells for specific markers or organelles of interest, which can be subsequently separated with flow sorting technology. Scanning microscopy, which combines microscopy with cytometry, has the advantage of monitoring single cells within a growing cell culture and existing inter-cellular interactions over time, while flow cytometry has the advantages of higher throughput. Following image cytometry, microdissection of individual cells allows for downstream single-cell assays, however microdissection often requires fixation of samples and/or manipulation of cells, which perturbs normal cellular physiology and limits these methods to end-point assays (ie. DNA or RNA).

Single-cell assays have started to emerge as viable methods for associating single-cell sequence analysis to phenotypes (Navin, Kendall et al. 2011). These include breakthroughs in single cell PCR (Pierce and Wangh 2007), whole-genome amplification (Treff, Su et al. 2011), and proteomics (Cohen, Dickerson et al. 2008). Lab-on-a-chip devices, which combine microscopy and integrated sensors, allow for high resolution characterization of single cell processes and metabolism (Lidstrom and Meldrum 2003). In these devices, cells are typically grown or deposited into wells with integrated sensors on optically clear chips where growth, substrate/product flux and other life and death characteristics can be controlled and measured. Typically single-cell measures of substrate or product flux require sub-pico to sub-femtomolar resolution, which is achieved using fluorescent dyes (Ryan, Ren et al. 2011).

Oxygen consumption is integral to metabolic measurements related to cellular life and death processes. Roughly 80% of the oxygen consumption rate (OCR) in a living cell is due to oxidative phosphorylation occurring inside mitochondria (Wu, Neilson et al. 2007). Oxygen

consumption fluctuates during the cell cycle (Novak and Mitchison 1990), as well as during death stimuli, decreasing immediately prior to apoptosis (Hynes, O'Riordan et al. 2005), and increasing in response to oxidative stress and upon onset of apoptosis (Tewari, Belenghi and Levine 2002). In addition to acute changes, mitochondrial function has been observed to change chronically in different disease states such as neural degeneration, diabetes, aging and cancer (Wallace 2010), thus measuring heterogeneity of OCR at single-cell resolution may provide discoveries that have not yet been observed with less sensitive methods.

Manometers and Clark electrodes (Renger and Hanssum 2009), designed to measure OCR in tissues, are not scalable to measuring OCR at single-cell levels since electrode-based respirometry assays consume oxygen as part of the detection process, require stirring for re-equilibration, and are difficult to incorporate into a gas-impermeable system. Several optical measurement systems exist that measure respirometry with platinum-porphyrin compounds, providing sub-femtomolar oxygen concentration measurements (Wilson, Vanderkooi et al. 1987; O'Mahony, O'Donovan et al. 2005; O'Donovan, Twomey et al. 2006); however, existing systems have difficulty sealing or are made of gas-permeable materials, and measure oxygen flux rates (with significant error) instead of absolute oxygen consumption rates. Thus far, the only known method for directly measuring oxygen at single-cell resolution has been platinum-porphyrin sensors inside diffusionally-sealed borosilicate glass chambers.

For the second part of my thesis work, I collaborated with bioengineers at the Microscale Life Sciences Center at the University of Washington to develop a gas-impermeable chip-based system capable of measuring oxygen consumption rates of single cells. Our development team included experts in cell biology, microscopy, automation, software, dye chemistry and sensors. The major goals of this collaboration were to 1) develop technology for monitoring life processes at single-cell resolution, and 2) measure single-cell OCR heterogeneity that predisposes individual cells to life or death. Although low throughput of numbers of cells measured limited experiments that were able to be performed on this device, with some modifications the prototype device that I participated in developing would enable future experiments to characterize how heterogeneity of OCR in cells relates to mitochondrial dysfunction, sensitivity to inhibitors and/or altered metabolism.

Tissue Culture. Primary Barrett's esophageal cell lines CP-A, CP-B, CP-C and CP-D (Palanca-Wessels, Barrett et al. 1998), adapted for serum-free growth by the Carlo Maley lab (University of California San Francisco), were cultured in keratinocyte serum-free media (KSFM) with 5ug/L hEGF and 50mg/L bovine pituitary extract (KSFM and supplements from Invitrogen). Cells seeded for imaging experiments were transferred to identical media that was phenol red free (custom order from Invitrogen) and filtered through a 40nm filter. Medium was re-stocked every month to preserve growth quality. All cell lines were grown in a humidified 37°C incubator with 5% CO_2, and passaged at 50-80% confluency, once to twice weekly. Passaging was performed using 0.05% Trypsin-EDTA (Invitrogen) to minimize over-trypsinization.

Since several EA cell lines in existing biorepositories have been determined to be of non-esophageal tumor type (Boonstra, van Marion et al. 2010), we verified the identity of each cell line using the AmpFlSTR Identifiler kit (Applied Biosystems) and DNA content flow cytometry was used to determine ploidy and cell cycle. Cell cultures were mycoplasma tested by MycoSensor PCR kit (Stratagene) and cell lines were refreshed from stock within 20 passages, or upon detection of changes in DNA cell cycle profile or mycoplasma contamination.

Microscopy platform. For imaging, a Nikon Eclipse Ti microscope with an automated stage, a full spectrum light source, an epifluorescent 483nm laser, an Andor iStar ICCD camera and shutter were used (Figure 1a). The microscopy system was enclosed in a temperature-controlled Plexiglas chamber pre-warmed to 37°C. Specialized automation software allowed for repetitive multi-step imaging experiments and remote access software allowed for remote control of the microscope in light-free conditions, in order to minimize the background signal.

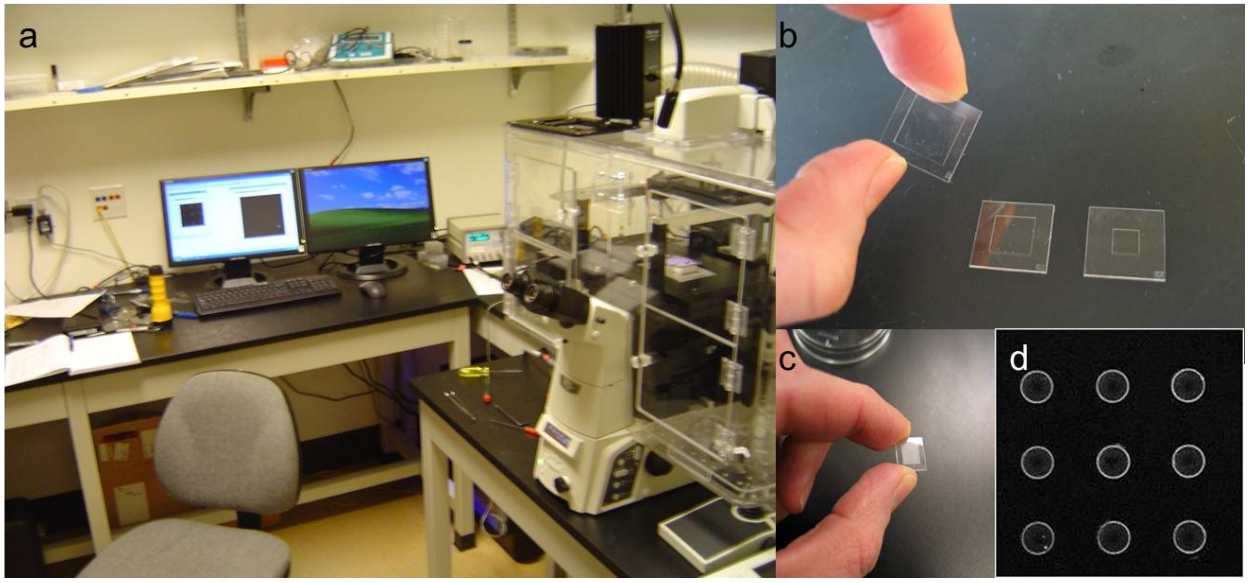

Figure 1: Microscopy system for measurement of single-cell oxygen consumption rates, displaying a) microscopy platform and setup, b) macrowell chips for analysis of bulk culture OCR, c) single-cell well chips with d) arrays of wells with embedded luminescent platinum-porphyrin ring sensors.

Fluorescent dyes that avoid spectral overlap were chosen to measure several biological parameters in series with oxygen consumption rate (Table 1).

Biological measurement	Dye	Excitation/Emission wavelength measured (nm)
Live cell (membrane integrity)	Calcein AM	483/530*
Apoptosis (early)	Annexin V-Alexa fluor 680 conjugate	680/702
Apoptosis (late)	Sytox Orange	543/570
Nuclear content (cell cycle stage)	Hoechst 33342	355/460
Mitochondrial mass	Mitotracker Green	483/530*
Oxygen consumption rate	Platinum-porphyrin	393/650

Table 1: Fluorescent dyes selected to measure biological parameters serially on chip system. Excitation and emission at indicated peak wavelengths was achieved using bandpass filters. *Due to overlapping spectra in Calcein AM and Mitotracker green, cells were stained with these dyes in independent experiments.

Live and dead cell imaging. Calcein AM is a cell-permeable non-fluorescent compound which becomes cell-impermeable and fluorescent following hydrolysis of its acetomethyl-ester group inside viable cells. Sytox Orange is a nucleic acid stain which enters fragmented cells at late stages of apoptosis and fluoresces when bound to dsDNA. Sytox Orange was believed to be cell-impermeable, however at high enough concentrations it penetrates into live cells, and stains their nuclei over time. Thus, an appropriate Sytox Orange concentration was selected to avoid false-positive dead cell staining for the duration of the OCR experiments.

To detect live and dead cells, growing cells were stained with 2.5μM Calcein AM and 0.5 μM Sytox Orange (Invitrogen) in phenol red-free growth media for 20 minutes in a humidified 37°C incubator with 5% CO_2. To avoid over-exposure to Calcein AM, cells were transferred to growth media containing only 0.5 μM Sytox Orange and imaged.

Annexin V is a protein ligand for extra-cellular phosphoserine, which appears as an early marker of apoptosis in most cells. To detect early apoptosis, growing cells were stained with 5μg/ml Annexin V-Alexafluor 680 conjugate (Invitrogen/Nexins Research BV #35109) in medium and incubated for 10 minutes. After medium was replaced, imaging was performed.

Cell cycle imaging. Hoechst 33342, a cell-permeable viable cell nuclear dye which fluoresces upon dsDNA binding, was used to quantitate cellular DNA content and to determine the stage of the cell cycle. Growing cells were stained with 10μM Hoechst 33342 (Invitrogen) in phenol red-free growth media for 30 minutes in a humidified 37°C incubator with 5% CO_2, and imaged.

The image cytometry assay was validated with flow cytometry with a sub-aliquot of cells that were grown to 50-70% confluency and harvested with 0.05% trypsin (Invitrogen). Cells were centrifuged at 100g for six minutes and resuspended in KSFM media (Invitrogen) to a concentration of 1 million cells/ml. Cells were diluted 1:2 and stained with a solution

containing a final concentration of 10μM Hoechst 33342 for 30 minutes at 37°C. Samples were measured by flow cytometry on the Beckton-Dickinson LSR-2 instrument. Analysis was performed using FlowJo software (Treestar, Ashland, OR).

To standardize for nuclear content between experiments, chick-red blood cells (CRBC, Biosure,Grass Valley, CA), which are traditionally used as a nuclear content standard in flow-cytometry, were dried on slides, fixed with 70% ethanol, and stored in the dark at room temperature. Slides were stained with 10μM Hoechst 33342 in phenol red-free media, covered under a coverslip, and immediately imaged.

To control for daily microscopy variations, fresh 2.5μm blue Inspeck microbeads (Invitrogen) were diluted in deionized water, sonicated to break up clumps, dried on slides, and imaged at 60X magnification, using the same filters as used for Hoechst 33342. Bead fluorescence intensities from a concentrated stock solution were verified to not change over time by the manufacturer and were used as a fluorescent standard.

Chroma blue slides were used to normalize images for field-of-view position effects by imaging using the same filters as used for Hoechst 33342.

Mitochondrial mass imaging. Mitotracker green is a cell-permeable dye that localizes to the mitochondria in a potential-independent fashion and can be used to quantitate mitochondrial mass in living cells. Growing cells were stained with phenol red-free cell media containing 10μM Mitotracker green for 20 minutes in a humidified 37°C incubator with 5% CO_2. Media was replaced with dye-free media and cells were imaged.

Chroma green slides were used to normalize images for field-of-view position effects by imaging using the same filters as used for Mitotracker green.

Oxygen consumption rate measurements. Oxygen consumption rates (OCR) were measured using 1μm platinum-porphyrin carboxylate-modified microspheres (Invitrogen; 1μm are discontinued but available as 40nm beads) rinsed in deionized water. When platinum-porphyrin is excited at 393nm, it luminesces and the phase of the luminescence can be converted to oxygen concentration (Molter, McQuaide et al. 2009). Sensors are deposited onto borosilicate and fused-silica chips of two major designs: Macrowell and single-cell well chips (Figure 1 b and c respectively). For macrowell chips, the sensors were deposited by gently touching a pipette tip to the glass surface, then allowing the spot to air-dry. For single-cell well chips, the sensors were injected with a pico-injector into the wells and allowed to dry, accumulating at the edges of the well due to the "coffee ring effect" (Figure 1d). Chips and sensors were then baked at 140°C for 20 minutes to melt the beads and promote adhesion.

To ensure consistent positioning during repeated piston sealing events, chips were held in place in a media-containing stainless steel chip holder with a built-in quartz viewing window for imaging. The chip holder was placed on the microscopy platen and the air above the chip and media were humidified via a gas line and enclosed with parafilm. A manifold containing the sealing-piston was mounted over the microscope platen and centrally aligned over an array of interest to allow a descending piston to seal all nine wells in the array. To ensure a proper seal after a piston descent, a characteristic laser diffraction pattern between the chip surface and lid was inspected visually after exciting with a 488nm laser and detecting at 530nm. Using this

method, successful gas-impermeable seals produced a "fringe pattern", named after the uniform radiating ring at the fringes of the wells, and uniform black rings on the well lips (Figure 12).

OCR measurements on macrowell chips. Oxygen consumption rates from a population of cells was measured using borosilicate glass chips with well dimensions that were 1cm x 1cm x 45µm deep, resulting in a volume of 4.5µl. These macrowell chips with sensor were prepared as described previously (Strovas, McQuaide et al. 2010). Briefly, approximately 0.1µl of beads were deposited onto a plasma-etched chip for one minute to make it hydrophobic and allowed to dry. Sensor patches were cured for 10 minutes at 170°C to melt the microspheres and cause adhesion. The chips were sterilized by immersion in 70% ethanol, and immediately rinsed serially three times in nanopure water and dried. To prevent cell adhesion to lips of the chips, ethanol-sterilized Blue Tack tape (Semiconductor Equipment Corporation, Moorpark, CA) was adhered to the lips and excess removed with a sterile scalpel.

18 hours prior to OCR measurement experiments, 100k cells in 1ml media were seeded onto macrowell chips inside wells of a 12-well plate, to obtain approximately 10k-20k live cells in the macrowell the following day. Following overnight growth, the Blue Tack tape was removed and the seeded chip was transferred to a chip holder with pre-warmed 40nm-filtered phenol red-free media containing 0.5µM Sytox Orange and stained for 20 minutes. The chip holder was then transferred to a heated microscopy system and imaged. The experiment was aborted if greater than 1% dead cells or toxicity in patches was observed. Macrowell chips were covered with a glass coverslip and pressure was temporarily applied to the lip to create a glass-upon-glass seal. Three serial OCR measurements were performed for 30 minutes each, while avoiding drawdowns below 10% oxygen. The serial measurements were alternated between two seeded chips to allow cells to recover between oxygen drawdowns and Sytox Orange was imaged following each OCR measurement to verify that the OCR assay was not causing cell death. Following the three OCR measurements, the medium was replaced with medium containing 10µM Hoechst 33342 and 10µM Mitotracker and incubated 30 minutes at 37°C before imaging. A blue and green autofluorescent Chroma slide was imaged in order to normalize intensity across the field of view. Analysis of OCR and cell quantitation was performed using Matlab, CellProfiler and Microsoft Excel.

OCR measurements on single-cell microwell chips. The borosilicate microwell chips used in this assay have nine separate arrays, each consisting of nine 474 picoliter wells. Microwell chips were prepared as described previously (Molter, McQuaide et al. 2009), except for use of deep reactive-ion etching with a Ni mask, to obtain more homogeneous well volumes, and picoinjection of Pt-porphyrin sensor deposition with lower temperature curing (140°C for 20 minutes instead of 170°C for 10 minutes, as reported previously), which allowed for more homogeneous sensor deposition and higher sensor signal-to-noise, respectively. Immediately prior to seeding, microwell chips were sterilized by immersion in 70% ethanol, rinsed with cell culture-grade water (Gibco #A12873), and kept wet in warm media in Falcon 12-well plates (Becton Dickinson).

Cells were seeded at 24k cells in 1ml media on microwell chips and grown overnight. The following day, the chips were transferred to a chip holder containing pre-warmed phenol red-free media with Calcein AM and Sytox Orange and stained for 20 minutes in a 37°C incubator. The media was replaced with Sytox Orange-only media, the chip holder was transferred to a heated microscopy system and the cells were imaged. A humidified 20% oxygen gas-line

providing positive air pressure was installed under a piece of parafilm stretched over the chip holder. Arrays with wells containing a single live cell and at least one empty well (to use as a no cell control) were selected for OCR measurements. Following the centering of an array in the field of view, the piston was lowered with a force of 10 lbs. and sealing was confirmed by imaging fringe patterns around each well. If a poor seal was observed, the piston was raised, re-centered over the array, and lowered to reset the seal. Following a successful seal, three serial OCR measurements were performed for approximately 7 minutes each (with the CP-A cell line) being careful to avoid drawing down below 10% oxygen. Cells were allowed to recover between OCR measures by alternating between two different arrays during the serial measurements. Following imaging on all selected arrays on a chip, media containing 10μM Hoechst 33342 and 10μM Mitotracker green was added, incubated for 30 minutes at 37°C, replaced with media containing only Hoechst 33342 (to avoid high background signal from Mitotracker green) and imaged. A blue and green autofluorescent Chroma slide was imaged in order to normalize intensity across the field of view. Analysis of OCR was performed using Matlab, CellProfiler and Microsoft Excel.

Oxygen sensor calibration. Following OCR experiments, chips were stored in the dark and calibrated within a week of the experiment to ensure integrity of the sensor. Chips were placed in the chip holder with 1ml of cell media and a positive air-pressure environment was created by flowing gases through a filtered syringe under a piece of parafilm. Chips were serially exposed to nitrogen and oxygen gases mixed in the correct ratio to achieve the desired concentration of oxygen (0%, 10% and 20% O_2), and sensor readings were taken for all of the arrays that had single-cell OCR measurements in prior experiments. The single-cell OCR measures obtained in prior experiments were corrected using the well-specific calibration values measured for each oxygen concentration. An identical calibration process was used for the bulk cell chips, except that only a single sensor was calibrated in this case.

Quantitative image cytometry standards. To develop an intra-experimental image cytometry standard for Hoechst 33342 and Mitotracker green staining, a macrowell chip was prepared as described in the microwell chip section above, stained at 37°C for 30 minutes with 10μM Hoechst 33342 and 10μM Mitotracker green, and 10k cells were imaged. A blue and green autofluorescent Chroma slide was imaged in order to normalize intensity across the field of view. Quantitative analysis of integrated intensity for each cell was performed using CellProfiler and Microsoft Excel.

DEVELOPMENT OF SINGLE-CELL OCR MEASUREMENT SYSTEM

Microwell chips were designed to measure single-cell OCR while being suitable optically to take advantage of many existing fluorometric assays. Image cytometry assays for live/dead cells using Calcein AM/Sytox Orange, cell cycle imaging using Hoechst 33342, and mitochondrial mass using Mitrotracker green were developed for these chips as part of this thesis.

LIVE AND DEAD CELL STAINING USING CALCEIN AM AND SYTOX ORANGE

To develop a live and dead cell assay for a four hour single-cell OCR experiment that avoided repetitive media exchanges, we required dyes which could be left in the media that were not toxic to growing cells during prolonged exposure. Calcein AM and Sytox Orange were chosen for their simple staining methods, low toxicity over time and spectral characteristics (Figure 2). Calcein AM is a dye that accumulates inside cells during staining and, once media is replaced, the dye is found to be stable within the cells for the duration of the experiment.

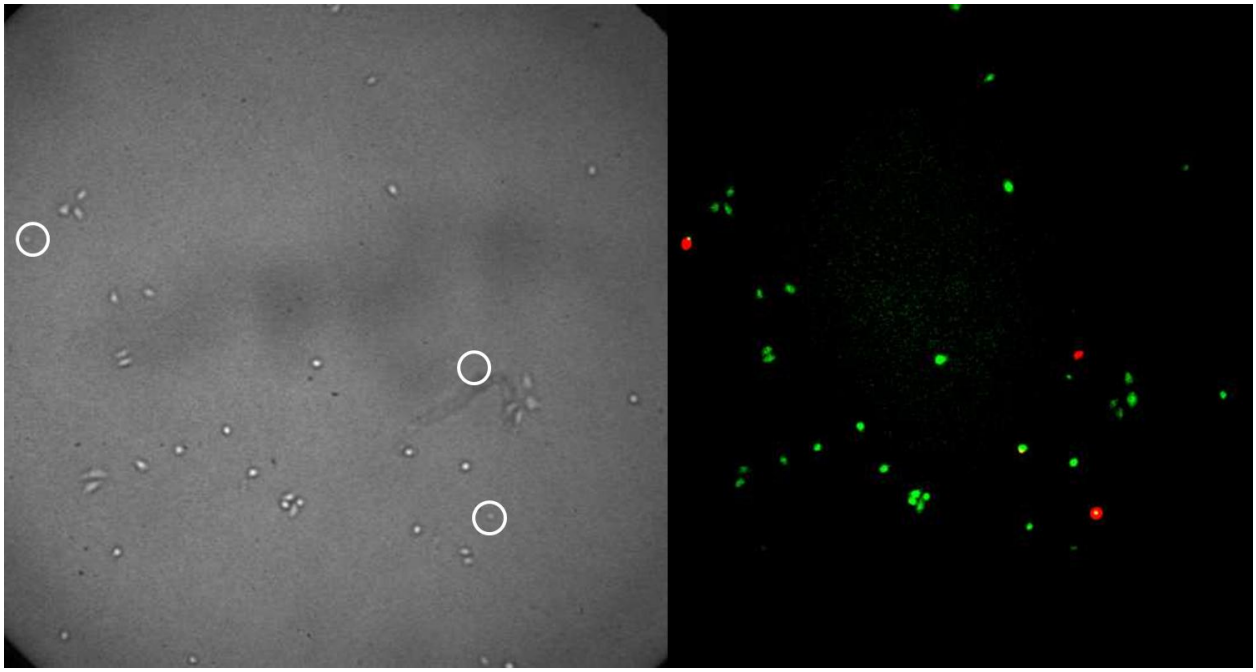

Figure 2: Live-dead assay of cells under bright field (left) and fluorescent (right) microscopy following staining with Calcein AM for live cells (green) and Sytox Orange for apoptosis (red) (10X magnification). Note the loss of refractive properties in dead cells (white circles, left) that stain with Sytox Orange.

Sytox Orange stains cells in late stages of apoptosis, and is reported by the manufacturer to be impermeable to viable cells (Invitrogen); however we discovered that at concentrations of 5μM Sytox Orange entered living cells after being present in media for 30 minutes (Figure 3). To reduce the number of false positive dead cells, we tested four different Sytox Orange concentrations (0.1, 0.5, 1, and 5μM) and found that concentrations of 1μM or lower produced

negligible false positive staining. 0.5μM Sytox Orange was used as a working concentration in subsequent assays.

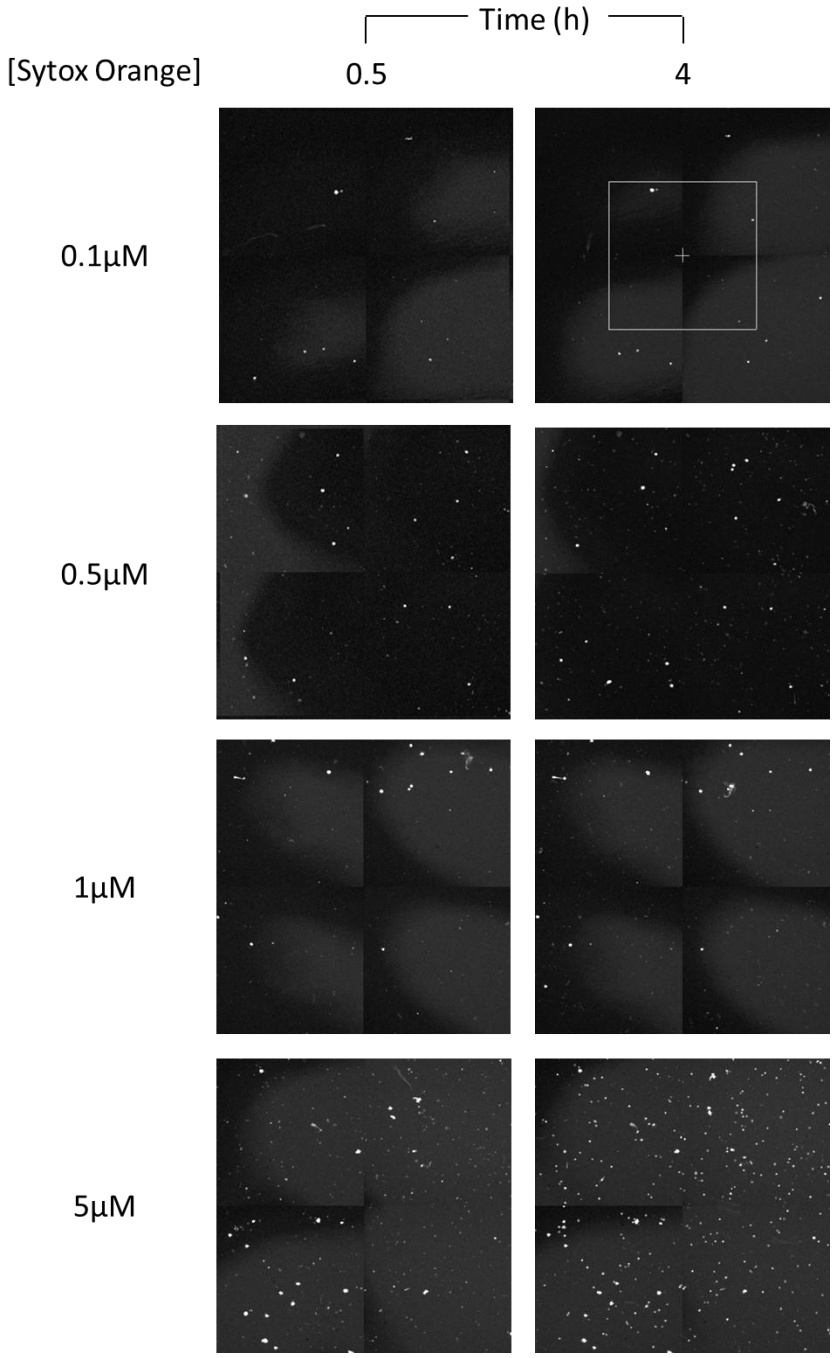

Figure 3: Sytox Orange is cell-permeable at high concentrations over the course of a 4 hour experiment. Images of cells stained with Sytox Orange (white spots, 10X magnification) show that cell permeability of this dye is concentration-dependent. 0.5μM was chosen as a working concentration with low false positive staining for a four hour experiment. Note: Images were not background corrected and contrast was uniformly increased to highlight the dimly fluorescing cells.

As a positive apoptosis-control, incubation with 100nM staurosporine, a broad-spectrum kinase inhibitor, overnight produced >20% cell death in most cell lines (data not shown). To detect early stages of apoptosis in cells, we tested Annexin V-Alexafluor 680 conjugate; however due to high background signal and lack of a consistent early-apoptosis controlthis method was not used (data not shown).

CELL CYCLE STAINING USING HOECHST 33342

The stage of the cell cycle is known to affect many aspects of cellular metabolism, including cellular oxygen consumption rate (OCR) (Novak and Mitchison 1990). Synchronization of cells to produce a homogeneous population is challenging since individual cells released from cell-cycle block induced by chemical means are known to exit from arrest in a stochastic fashion (Darzynkiewicz, Traganos et al. 1981). Given these findings, several methods were attempted to induce synchronization through less harsh methods including 1) cell growth to confluency, 2) mitotic shake-off and 3) flow sorting. The first two methods were not able to successfully synchronize BE cell lines, and the last method was not able to provide a sufficient number of viable cells (data not shown).

Since synchronization was unsuccessful, I decided to measure cell cycle directly with the fluorescent cell-permeable nuclear dye, Hoechst 33342. Cell cycle imaging by image cytometry on macrowell chips was validated against cell cycle assessed by flow cytometry. Similar distributions were obtained between cells analyzed by image and flow cytometry, except for a much smaller coefficient of variance in the G1 and G2 peak by flow cytometry (Figure 4).

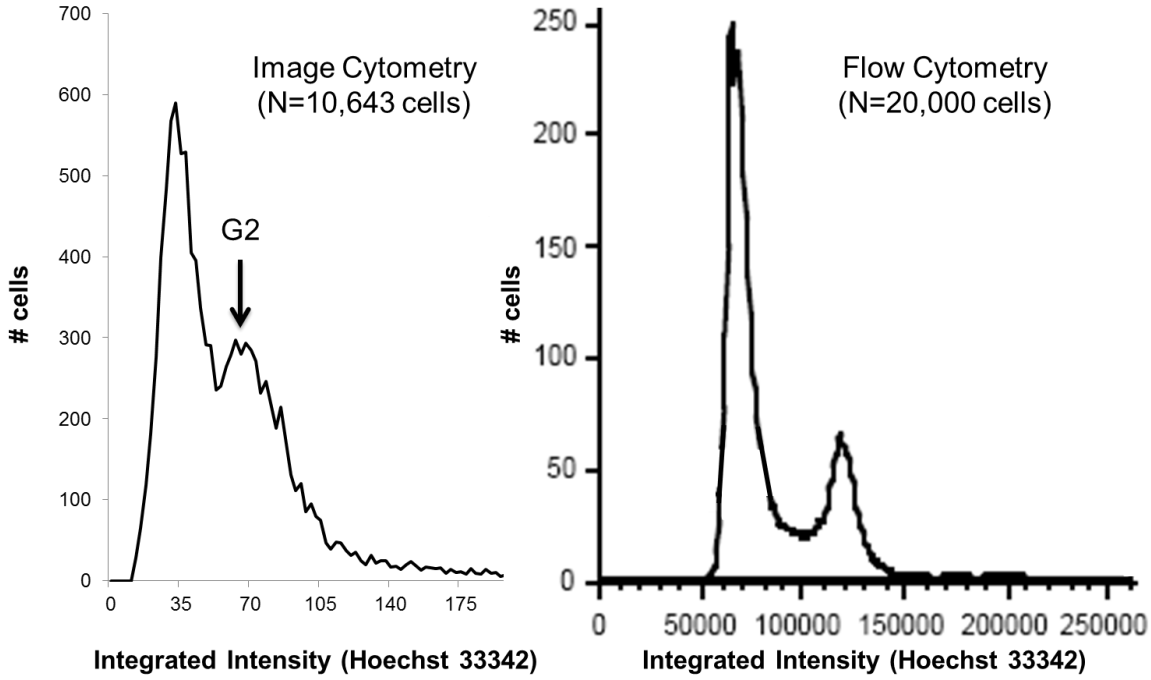

Figure 4: Hoechst 33342-stained CP-A histograms as measured by image (left) and flow cytometry (right). G2 peak in image cytometry (arrow) demonstrates a higher coefficient of variance than flow cytometry, which is more difficult to discriminate.

Chick-red blood cells (CRBCs), which are traditionally used as a nuclear content standard in flow-cytometry, were fixed, stained and imaged to determine if they could be used as an inter-experimental Hoechst 33342 staining control (Figure 5). In preliminary experiments, focus of the imaged CRBCs tended to drift with location on the slide (data not shown), which was not possible to correct with existing autofocus routines due to a z-axis step size that was too coarse, thus this control was abandoned.

In order to control for daily instrument variations, 2.5µm blue Inspeck microbeads were imaged to test excitation and emission intensity in the same area of the spectrum as Hoechst 33342. These microbeads are guaranteed by manufacturer to produce consistent fluorescent intensities, within a given lot and the same lot of microbeads was utilized between experiments conducted as part of this thesis. To correct for uneven illumination of the field-of-view, a blue Chroma autofluorescent slide image was used to normalize fluorescent intensity based on location (Figure 6).

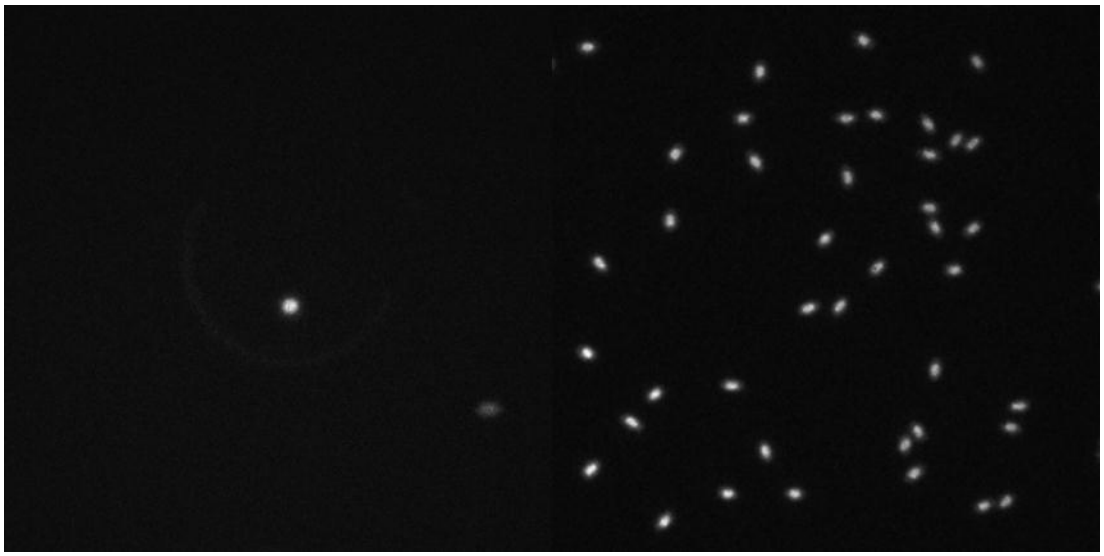

Figure 5: Imaging of Hoechst 33342-stained CP-A cell growing inside a microwell (left, 20X magnification) and ethanol-fixed chick red blood cell controls on a slide (right, 60X magnification).

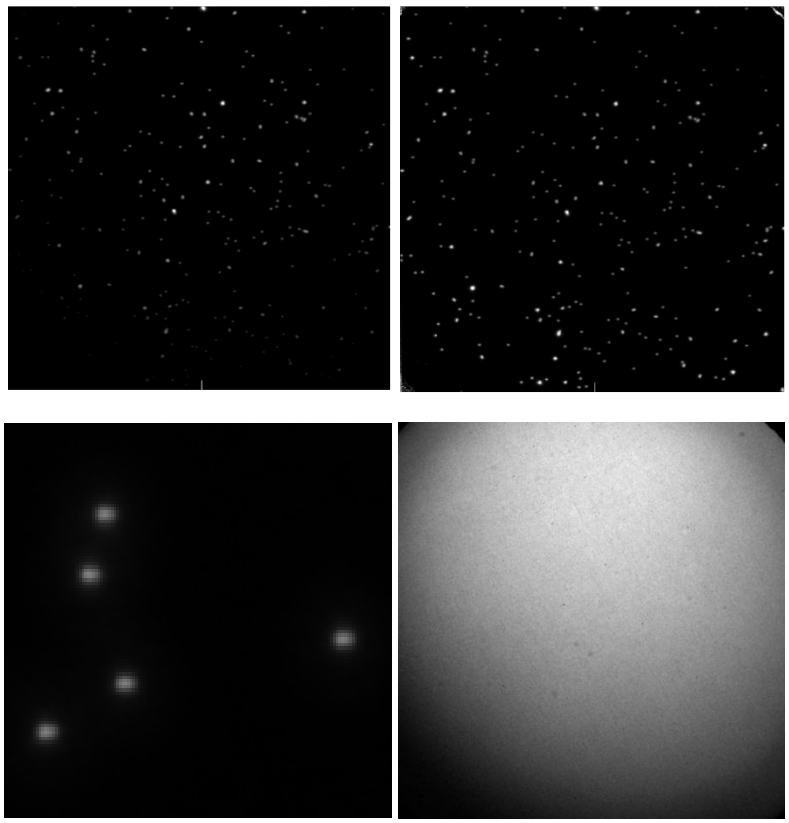

Figure 6: Normalization of 2.5μm blue Inspeck microbead images showing pre-normalized (top left) and normalized (top right) images (20X magnification). A close up of beads is shown (bottom left). Fluorescent intensities for each location in the field-of-view were normalized using a blue Chroma autofluorescent slide image (bottom right).

MITOCHONDRIAL MASS STAINING USING MITOTRACKER GREEN

Mitochondrial content within a cell may contribute to single cell OCR heterogeneity; therefore Mitotracker green, a cell-permeable mitochondrial potential-independent dye which localizes to the mitochondria, was used to stain cells to measure mitochondrial mass. Cells stained with this dye demonstrated heterogeneous total dye uptake related to size and morphology of the cell (Figure 7).

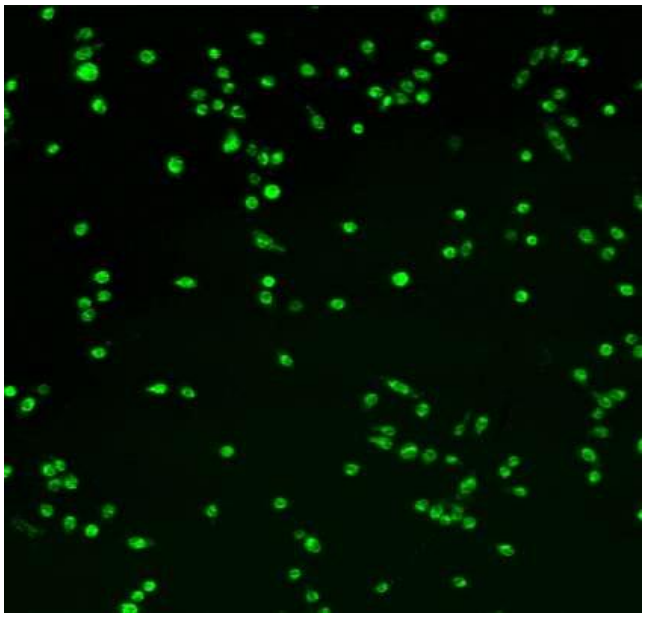

Figure 7: Mitochondrial mass staining of CP-A cells with Mitotracker green, demonstrating heterogeneity observed (10X magnification).

Using CellProfiler, two parameters were adjusted to identify and separate cells: intensity threshold and minimum cell size. Intensity threshold adjustment was optimized, since at too low threshold cells and background were merged, while at too high threshold areas of cytoplasm and small cells which were faintly stained were excluded. A minimum cell size was also optimized, to remove debris and to prevent dividing larger cells into smaller ones. Upon analysis with CellProfiler software, three problems were discovered with quantitation of Mitotracker green in cells (Fig. 8):

1. Split cells – Some cells, especially those with centrally-located nuclei, were divided and counted as two.
2. Merged cells - Some cells when growing close together were merged and counted as one.
3. Small cells excluded from counting – Small cells, which typically have less intense staining due to low amounts of mitochondrial dye , may not have enough stained area above the intensity threshold to overcome the CellProfiler size cutoff.

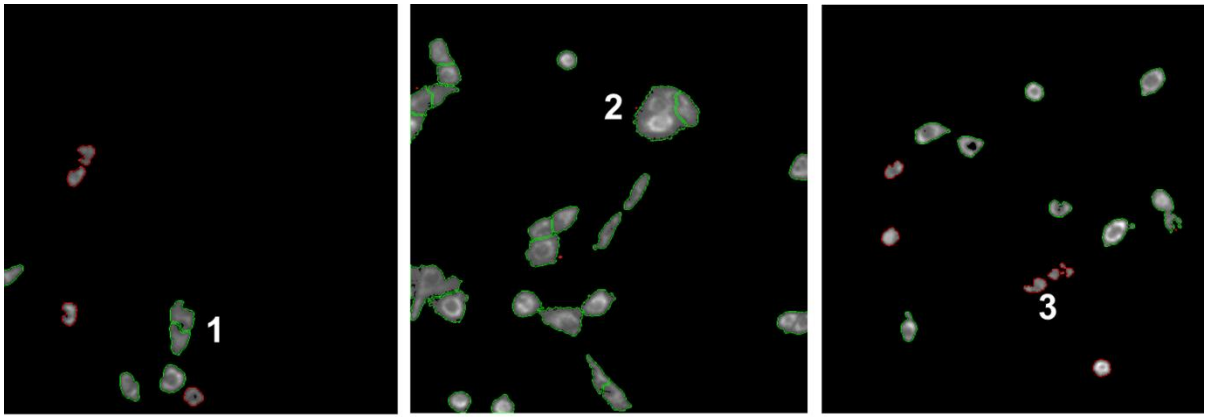

Figure 8: Mitochondrial mass staining with Mitotracker green, shows cells detected by CellProfiler (outlined in green) and those excluded based on size threshold (outlined in red; 10X magnification). The enumerated cells highlight the main problems of cell counting including 1) division of cells with centrally-located nuclei 2) merging of cells clustered together and 3) exclusion of cells due to small size and low fluorescence due to decreased uptake.

To overcome these problems, cell boundary staining was briefly tested with Vybrant DiD cell membrane dye (Invitrogen) but this method did not produce well-defined cell boundaries (data not shown). A cytoplasmic stain may provide better cell boundary definition, however this was not attempted. Given these image analysis limitations, the mitochondrial mass histogram in CP-A cells is skewed towards a right-tailed distribution (Fig. 9). This is likely due to an artificially high number of cells which are a result of cells being merged (described in problem #2 above).

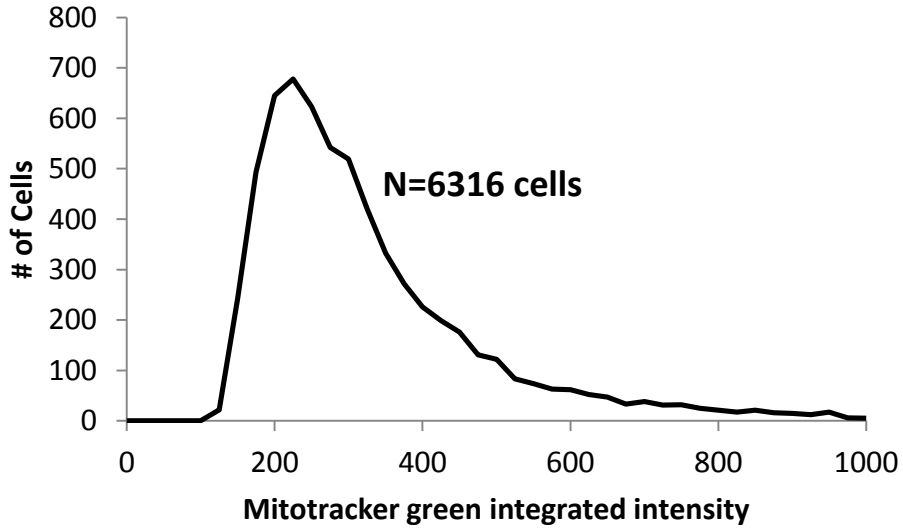

Figure 9: CP-A mitochondrial mass distribution derived from Mitotracker green staining, displays a right-tailed distribution. Note that this effect may be due to high numbers of merged cells detected during Mitotracker green image cytometry analysis.

To develop a method for measuring heterogeneity of OCR at single-cell resolution, a chip was designed with the following specifications:

- A sensor that is sensitive at sub-picomolar oxygen concentrations: platinum (Pt)-porphyrin.
- A surface that allows the cells to adhere (hydrophilic), yet also allows the sensors to adhere (without relying on hydrophobilicity or sialination). Chambers that are gas-impermeable: glass-to-glass seal.
- Non-toxic environment: sensor needs to be adhered in wells without glues; piston-lid needs to be adhered with non-toxic glue.

Chip design and sensor deposition. A compromise for chip design was reached with a borosilicate (and later fused-silica) glass, etched-well chip that provides a hydrophilic, gas-impermeable environment when sealed with a glass lid (Fig. 10). Chips were designed to have a raised seal-ridge around wells to enhance sealing by avoiding cells that adhere to the chip surface in the inter-well space.

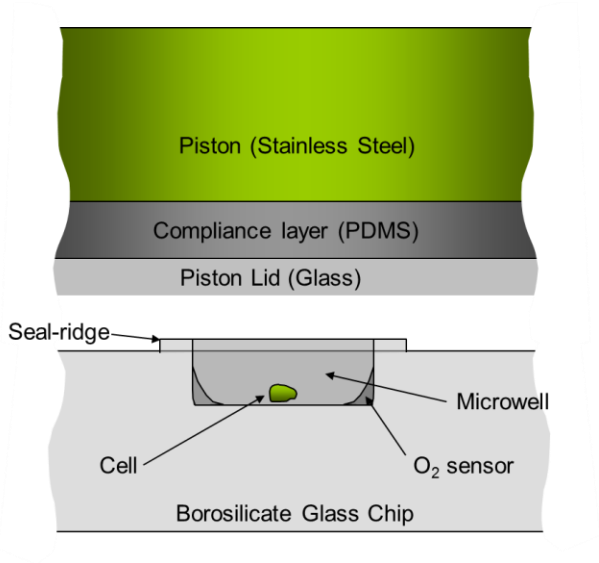

Figure 10: Setup of one-of-nine single-cell microwells and a piston prior to sealing. Cells are seeded into microwells in borosilicate glass chips, containing Pt-Porphyrin oxygen sensors. After the piston descends, the glass-to-glass interface between the piston lid and seal-ridge is able to form an oxygen-impermeable system in the microwell. The polydimethylsiloxane (PDMS) compliance layer prevents fracture of glass when pressure is applied on the lid.

Pt-porphyrin embedded in polystyrene microspheres was deposited into the wells by pico-injector and adhered by baking at 140°C for 20 minutes (Fig. 11). Sensors adhered in this way eventually delaminated from the surface, but were reliable for a four hour experiment consisting of three or four OCR measurements per well. Delamination was presumed to be

caused by convection currents caused by piston action and the relatively weak forces keeping the sensor adhered to the surface of the chip. Following experiments, undamaged chips could be re-used by cleaning with sulfuric acid and replacing fresh Pt-porphyrin sensors into the wells.

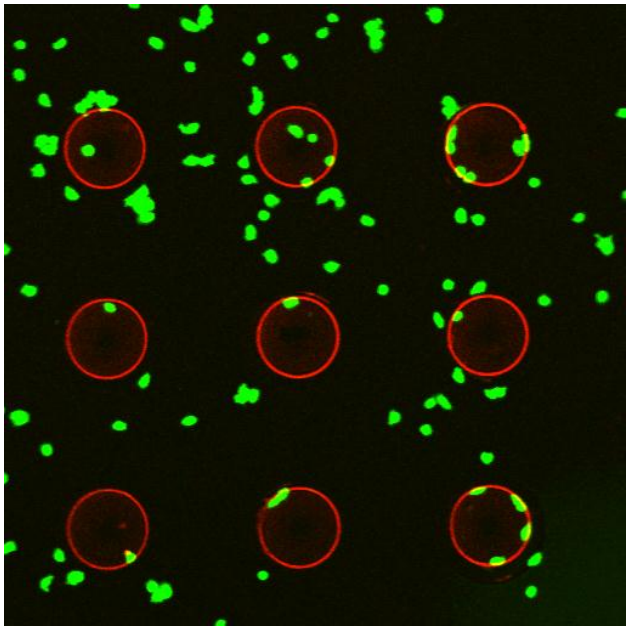

Figure 11: Typical cell seeding visualized by staining with Calcein AM (green) on a single-cell microwell chip (10X magnification). Platinum-porphyrin sensors (red) are seen adhered primarily to the bottom exterior of each microwell in the characteristic "coffee ring effect".

Piston and lid design. The piston and lid were designed in a way to be modular to allow for rapid replacement if lid detachment occurs during drawdown experiments. Lid detachment was detected by looking at the bright field image during piston alignment with the array. If a piston came down without the lid, it damaged the cells in the array and potentially cast debris across the entire chip, typically causing the experiment to be aborted. In such cases, the remainder of the chip was inspected to determine if it could be salvaged for further use. The piston-lid design was later redesigned with a hollow cylindrical PDMS mounted on a stainless steel spoke glued to the lid, allowing for quicker re-mounting of new pistons and less frequent lid failure.

After the microwells were sealed with applied pressure by the piston-lid, air-tight seals were verified by examining "fringe patterns" produced by the diffraction of a 488nm laser between the chip surface and lid, by imaging emission at 530nm (Fig. 12). Breaks in fringe patterns indicated poor sealing due to misalignment of the piston with the center of the arrays, or cells or other forms of debris. To deal with misalignment, re-centering the piston was effective at establishing good seals. Filtering cell medium prior to use through a 40nm filter was effective at reducing debris and improving likelihood of good seals. If glass debris was found, this typically indicated a lid (or more uncommonly a chip) fractured and, depending on the extent of debris, resulted in aborting the experiment since applying pressure onto glass debris often produced a chip fracture.

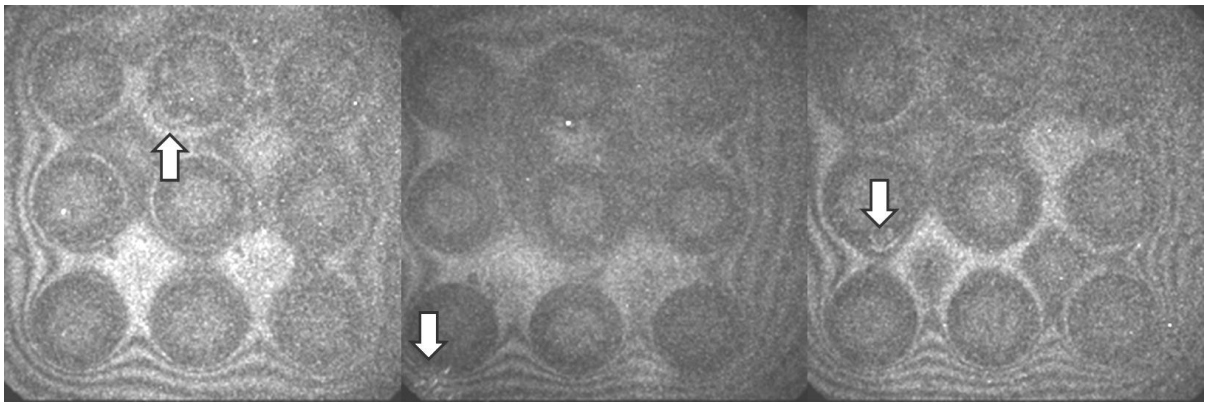

Figure 12: Uniform fringe patterns from 488nm laser light diffraction between lid and chip indicate proper seals in wells (10X magnification). Examples of fringe pattern defects in wells which are improperly sealed (arrows) show deviations from solid black lip around most wells.

Attention to toxic-free and contamination-free design. When designing devices for single-cell monitoring, it is vital that individual cells are handled uniformly and growth conditions do not impact cell function. As mentioned previously, several materials used in this device were specifically chosen to avoid cell toxicity. Sensors were adhered in a way that avoided potential toxicity from glues and sialination. Polydimethylsiloxane (PDMS), a material that is generally biocompatible, was used in the piston as a compliance layer. Biocompatible surgical glue was used to attach the lid to the piston, and the assembled piston was cured in a UV chamber prior to use, in order to avoid leaching of glue into medium.

To avoid bacterial contamination, chips were sterilized with ethanol and sterile water washes. It was discovered that residues from ethanol that dried could produce uneven patches of cell toxicity. Care was then taken to avoid drying the chips by keeping the chips wetted during and in between washes. To avoid contamination during experiments, the chip holder was covered with parafilm and maintained in a positive pressure air environment with a filtered gas line. Penicillin and streptomycin were present in cell culture media to slow bacterial growth.

Macrowell OCR experiments. Macrowell chips were initially tested to determine OCR of cell populations; however in independent experiments by Drs. Tom Paulson and Michael Konopka high variability between replicate experiments was reported. It was concluded that this variability is either due to significant oxygen leakage from the macrowells due to poor sealing and/or cell overgrowth on the sensor contributing to sensor noise (data not shown). Despite the problems encountered in measuring OCR, macrowells still provided a useful platform for measuring cell cycle and mitochondrial mass distributions in populations (with Hoechst 33342 and Mitotracker green respectively) to use as a quantitative standard for staining on single-cell chips.

Single-cell OCR experiments. Seeding concentrations were optimized for single-cell chips to produce one empty well (control) and several single cell wells for each array, 16 hours after seeding. Arrays with the most live single-cell wells, as detected by Calcein AM staining (or bright field cells without Sytox Orange uptake), were prioritized for OCR measures. Arrays with no empty or single-cell wells were re-examined at the end of OCR measuments on the prioritized arrays, since cell seeding tends to be a dynamic phenomenon due to cell motility and detachment over the course of a typical four-hour experiment.

Following successful sealing, single-cell OCRs were measured. Since higher concentrations of oxygen produce higher levels of variability in Pt-porphyrin sensors, oxygen concentrations readings from single-cell wells were taken from measurements that fell below this early high-variability region, typically 6ppm and below (Fig. 13a). Following experiments, chips were set aside and calibrated (Fig. 13b). *A priori* calibration was initially considered and is typically preferable with sensor systems but was not possible due to problems with sensor delamination over the high duration of time that calibration required.

(a) (b)

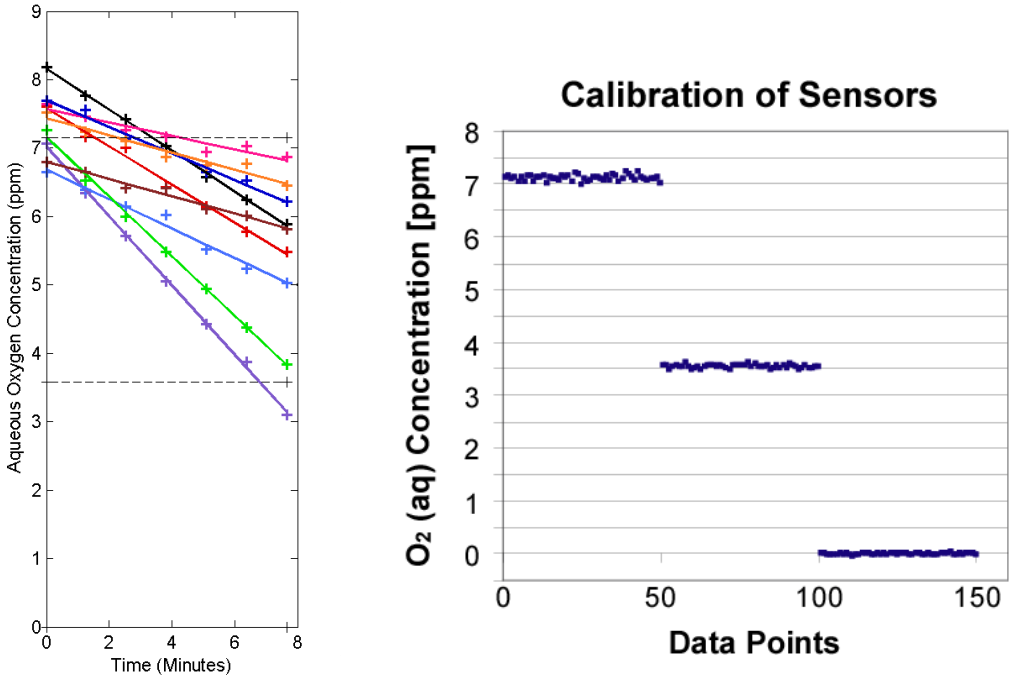

Figure 13: CP-A cells seeded on single-cell microwell chips had (a) oxygen consumption rates measured and calculated from slopes. Following OCR experiments, individual sensors were (b) calibrated at 20% (7ppm), 10% (3.5ppm) and 0% (0ppm) of oxygen. Higher concentrations of oxygen were observed to produce higher levels of measurement variability.

As a final validation of the single-cell OCR measurement technology, 79 single-cell CP-A cell line OCRs were measured (Fig. 14). This histogram profile was independently confirmed on a comparable platform by Laimonas Kelbauskas in Deirdre Meldrum's lab at Arizona State University (ASU), which used a sartomer-embedded platinum-porphyrin dye, with a sensor-on-lid configuration. Although the single-cell measurements were comparable, the measurements from ASU were right-shifted in comparison to ours. Interestingly, a second OCR peak was detected around 1.5fmol/min/cell in both sets of experiments. It was observed that cells displaying elongated morphology tended to have higher OCRs around this peak, although only a small number of cells of this type were observed during the course of our measures.

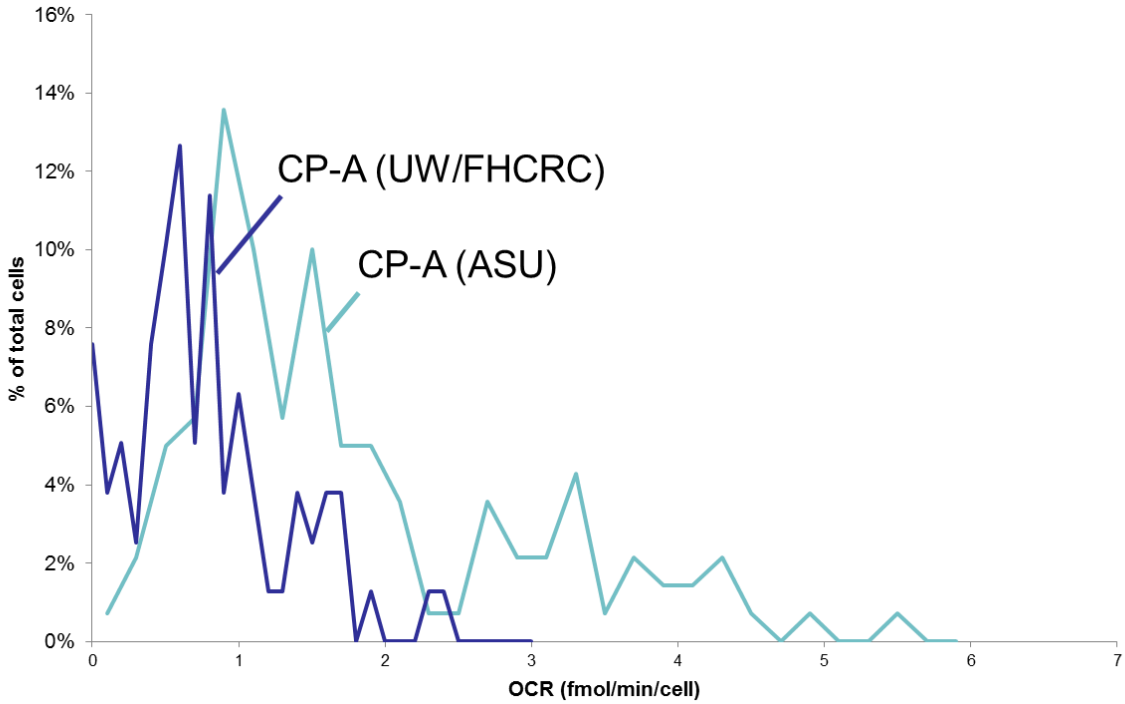

Figure 14: Single cell OCR heterogeneity profiles were measured in the CP-A cell line by two different groups, FHCRC/UW (N=79 cells) and ASU (N=140 cells).

DISCUSSION

In the second part of my thesis, I assisted in the development and testing of a system to measure single-cell oxygen consumption rates. Compared to systems that perform similar measurements, our instrument is able to perform measurements in gas-impermeable chambers that are able to sensitively measure single-cell OCR with minimal toxicity.

On our system, we established methods for serially measuring cell cycle and OCR on cells from the CP-A Barrett's esophagus cell line. We also attempted to measure mitochondrial mass but encountered problems with delineating cell boundaries and this may be overcome by cytoplasmic staining in future experiments. The distribution of OCR heterogeneity observed on our system was confirmed by similar OCR distributions observed by independent testing on a platform at Arizona State University. Due to low throughput of the single-cell OCR system, OCR measurements have yet to be tested in combination with cell cycle and/or mitochondrial mass.

One limitation of our system is low throughput. Each experiment, barring a lid or chip fracture event, collected on average 12 single-cell OCRs per 8 hour day. The major bottlenecks for throughput in our system were single-cell cell seeding and lid and sensor failure. The method used to seed cells resulted in random dispersal of cells onto chips, which averaged approximately 2 wells with single cells, even after optimization. Several techniques for directed seeding, such as cell injection systems and laser tweezers-based cell manipulation, were attempted by other collaborators in this grant, however BE cells are motile and, unless sealed, can escape well compartments during overnight growth. Other ideas proposed include micropatterning the cell surface to produce hydrophilic surfaces preferential for growth exclusively within the wells or redesigning the system to allow for microfluidics-based cell seeding. Lid detachment was a major obstacle to high-throughput since detection of lid detachment introduces a manual step into the experimental process and resulted in frequent failure of experiments. Lid detachment was prevented marginally by redesigning the piston-lid, but was still a relatively frequent occurance.

Sensor detachment during experiments or during calibration was also a problem to OCR data acquisition but has been corrected by better curing and adhesion methods. One design modification, tested by ASU, was to attach the sensors to the lid, which does not need to be hydrophilic for cell attachment and allows for different materials and manufacturing methods to be used.

Several emerging technologies may enable novel association experiments between OCR and other characteristics of individual cells in a population. As part of this multi-center grant, collaborative efforts were explored with Dr. Larry Wangh to perform single cell PCR and Dr. Norm Dovichi to perform single cell proteomics (Pierce and Wangh 2007; Cohen, Dickerson et al. 2008). Other emerging technologies may eventually enable single-cell genomics to be performed on single cells (Treff, Su et al. 2011).

This platform is amenable to expanding sensors to include other types that measure changes in pH, ATP and Ca2+. Metabolic nanosensors capable of measuring cytokines or other metabolites such as glucose and lactate have also been investigated through collaborations with Dr. Babak Parviz's group. Since my work in this thesis involved development of the prototype OCR measurement system, work in this thesis did not directly explore biological implications of OCR heterogeneity. However, we now have the tools to concurrently measure OCR with other

cell processes. Changes in oxygen consumption may indicate mitochondrial dysfunction and/or predisposition of cells towards a particular energy metabolism. Since changes in mitochondrial function have been reported in cancers, neurodegenerative diseases, sperm fertility and aging (Wallace 2010), we predict that monitoring oxygen consumption with single-cell resolution may produce discoveries for these conditions which have not been possible with higher scale methods.

REFERENCES

Boonstra, J. J., R. van Marion, et al. (2010). "Verification and unmasking of widely used human esophageal adenocarcinoma cell lines." Journal of the National Cancer Institute **102**(4): 271-274.

Cohen, D., J. A. Dickerson, et al. (2008). "Chemical cytometry: fluorescence-based single-cell analysis." Annual review of analytical chemistry **1**: 165-190.

Cooke, S. L., J. Temple, et al. (2011). "Intra-tumour genetic heterogeneity and poor chemoradiotherapy response in cervical cancer." British journal of cancer **104**(2): 361-368.

Coons, S. W., P. C. Johnson, et al. (1995). "Cytogenetic and flow cytometry DNA analysis of regional heterogeneity in a low grade human glioma." Cancer Res **55**(7): 1569-1577.

Darzynkiewicz, Z., F. Traganos, et al. (1981). "Rapid analysis of drug effects on the cell cycle." Cytometry **1**(4): 279-286.

Gonzalez-Garcia, I., R. V. Sole, et al. (2002). "Metapopulation dynamics and spatial heterogeneity in cancer." Proceedings of the National Academy of Sciences of the United States of America **99**(20): 13085-13089.

Harper, M. E., A. Antoniou, et al. (2002). "Characterization of a novel metabolic strategy used by drug-resistant tumor cells." The FASEB journal : official publication of the Federation of American Societies for Experimental Biology **16**(12): 1550-1557.

Hynes, J., T. C. O'Riordan, et al. (2005). "Fluorescence based oxygen uptake analysis in the study of metabolic responses to apoptosis induction." Journal of immunological methods **306**(1-2): 193-201.

Lewontin, R. C. (1970). "The Units of Selection." Annual Review of Ecology and Systematics **1**: 1-18.

Lidstrom, M. E. and D. R. Meldrum (2003). "Life-on-a-chip." Nat Rev Microbiol **1**(2): 158-164.

Limke, T. L. and W. D. Atchison (2009). "Application of single-cell microfluorimetry to neurotoxicology assays." Current protocols in toxicology / editorial board, Mahin D. Maines **Chapter 12**: Unit 12 15.

Maley, C. C., P. C. Galipeau, et al. (2006). "Genetic clonal diversity predicts progression to esophageal adenocarcinoma." Nat Genet **38**(4): 468-473.

Molter, T. W., S. C. McQuaide, et al. (2009). "A microwell array device capable of measuring single-cell oxygen consumption rates." Sensors and actuators. B, Chemical **135**(2): 678-686.

Novak, B. and J. M. Mitchison (1990). "Changes in the rate of oxygen consumption in synchronous cultures of the fission yeast Schizosaccharomyces pombe." Journal of cell science **96 (Pt 3)**: 429-433.

Nowell, P. C. (1976). "The clonal evolution of tumor cell populations." Science **194**(4260): 23-28.

O'Donovan, C., E. Twomey, et al. (2006). "Development of a respirometric biochip for embryo assessment." Lab on a chip **6**(11): 1438-1444.

O'Mahony, F. C., C. O'Donovan, et al. (2005). "Optical oxygen microrespirometry as a platform for environmental toxicology and animal model studies." Environmental science & technology **39**(13): 5010-5014.

Palanca-Wessels, M. C., M. T. Barrett, et al. (1998). "Genetic analysis of long-term Barrett's esophagus epithelial cultures exhibiting cytogenetic and ploidy abnormalities." Gastroenterology **114**(2): 295-304.

Pierce, K. E. and L. J. Wangh (2007). "Linear-after-the-exponential polymerase chain reaction and allied technologies. Real-time detection strategies for rapid, reliable diagnosis from single cells." Methods in molecular medicine **132**: 65-85.

Renger, G. and B. Hanssum (2009). "Oxygen detection in biological systems." Photosynthesis research **102**(2-3): 487-498.
Ryan, D., K. Ren, et al. (2011). "Single-cell assays." Biomicrofluidics **5**(2): 21501.
Salk, J. J., E. J. Fox, et al. (2010). "Mutational heterogeneity in human cancers: origin and consequences." Annual review of pathology **5**: 51-75.
Strovas, T. J., S. C. McQuaide, et al. (2010). "Direct measurement of oxygen consumption rates from attached and unattached cells in a reversibly sealed, diffusionally isolated sample chamber." Advances in bioscience and biotechnology **5**(5): 398-408.
Treff, N. R., J. Su, et al. (2011). "Single-cell whole-genome amplification technique impacts the accuracy of SNP microarray-based genotyping and copy number analyses." Molecular human reproduction **17**(6): 335-343.
Wallace, D. C. (2010). "Mitochondrial DNA mutations in disease and aging." Environmental and molecular mutagenesis **51**(5): 440-450.
Wilson, D. F., J. M. Vanderkooi, et al. (1987). "A versatile and sensitive method for measuring oxygen." Advances in experimental medicine and biology **215**: 71-77.
Wright, G. L., I. G. Maroulakou, et al. (2008). "VEGF stimulation of mitochondrial biogenesis: requirement of AKT3 kinase." The FASEB journal : official publication of the Federation of American Societies for Experimental Biology **22**(9): 3264-3275.
Wu, M., A. Neilson, et al. (2007). "Multiparameter metabolic analysis reveals a close link between attenuated mitochondrial bioenergetic function and enhanced glycolysis dependency in human tumor cells." American journal of physiology. Cell physiology **292**(1): C125-136.

CHAPTER 3

CONCLUSIONS

This thesis is the first investigation of the presence of the Warburg Effect in premalignant cell lines. Although the Warburg effect has been studied for nearly a century in cancer cells, the stage of progression at which it develops is poorly understood. Using Barrett's esophagus (BE) cell lines derived from patients, more genetically unstable cell lines were found to have higher glycolysis and a more pronounced Crabtree effect than a more stable BE cell line. Contrary to Warburg's original speculation that damaged mitochondria are associated with glycolytic increases in cancer cells, BE cells compensate for glycolytic inhibition with increased oxidative phosphorylation, indicating at least partially functioning mitochondria. The finding that neoplastic cells have heterogeneous energy metabolism suggests several possible research directions for monitoring neoplastic progression and therapeutic strategies for BE, discussed in the following sections.

As part of this thesis, I had the opportunity to work alongside a bioengineering team at the University of Washington to develop a chip-based system to measure single-cell oxygen consumption rate (OCR) and other characteristics, such as cell cycle, mitochondrial mass and apoptosis, in series. The measure of single-cell OCR, a central aspect of energy metabolism, enables novel discoveries of cellular function that is not possible at population levels. In this chapter, possible improvements, features and experiments with this newly developed technology are discussed.

FUTURE DIRECTIONS: GLYCOLYTIC HETEROGENEITY IN BE CELL LINES

Recent cancer research contributing to the Tumor Cancer Genome Atlas is providing complete sequences of many cancers (Wood, Parsons et al. 2007; Cancer_Genome_Atlas_Research_Network 2008; Ding, Getz et al. 2008); however, there is significant difficulty in finding novel individual genes that promote progression since cancer rarely result from the dysfunction of an individual gene but instead through interacting networks and large-scale deletions of multiple compensatory factors that contribute to loss of growth control (Hanahan and Weinberg 2011). To overcome the genetic heterogeneity seen in tumors, advancing technologies are making new approaches available and detection of downstream metabolic markers, such as upregulated glycolysis, may be useful in determining the risk of progression.

Due to the lower efficiency of ATP generation per glucose molecule, cells that increase their glycolysis require a higher influx of glucose. For the past four decades, knowledge of this increased glucose flux has led to cancer detection via whole-body imaging by positron-emission tomography (PET), in which cancer cells can be differentiated from surrounding tissue by elevated rates of radioactive glucose analogue uptake (Gambhir 2002). Several cancers are known to be predominantly glycolytic, including brain cancer, colon adenocarcinomas, clear-cell renal cell carcinoma and fast-growing hepatomas (Moreno-Sanchez, Rodriguez-Enriquez et al. 2007). Of these, colon cancer progression is most similar to BE to EA, sharing a self-renewing epithelium which is designed to proliferate and slough off. Increased glycolysis may evolve to accompany the ongoing proliferative program of this tissue.

Findings of increased glycolysis in cancers has led researchers to design metabolism-specific therapies targeting this pathway (Kim and Dang 2006) (Chen, Lu et al. 2007). Treatment with 2-deoxyglucose (2-DG) was found to significantly increase cytotoxicity of cisplatin in head and neck cancer cells by increasing oxidative stress (Simons, Ahmad et al. 2007); however there are concerns that treatment with 2-DG would adversely affect the glycolytic metabolism critical for brain and heart function (Fulda, Galluzzi et al. 2010). Since BE cells maintain both glycolytic and oxidative phosphorylation, glycolytic inhibition is unlikely to be a viable therapy due to compensation by mitochondria. Identification of glycolytic regions in BE and EA may facilitate localized topical therapy, since hypoxic regions are resistant to photodynamic therapy, and have limited blood flow, which reduces efficiency of drug delivery.

During neoplastic progression clones evolve and expand across the BE segment. The ability to modulate glycolysis may be advantageous to clones during selection and be associated with progression *in vivo*. If glycolysis can detected by measuring lactate levels of fresh biopsies or by fluorescent tissue imaging of redox changes (Georgakoudi, Jacobson et al. 2002), then a future *in vivo* experiment would be able to determine if glycolytic regions detected in endoscopic surveillance for early detection of cancer are associated with risk of progression to EA. Comparing somatic chromosome alterations in glycolytic versus non-glycolytic BE biopsies in patients would further determine if increased glycolysis is associated with regions of increased chromosomal instability or if it is an independent marker of progression. However, current approaches to cancer therapy have not resolved the clinical dilemma of overdiagnosis of non-lethal cancers and underdetection of lethal cancers therefore any therapeutic use of glycolysis as a biomarker must be carefully explored and validated.

The findings that glycolysis is heterogeneous in BE cell lines raises the question 'How does this adaptation arise?' Increased glycolysis has been associated with actively proliferating cells (Brand 1997), and BE is a hyperproliferative tissue is the esophagus, so adaptation of higher rates of glycolysis may be selected for among competing clones following an ulcerative event. Glycolysis, via the pentose phosphate pathway, also mediates the generation of reactive oxygen species (ROS) through NADPH synthesis and subsequent glutathione regeneration and may be selected in an environment with elevated extracellular ROS caused by periodic bile-acid reflux or chronic inflammation. The protective effects of NSAIDs, which decrease systemic inflammation, are known to decrease risk in BE patients likely as a result of decreased systemic ROS (Galipeau, Li et al. 2007; Rothwell, Fowkes et al. 2011). Understanding if cells are adapted to overcome ROS from intrinsic sources (ie. mitochondrial dysfunction) or extrinsic sources (ie. hypoxia, bile-salts or inflammation), would aid in designing better preventative strategies in patients.

My findings in BE cell lines have been limited by the low number of BE cell lines available and by inadequate control cell lines. At the time of these experiments, a single p53 wild-type cell line with low levels of genetic alteration (CP-A) was available; additional cell lines with low levels of genetic instability would greatly improve the statistical confidence of our findings. In most prior studies that utilized BE cultures, EPC-2 and HET-1A were used as normal squamous esophageal control lines. However EPC-2 was found to be aneuploid (Chapter 1), and HET-1A is transformed with SV40 large T-antigen and forms dysplastic epithelium in organotypic culture (Underwood et al, 2010). Until recently the origin of BE cells was unknown and so squamous epithelium has been used as a control cell line. Recently Dr. McKeon et al discovered a reservoir of embryonic-stage cells at the gastro-esophageal junction in p63 null-mouse models with

cryptic epithelium having gene-expression profiles similar to BE (Wang, Ouyang et al. 2011). Isolation of cell lines derived from these GE junction cells would provide a new type of cell line for BE studies, providing a more accurate BE-precursor control. Finally, only a small number of esophageal adenocarcinoma (EA) cell lines remain after several were found to have been of non-esophageal origin (Boonstra, van Marion et al. 2010). Submission of the limited remaining EA cell lines to public biorepositories by the founding labs would accelerate future research of this cancer.

Most cell lines undergo significant genetic alterations during establishment and passaging in tissue culture, raising a concern about how accurately they represent cell growth characteristics *in vivo*. The genomes of BE cell lines used in this study contain remarkably similar levels of genetic instability to biopsies from patients from which they were derived, despite being adapted to and passaged in tissue culture. Given the genetic similarity of the cell lines to patient biopsies, they represented a reasonable *ex vivo* model to use for studying metabolism. Analysis of the BE cell line genome alterations did not reveal glycolytic genes to be consistently altered, however the low number of cell lines in this study limit our ability to comprehensively survey genes that affect glycolytic metabolism. However, interpretation of genetic effects on metabolism can be difficult due to the network and redundancy effects of genes.

Mutations in the mitochondrial genome have been suggested as a marker of BE progression in several studies (Miyazono, Schneider et al. 2002; Sui, Zhou et al. 2006). Despite having active mitochondria, mitochondrial genome analysis revealed that most cell lines have mutations in coding mitochondrial genes and CP-A and CP-C have partial mutations, suggesting sub-populations with diverse mutations present. Recent work by a collaborator at Brandeis supports this concept, with a finding of multiple mitochondrial genome variants present within different cells of the population and even within single cells. The BE cell lines displayed different OCRs at a population level and technology developed in this thesis enables further investigation of phenotypic differences using single-cell OCR measurements.

FUTURE DIRECTIONS: OCR HETEROGENEITY MEASUREMENT PLATFORM

The technology developed in this thesis enables OCR measurements at a single cell level which make it possible to design experiments to investigate the mechanisms of metabolic heterogeneity at high resolution. Since decreased oxygen consumption is an early sign of cell death (Hynes, O'Riordan et al. 2005), this assay, combined with other downstream measurements may produce a very sensitive method for discovery of why some individual cells are more susceptible to death as a result of treatment with drugs or due to injury. Most drugs and antibiotics undergo specialized testing to determine if they have off-target mitochondrial toxicity (Nadanaciva, Bernal et al. 2007), and this assay may provide insight into whether the effects of these drugs are associated with OCR of individual cells and, unlike most other assays, to further characterize the individual cells that display sensitivity. Several mitochondrial characteristics may contribute to the heterogeneity of OCR including mitochondrial mass, potential and genotype. Mitochondrial mass and potential may be measured using fluorometric assays using mitochondrial dye staining methods, such as Mitotracker green or JC-1 (Invitrogen). As part of our multi-center CEGS grant, Dr. Larry Wangh's laboratory at Brandeis University have started investigating single-cell mitochondrial genotyping, which would enable experiments associating single-cell OCRs with mitochondrial genome mutations.

A major limitation of our method is throughput, although possible solutions have been proposed in Chapter 2. Increased throughput would provide data for greater statistical power, for additional measures for tests of reproducibility and detection of rare clones in a population. Throughput would be greatly improved by developing and implementing a fully-automated process as designed but aborted. The major problems to achieve automation were technical issuess with lid detachment, breakage and sealing. This necessitated frequent user intervention during single-cell OCR measurement experiments. Integrating microfluidics to the technology to improve throughput capacity with additionalassays would advance this platform.. . Microfluidics would enable experiments to test drug doses or nutrient levels on individual cells with treatment-free controls in each experiment.

Our single-cell chip OCR platform allows for addition of other assays that complement metabolic characterization or other cellular processes. To measure rates of glycolysis, pH sensors to measure extra-cellular acidification have been tested in pilot experiments at ASU. Commercially available dyes in the SNARF-family may also allow intracellular staining of pH. However, both of these methods require use of unbuffered media, as used in Seahorse assays to measure OCR described above, which may affect cell viability in longer experiments. To measure overall energy level within cells, an ATP assay, using a luciferase or ATP-sensitive dyes, could be done as an end-point analysis. As part of the interdisciplinary grant that funded this research, there was also exploration into intracellular ATP sensors by Dr. Alex Jen's laboratory at UW. To measure substrates, a glucose assay may be designed using either an enzymatic assay or nanowire sensors, which have been explored in collaboration with Dr. Babak Parviz's laboratory at UW. Finally, end-point assays that involve emerging single-cell genotyping, transcriptomics or proteomics technologies may provide additional downstream characterization of cells of interest.

SUMMARY

Knowledge that glycolysis is heterogeneous in premalignant cell lines opens novel directions in research and treatment of Barrett's esophagus and possibly other neoplasias. Work in this thesis characterized BE cell lines; however supporting evidence *in vivo* suggests that these findings are applicable to patients. If glycolytic regions in patients produce increased risk of progression to esophageal adenocarcinoma, these findings may have implications for surveillance and/or therapy for BE and EA.

The development of the single-cell OCR measurement technology in this thesis allows for detection of OCR with better resolution than was previously available in assays that did not produce a gas-impermeable interface. The establishment of other serial fluorometric assays enables experiments investigating association of OCR measurements to other cell characteristics at unprecedented resolution.

REFERENCES

Abnet, C. C., N. D. Freedman, et al. (2009). "Non-steroidal anti-inflammatory drugs and risk of gastric and oesophageal adenocarcinomas: results from a cohort study and a meta-analysis." Br J Cancer **100**(3): 551-557.
Baatar, D., M. K. Jones, et al. (2002). "Esophageal ulceration triggers expression of hypoxia-inducible factor-1 alpha and activates vascular endothelial growth factor gene - Implications for angiogenesis and ulcer healing." American Journal of Pathology **161**(4): 1449-1457.
Bensaad, K., A. Tsuruta, et al. (2006). "TIGAR, a p53-inducible regulator of glycolysis and apoptosis." Cell **126**(1): 107-120.
Berridge, M. V., P. M. Herst, et al. (2010). "Metabolic flexibility and cell hierarchy in metastatic cancer." Mitochondrion **10**(6): 584-588.
Blagosklonny, M. V., W. G. An, et al. (1998). "p53 inhibits hypoxia-inducible factor-stimulated transcription." Journal of Biological Chemistry **273**(20): 11995-11998.
Bonde, P., D. Gao, et al. (2007). "Duodenal reflux leads to down regulation of DNA mismatch repair pathway in an animal model of esophageal cancer." The Annals of thoracic surgery **83**(2): 433-440; discussion 440.
Boonstra, J. J., R. van Marion, et al. (2010). "Verification and unmasking of widely used human esophageal adenocarcinoma cell lines." Journal of the National Cancer Institute **102**(4): 271-274.
Brand, K. (1997). "Aerobic glycolysis by proliferating cells: protection against oxidative stress at the expense of energy yield." Journal of bioenergetics and biomembranes **29**(4): 355-364.
Brandon, M. C., E. Ruiz-Pesini, et al. (2009). "MITOMASTER: a bioinformatics tool for the analysis of mitochondrial DNA sequences." Hum Mutat **30**(1): 1-6.
Bytzer, P., P. B. Christensen, et al. (1999). "Adenocarcinoma of the esophagus and Barrett's esophagus: a population- based study." Am J Gastroenterol **94**(1): 86-91.
Cancer_Genome_Atlas_Research_Network (2008). "Comprehensive genomic characterization defines human glioblastoma genes and core pathways." Nature **455**(7216): 1061-1068.
Cardone, R. A., V. Casavola, et al. (2005). "The role of disturbed pH dynamics and the Na+/H+ exchanger in metastasis." Nature reviews. Cancer **5**(10): 786-795.
Casciari, J. J., S. V. Sotirchos, et al. (1988). "Glucose diffusivity in multicellular tumor spheroids." Cancer Res **48**(14): 3905-3909.
Chang, C. L., P. Lao-Sirieix, et al. (2007). "Retinoic acid-induced glandular differentiation of the oesophagus." Gut **56**(7): 906-917.
Chen, G., J. Izzo, et al. (2009). "Different redox states in malignant and nonmalignant esophageal epithelial cells and differential cytotoxic responses to bile acid and honokiol." Antioxidants & redox signaling **11**(5): 1083-1095.
Chen, Z., W. Lu, et al. (2007). "The Warburg effect and its cancer therapeutic implications." Journal of bioenergetics and biomembranes **39**(3): 267-274.
Chiche, J., K. Ilc, et al. (2009). "Hypoxia-inducible carbonic anhydrase IX and XII promote tumor cell growth by counteracting acidosis through the regulation of the intracellular pH." Cancer research **69**(1): 358-368.
Cohen, D., J. A. Dickerson, et al. (2008). "Chemical cytometry: fluorescence-based single-cell analysis." Annual review of analytical chemistry **1**: 165-190.
Cook, M. B., C. P. Wild, et al. (2007). "Risk of mortality and cancer incidence in Barrett's esophagus." Cancer Epidemiol Biomarkers Prev **16**(10): 2090-2096.
Cooke, S. L., J. Temple, et al. (2011). "Intra-tumour genetic heterogeneity and poor chemoradiotherapy response in cervical cancer." British journal of cancer **104**(2): 361-368.

Coons, S. W., P. C. Johnson, et al. (1995). "Cytogenetic and flow cytometry DNA analysis of regional heterogeneity in a low grade human glioma." Cancer Res **55**(7): 1569-1577.
Corley, D. A., T. R. Levin, et al. (2002). "Surveillance and Survival in Barrett's Adenocarcinomas: A Population- Based Study." Gastroenterology **122**(3): 633-640.
Crabtree, H. G. (1929). "Observations on the carbohydrate metabolism of tumours." The Biochemical journal **23**(3): 536-545.
Czernin, J. and M. E. Phelps (2002). "Positron emission tomography scanning: current and future applications." Annual review of medicine **53**: 89-112.
Dang, C. V. (2010). "p32 (C1QBP) and cancer cell metabolism: is the Warburg effect a lot of hot air?" Molecular and cellular biology **30**(6): 1300-1302.
Darzynkiewicz, Z., F. Traganos, et al. (1981). "Rapid analysis of drug effects on the cell cycle." Cytometry **1**(4): 279-286.
De Gottardi, A., J. M. Dumonceau, et al. (2006). "Expression of the bile acid receptor FXR in Barrett's esophagus and enhancement of apoptosis by guggulsterone in vitro." Mol Cancer **5**: 48.
de Groof, A. J., M. M. te Lindert, et al. (2009). "Increased OXPHOS activity precedes rise in glycolytic rate in H-RasV12/E1A transformed fibroblasts that develop a Warburg phenotype." Molecular cancer **8**: 54.
Diaz-Ruiz, R., M. Rigoulet, et al. (2011). "The Warburg and Crabtree effects: On the origin of cancer cell energy metabolism and of yeast glucose repression." Biochimica et biophysica acta **1807**(6): 568-576.
Ding, L., G. Getz, et al. (2008). "Somatic mutations affect key pathways in lung adenocarcinoma." Nature **455**(7216): 1069-1075.
Dvorak, K., C. M. Payne, et al. (2007). "Bile acids in combination with low pH induce oxidative stress and oxidative DNA damage: relevance to the pathogenesis of Barrett's oesophagus." Gut **56**(6): 763-771.
Dwarkanath, B. S., F. Zolzer, et al. (2001). "Heterogeneity in 2-deoxy-D-glucose-induced modifications in energetics and radiation responses of human tumor cell lines." International journal of radiation oncology, biology, physics **50**(4): 1051-1061.
Elstrom, R. L., D. E. Bauer, et al. (2004). "Akt stimulates aerobic glycolysis in cancer cells." Cancer research **64**(11): 3892-3899.
Epstein, A. C., J. M. Gleadle, et al. (2001). "C. elegans EGL-9 and mammalian homologs define a family of dioxygenases that regulate HIF by prolyl hydroxylation." Cell **107**(1): 43-54.
Fatyol, K. and A. A. Szalay (2001). "The p14(ARF) tumor suppressor protein facilitates nucleolar sequestration of hypoxia-inducible factor-1 alpha (HIF-1 alpha) and inhibits HIF-1-mediated transcription." Journal of Biological Chemistry **276**(30): 28421-28429.
Ferguson, H. R., C. P. Wild, et al. (2008). "Cyclooxygenase-2 and inducible nitric oxide synthase gene polymorphisms and risk of reflux esophagitis, Barrett's esophagus, and esophageal adenocarcinoma." Cancer epidemiology, biomarkers & prevention : a publication of the American Association for Cancer Research, cosponsored by the American Society of Preventive Oncology **17**(3): 727-731.
Fichter, C. D., C. Herz, et al. (2011). "Occurrence of multipolar mitoses and association with Aurora-A/-B kinases and p53 mutations in aneuploid esophageal carcinoma cells." BMC cell biology **12**: 13.
Frezza, C. and E. Gottlieb (2009). "Mitochondria in cancer: not just innocent bystanders." Seminars in cancer biology **19**(1): 4-11.
Fulda, S., L. Galluzzi, et al. (2010). "Targeting mitochondria for cancer therapy." Nature reviews. Drug discovery **9**(6): 447-464.
Galipeau, P. C., X. Li, et al. (2007). "NSAIDs modulate CDKN2A, TP53, and DNA content risk for future esophageal adenocarcinoma." PLoS Med **4**: e67.

Galipeau, P. C., X. Li, et al. (2007). "NSAIDs modulate CDKN2A, TP53, and DNA content risk for progression to esophageal adenocarcinoma." PLoS Med **4**(2): e67.
Gambhir, S. S. (2002). "Molecular imaging of cancer with positron emission tomography." Nat Rev Cancer **2**(9): 683-693.
Gatenby, R. A. and R. J. Gillies (2004). "Why do cancers have high aerobic glycolysis?" Nature Reviews Cancer **4**(11): 891-899.
Gatenby, R. A. and R. J. Gillies (2008). "A microenvironmental model of carcinogenesis." Nat Rev Cancer **8**(1): 56-61.
Georgakoudi, I., B. C. Jacobson, et al. (2002). "NAD(P)H and collagen as in vivo quantitative fluorescent biomarkers of epithelial precancerous changes." Cancer research **62**(3): 682-687.
Goldblatt, H. and G. Cameron (1953). "Induced malignancy in cells from rat myocardium subjected to intermittent anaerobiosis during long propagation in vitro." The Journal of experimental medicine **97**(4): 525-552.
Golshani-Hebroni, S. G. and S. P. Bessman (1997). "Hexokinase binding to mitochondria: a basis for proliferative energy metabolism." Journal of bioenergetics and biomembranes **29**(4): 331-338.
Gonzalez-Garcia, I., R. V. Sole, et al. (2002). "Metapopulation dynamics and spatial heterogeneity in cancer." Proceedings of the National Academy of Sciences of the United States of America **99**(20): 13085-13089.
Graeber, T. G., C. Osmanian, et al. (1996). "Hypoxia-mediated selection of cells with diminished apoptotic potential in solid tumours." Nature **379**(6560): 88-91.
Greenhough, A., H. J. Smartt, et al. (2009). "The COX-2/PGE2 pathway: key roles in the hallmarks of cancer and adaptation to the tumour microenvironment." Carcinogenesis **30**(3): 377-386.
Griffiths, E. A., S. A. Pritchard, et al. (2007). "Increasing expression of hypoxia-inducible proteins in the Barrett's metaplasia-dysplasia-adenocarcinoma sequence." Br J Cancer **96**(9): 1377-1383.
Guppy, M., E. Greiner, et al. (1993). "The role of the Crabtree effect and an endogenous fuel in the energy metabolism of resting and proliferating thymocytes." European journal of biochemistry / FEBS **212**(1): 95-99.
Hanahan, D. and R. A. Weinberg (2000). "The hallmarks of cancer." Cell **100**(1): 57-70.
Hanahan, D. and R. A. Weinberg (2011). "Hallmarks of cancer: the next generation." Cell **144**(5): 646-674.
Harada, H., H. Nakagawa, et al. (2003). "Telomerase induces immortalization of human esophageal keratinocytes without p16INK4a inactivation." Molecular cancer research : MCR **1**(10): 729-738.
Harper, M. E., A. Antoniou, et al. (2002). "Characterization of a novel metabolic strategy used by drug-resistant tumor cells." The FASEB journal : official publication of the Federation of American Societies for Experimental Biology **16**(12): 1550-1557.
Hewitson, K. S., L. A. McNeill, et al. (2002). "Hypoxia-inducible factor (HIF) asparagine hydroxylase is identical to factor inhibiting HIF (FIH) and is related to the cupin structural family." The Journal of biological chemistry **277**(29): 26351-26355.
Holmes, R. S. and T. L. Vaughan (2007). "Epidemiology and pathogenesis of esophageal cancer." Semin Radiat Oncol **17**(1): 2-9.
Hornig-Do, H. T., J. C. von Kleist-Retzow, et al. (2007). "Human epidermal keratinocytes accumulate superoxide due to low activity of Mn-SOD, leading to mitochondrial functional impairment." The Journal of investigative dermatology **127**(5): 1084-1093.

Hynes, J., T. C. O'Riordan, et al. (2005). "Fluorescence based oxygen uptake analysis in the study of metabolic responses to apoptosis induction." Journal of immunological methods **306**(1-2): 193-201.
Ivan, M., K. Kondo, et al. (2001). "HIFalpha targeted for VHL-mediated destruction by proline hydroxylation: implications for O2 sensing." Science **292**(5516): 464-468.
Jaakkola, P., D. R. Mole, et al. (2001). "Targeting of HIF-alpha to the von Hippel-Lindau ubiquitylation complex by O2-regulated prolyl hydroxylation." Science **292**(5516): 468-472.
Kern, K. A. and J. A. Norton (1987). "Inhibition of established rat fibrosarcoma growth by the glucose antagonist 2-deoxy-D-glucose." Surgery **102**(2): 380-385.
Kim, J. W. and C. V. Dang (2006). "Cancer's Molecular Sweet Tooth and the Warburg Effect." Cancer Res **66**(18): 8927-8930.
Kong, J., M. A. Crissey, et al. (2011). "Ectopic Cdx2 expression in murine esophagus models an intermediate stage in the emergence of Barrett's esophagus." PloS one **6**(4): e18280.
Kosoff, R. E., K. L. Gardiner, et al. (2011). "Development and characterization of an organotypic model of Barrett's esophagus." Journal of cellular physiology.
Lai, L. A., R. Kostadinov, et al. (2010). "Deletion at fragile sites is a common and early event in Barrett's esophagus." Mol Cancer Res **8**(8): 1084-1094.
Latif, F., K. Tory, et al. (1993). "Identification of the Vonhippel-Lindau Disease Tumor-Suppressor Gene." Science **260**(5112): 1317-1320.
Leese, H. J. and J. R. Bronk (1975). "Lactate formation by rat small intestine in vitro." Biochimica et biophysica acta **404**(1): 40-48.
Levine, D. S. and B. J. Reid (1992). Endoscopic diagnosis of esophageal neoplasms. Gastrointestinal Endoscopy Clinics of North America. G. A. Boyce and H. W. J. Boyce. Philadelphia, W. B. Saunders Co.**:** 395-413.
Lewontin, R. C. (1970). "The Units of Selection." Annual Review of Ecology and Systematics **1**: 1-18.
Li, X., P. C. Galipeau, et al. (2008). "Single nucleotide polymorphism-based genome-wide chromosome copy change, loss of heterozygosity, and aneuploidy in Barrett's esophagus neoplastic progression." Cancer Prev Res (Phila Pa) **1**(6): 413-423.
Lidstrom, M. E. and D. R. Meldrum (2003). "Life-on-a-chip." Nat Rev Microbiol **1**(2): 158-164.
Limke, T. L. and W. D. Atchison (2009). "Application of single-cell microfluorimetry to neurotoxicology assays." Current protocols in toxicology / editorial board, Mahin D. Maines **Chapter 12**: Unit 12 15.
Lopaschuk, G. D. and W. C. Stanley (1997). "Glucose metabolism in the ischemic heart." Circulation **95**(2): 313-315.
Lord, R. V., J. M. Park, et al. (2003). "Vascular endothelial growth factor and basic fibroblast growth factor expression in esophageal adenocarcinoma and Barrett esophagus." The Journal of thoracic and cardiovascular surgery **125**(2): 246-253.
Maley, C. C., P. C. Galipeau, et al. (2006). "Genetic clonal diversity predicts progression to esophageal adenocarcinoma." Nat Genet **38**(4): 468-473.
Matoba, S., J. G. Kang, et al. (2006). "p53 regulates mitochondrial respiration." Science **312**(5780): 1650-1653.
Miyazono, F., P. M. Schneider, et al. (2002). "Mutations in the mitochondrial DNA D-Loop region occur frequently in adenocarcinoma in Barrett's esophagus." Oncogene **21**(23): 3780-3783.
Molter, T. W., S. C. McQuaide, et al. (2009). "A microwell array device capable of measuring single-cell oxygen consumption rates." Sensors and actuators. B, Chemical **135**(2): 678-686.

Montgomery, E., M. P. Bronner, et al. (2001). "Reproducibility of the diagnosis of dysplasia in Barrett esophagus: a reaffirmation." Hum Pathol **32**(4): 368-378.
Moons, L. M., E. J. Kuipers, et al. (2007). "COX-2 CA-haplotype is a risk factor for the development of esophageal adenocarcinoma." The American journal of gastroenterology **102**(11): 2373-2379.
Moreno-Sanchez, R., S. Rodriguez-Enriquez, et al. (2007). "Energy metabolism in tumor cells." The FEBS journal **274**(6): 1393-1418.
Mustea, I. and T. Muresian (1967). "Crabtree effect in some bacterial cultures." Cancer **20**(9): 1499-1501.
Nadanaciva, S., A. Bernal, et al. (2007). "Target identification of drug induced mitochondrial toxicity using immunocapture based OXPHOS activity assays." Toxicology in vitro : an international journal published in association with BIBRA **21**(5): 902-911.
Navin, N., J. Kendall, et al. (2011). "Tumour evolution inferred by single-cell sequencing." Nature **472**(7341): 90-94.
Neto, C. A., H. Zhuang, et al. (2001). "Detection of Barrett's esophagus superimposed by esophageal cancer by FDG positron emission tomography." Clinical nuclear medicine **26**(12): 1060.
Nishihira, T., Y. Hashimoto, et al. (1993). "Molecular and cellular features of esophageal cancer cells." Journal of cancer research and clinical oncology **119**(8): 441-449.
Nolop, K. B., C. G. Rhodes, et al. (1987). "Glucose utilization in vivo by human pulmonary neoplasms." Cancer **60**(11): 2682-2689.
Novak, B. and J. M. Mitchison (1990). "Changes in the rate of oxygen consumption in synchronous cultures of the fission yeast Schizosaccharomyces pombe." Journal of cell science **96 (Pt 3)**: 429-433.
Nowell, P. C. (1976). "The clonal evolution of tumor cell populations." Science **194**(4260): 23-28.
O'Donovan, C., E. Twomey, et al. (2006). "Development of a respirometric biochip for embryo assessment." Lab on a chip **6**(11): 1438-1444.
O'Mahony, F. C., C. O'Donovan, et al. (2005). "Optical oxygen microrespirometry as a platform for environmental toxicology and animal model studies." Environmental science & technology **39**(13): 5010-5014.
Orlando, R. C. (2006). Mucosal Defense in Barrett's Esophagus. Barrett's Esophagus and Esophageal Adenocarcinoma. S. R. ed. Sharma P. Oxford, UK, Blackwell Publishing, Ltd**:** pp. 60-72.
Palanca-Wessels, M. C., M. T. Barrett, et al. (1998). "Genetic analysis of long-term Barrett's esophagus epithelial cultures exhibiting cytogenetic and ploidy abnormalities." Gastroenterology **114**(2): 295-304.
Palanca-Wessels, M. C., A. Klingelhutz, et al. (2003). "Extended lifespan of Barrett's esophagus epithelium transduced with the human telomerase catalytic subunit: a useful in vitro model." Carcinogenesis **24**(7): 1183-1190.
Pierce, K. E. and L. J. Wangh (2007). "Linear-after-the-exponential polymerase chain reaction and allied technologies. Real-time detection strategies for rapid, reliable diagnosis from single cells." Methods in molecular medicine **132**: 65-85.
Pohl, H. and H. G. Welch (2005). "The role of overdiagnosis and reclassification in the marked increase of esophageal adenocarcinoma incidence." J Natl Cancer Inst **97**(2): 142-146.
Polednak, A. P. (2003). "Trends in survival for both histologic types of esophageal cancer in US surveillance, epidemiology and end results areas." Int J Cancer **105**(1): 98-100.
Possemato, R., K. M. Marks, et al. (2011). "Functional genomics reveal that the serine synthesis pathway is essential in breast cancer." Nature.

Postma, E., C. Verduyn, et al. (1989). "Enzymic analysis of the crabtree effect in glucose-limited chemostat cultures of Saccharomyces cerevisiae." Applied and environmental microbiology **55**(2): 468-477.
Przybytkowski, E., E. Joly, et al. (2007). "Upregulation of cellular triacylglycerol - free fatty acid cycling by oleate is associated with long-term serum-free survival of human breast cancer cells." Biochemistry and cell biology = Biochimie et biologie cellulaire **85**(3): 301-310.
Ramanathan, A., C. Wang, et al. (2005). "Perturbational profiling of a cell-line model of tumorigenesis by using metabolic measurements." Proc Natl Acad Sci U S A **102**(17): 5992-5997.
Reid, B. J., R. C. Haggitt, et al. (1988). "Observer variation in the diagnosis of dysplasia in Barrett's esophagus." Human Pathology **19**(2): 166-178.
Reid, B. J., X. Li, et al. (2010). "Barrett's oesophagus and oesophageal adenocarcinoma: time for a new synthesis." Nat Rev Cancer **10**(2): 87-101.
Renger, G. and B. Hanssum (2009). "Oxygen detection in biological systems." Photosynthesis research **102**(2-3): 487-498.
Rockett, J. C., K. Larkin, et al. (1997). "Five newly established oesophageal carcinoma cell lines: phenotypic and immunological characterization." British journal of cancer **75**(2): 258-263.
Rothwell, P. M., F. G. Fowkes, et al. (2011). "Effect of daily aspirin on long-term risk of death due to cancer: analysis of individual patient data from randomised trials." Lancet **377**(9759): 31-41.
Ryan, D., K. Ren, et al. (2011). "Single-cell assays." Biomicrofluidics **5**(2): 21501.
Salk, J. J., E. J. Fox, et al. (2010). "Mutational heterogeneity in human cancers: origin and consequences." Annual review of pathology **5**: 51-75.
Sampliner, R. E. (2002). "Updated guidelines for the diagnosis, surveillance, and therapy of Barrett's esophagus." Am J Gastroenterol **97**(8): 1888-1895.
Scheffler, I. E. (2001). "A century of mitochondrial research: achievements and perspectives." Mitochondrion **1**(1): 3-31.
Schornack, P. A. and R. J. Gillies (2003). "Contributions of cell metabolism and H+ diffusion to the acidic pH of tumors." Neoplasia **5**(2): 135-145.
Semenza, G. L. (2001). "Hypoxia-inducible factor 1: control of oxygen homeostasis in health and disease." Pediatric research **49**(5): 614-617.
Semenza, G. L. (2002). "HIF-1 and tumor progression: pathophysiology and therapeutics." Trends in Molecular Medicine **8**(4): S62-S67.
Simons, A. L., I. M. Ahmad, et al. (2007). "2-Deoxy-D-glucose combined with cisplatin enhances cytotoxicity via metabolic oxidative stress in human head and neck cancer cells." Cancer research **67**(7): 3364-3370.
Smallbone, K., R. A. Gatenby, et al. (2007). "Metabolic changes during carcinogenesis: potential impact on invasiveness." Journal of theoretical biology **244**(4): 703-713.
Song, S., S. Guha, et al. (2007). "COX-2 induction by unconjugated bile acids involves reactive oxygen species-mediated signalling pathways in Barrett's oesophagus and oesophageal adenocarcinoma." Gut **56**(11): 1512-1521.
Souba, W. W. (1993). "Glutamine and cancer." Annals of surgery **218**(6): 715-728.
Strovas, T. J., S. C. McQuaide, et al. (2010). "Direct measurement of oxygen consumption rates from attached and unattached cells in a reversibly sealed, diffusionally isolated sample chamber." Advances in bioscience and biotechnology **5**(5): 398-408.
Suganuma, K., H. Miwa, et al. (2010). "Energy metabolism of leukemia cells: glycolysis versus oxidative phosphorylation." Leukemia & lymphoma **51**(11): 2112-2119.

Sui, G., S. Zhou, et al. (2006). "Mitochondrial DNA mutations in preneoplastic lesions of the gastrointestinal tract: a biomarker for the early detection of cancer." Mol Cancer **5**: 73.
Sun, Q., X. Chen, et al. (2011). "Mammalian target of rapamycin up-regulation of pyruvate kinase isoenzyme type M2 is critical for aerobic glycolysis and tumor growth." Proceedings of the National Academy of Sciences of the United States of America **108**(10): 4129-4134.
Sussman, I., M. Erecinska, et al. (1980). "Regulation of cellular energy metabolism: the Crabtree effect." Biochimica et biophysica acta **591**(2): 209-223.
Taylor, M. D., P. W. Smith, et al. (2009). "Correlations between selected tumor markers and fluorodeoxyglucose maximal standardized uptake values in esophageal cancer." European journal of cardio-thoracic surgery : official journal of the European Association for Cardio-thoracic Surgery **35**(4): 699-705.
Thomas, T., K. R. Abrams, et al. (2007). "Meta analysis: Cancer risk in Barrett's oesophagus." Aliment Pharmacol Ther **26**(11-12): 1465-1477.
Thomlinson, R. H. and L. H. Gray (1955). "The histological structure of some human lung cancers and the possible implications for radiotherapy." British Journal of Cancer **9**: 539-549.
Treff, N. R., J. Su, et al. (2011). "Single-cell whole-genome amplification technique impacts the accuracy of SNP microarray-based genotyping and copy number analyses." Molecular human reproduction **17**(6): 335-343.
Vander Heiden, M. G., L. C. Cantley, et al. (2009). "Understanding the Warburg effect: the metabolic requirements of cell proliferation." Science **324**(5930): 1029-1033.
Vander Heiden, M. G., J. W. Locasale, et al. (2010). "Evidence for an alternative glycolytic pathway in rapidly proliferating cells." Science **329**(5998): 1492-1499.
Vaughan, T. L., L. M. Dong, et al. (2005). "Non-steroidal anti-inflammatory drugs and risk of neoplastic progression in Barrett's oesophagus: a prospective study." Lancet Oncol **6**(12): 945-952.
Wallace, D. C. (2010). "Mitochondrial DNA mutations in disease and aging." Environmental and molecular mutagenesis **51**(5): 440-450.
Wang, K. K. and R. E. Sampliner (2008). "Updated guidelines 2008 for the diagnosis, surveillance and therapy of Barrett's esophagus." Am J Gastroenterol **103**(3): 788-797.
Wang, X., H. Ouyang, et al. (2011). "Residual embryonic cells as precursors of a Barrett's-like metaplasia." Cell **145**(7): 1023-1035.
Warburg, O. (1956). "On the origin of cancer cells." Science **123**(3191): 309-314.
Warburg, O., F. Wind, et al. (1927). "The Metabolism of Tumors in the Body." The Journal of general physiology **8**(6): 519-530.
Weinhouse, S. (1956). "On respiratory impairment in cancer cells." Science **124**(3215): 267-269.
Weinhouse, S. (1967). "Glycolysis, respiration, and enzyme alterations in rat liver neoplasia." Science **158**(3800): 537.
Weinhouse, S. (1976). "The Warburg hypothesis fifty years later." Zeitschrift fur Krebsforschung und klinische Onkologie. Cancer research and clinical oncology **87**(2): 115-126.
Wilson, D. F., J. M. Vanderkooi, et al. (1987). "A versatile and sensitive method for measuring oxygen." Advances in experimental medicine and biology **215**: 71-77.
Wood, L. D., D. W. Parsons, et al. (2007). "The genomic landscapes of human breast and colorectal cancers." Science **318**(5853): 1108-1113.
Wright, G. L., I. G. Maroulakou, et al. (2008). "VEGF stimulation of mitochondrial biogenesis: requirement of AKT3 kinase." The FASEB journal : official publication of the Federation of American Societies for Experimental Biology **22**(9): 3264-3275.

Wu, M., A. Neilson, et al. (2007). "Multiparameter metabolic analysis reveals a close link between attenuated mitochondrial bioenergetic function and enhanced glycolysis dependency in human tumor cells." American journal of physiology. Cell physiology **292**(1): C125-136.

Xie, H., V. A. Valera, et al. (2009). "LDH-A inhibition, a therapeutic strategy for treatment of hereditary leiomyomatosis and renal cell cancer." Molecular cancer therapeutics **8**(3): 626-635.

Yen, C. J., J. G. Izzo, et al. (2008). "Bile acid exposure up-regulates tuberous sclerosis complex 1/mammalian target of rapamycin pathway in Barrett's-associated esophageal adenocarcinoma." Cancer research **68**(8): 2632-2640.

Younes, M., A. Ertan, et al. (1997). "Human erythrocyte glucose transporter (Glut1) is immunohistochemically detected as a late event during malignant progression in Barrett's metaplasia." Cancer Epidemiology Biomarkers & Prevention **6**(5): 303-305.

Yousef, F., C. Cardwell, et al. (2008). "The incidence of esophageal cancer and high-grade dysplasia in Barrett's esophagus: a systematic review and meta-analysis." Am J Epidemiol **168**(3): 237-249.

Zhong, H., A. M. De Marzo, et al. (1999). "Overexpression of hypoxia-inducible factor 1alpha in common human cancers and their metastases." Cancer research **59**(22): 5830-5835.

Zhong, H., N. Mabjeesh, et al. (2002). "Nuclear expression of hypoxia-inducible factor 1alpha protein is heterogeneous in human malignant cells under normoxic conditions." Cancer letters **181**(2): 233-238.

Zu, X. L. and M. Guppy (2004). "Cancer metabolism: facts, fantasy, and fiction." Biochemical and biophysical research communications **313**(3): 459-465.